Stony Brook University

Neuronal Control of Immunity

A Dissertation Presented

by

William Michael Hanes

to

The Graduate School

in Partial Fulfillment of the

Requirements

for the Degree of

Doctor of Philosophy

in

Molecular and Cellular Biology

(Immunology and Pathology)

Stony Brook University

December 2015

Stony Brook University

The Graduate School

William Michael Hanes

We, the dissertation committee for the above candidate for the

Doctor of Philosophy degree, hereby recommend

acceptance of this dissertation.

Kevin J. Tracey, MD – Dissertation Advisor
Adjunct Faculty, Department of Molecular Genetics and Microbiology

Nicholas Carpino, PhD – Chairperson of Defense
Associate Professor, Department of Molecular Genetics and Microbiology

Nancy C. Reich, PhD
Professor, Department of Molecular Genetics and Microbiology

Barbara Sherry, PhD
Investigator, Immunology & Infection, The Feinstein Institute for Medical Research

Ulf Andersson, MD, PhD
Professor/Senior Physician, Paediatric Reumatology, Karolinska Institutet

This dissertation is accepted by the Graduate School

Charles Taber
Dean of the Graduate School

Abstract of the Dissertation

Neuronal Control of Immunity

by

William Michael Hanes

Doctor of Philosophy

in

Molecular and Cellular Biology

(Immunology and Pathology)

Stony Brook University

2015

Control of immune responses is vital for maintenance of homeostasis. The immune system must be able to quickly respond to invading pathogens, while suppressing responses that could lead to autoimmunity and inflammation. Recent advances have revealed a role for the nervous system in maintaining homeostasis. In the prototypical neural reflex, during activation of the inflammatory reflex, vagus nerve signaling culminates on adrenergic signals translated to acetylcholine release by splenic T lymphocytes which activate receptor signals on macrophages to attenuate cytokine release. Many additional interactions remain to be elucidated. Herein, several novel immune-nervous interactions are characterized.

A newly-described neuronal reflex, which regulates antigen flow through the lymphatic system is described. Antigen flow through the lymphatic system is restricted when an animal has been immunized against it. We utilized fluorescently-labeled antigen imaged *in situ* in the lymphatic system, and found that neuronal interventions were able to modulate antigen localization. Antigen trafficking that is normally restricted in immunized mice was restored when nerve activity was blocked pharmaceutically or by genetically-driven neuron depletion. In addition, induction of neuronal activity restricted antigen in naïve mice. This establishes a role

for neurons in alteration of lymphatic trafficking and provides a new way for bioelectronic intervention to modulate immune function.

Vagus nerve stimulation inhibits inflammatory responses and modulates B cell antibody production. Galantamine, a centrally-acting acetylcholinesterase inhibitor is known to signal through the vagus nerve. Herein, use of this compound is shown to delay the onset of type 1 diabetes in a non-obese diabetic mouse model while inhibiting immune responses in a disease-specific manner. Daily administration of galantamine delayed the onset of hyperglycemia and insulitis, and decreased anti-insulin antibodies. These findings highlight a previously unrecognized anti-inflammatory effect of galantamine in preclinical type I diabetes.

Blood pressure is mediated by cholinergic signaling; however, the vasculature lacks cholinergic neurons. The source of acetylcholine has not yet been described. Acetylcholine-producing T cells are herein described as being necessary and vital to maintenance of blood pressure. To support this study, I produced a T cell line that overproduces ChAT. The functional role of T_{ChAT} is verified using *in vivo* mouse studies of blood pressure variation in different phenotypic backgrounds. This new role for T cells acting as interneurons expands our understanding of the role of the immune system.

In addition, these T cells increase cholinergic signaling in response to β2-adrenergic receptor ligand binding. Until now, study of specific T cell responses to β2-adrenergic receptor activation *in vivo* has been impossible as numerous other cell types also respond to β2-adrenergic receptor. A novel use of optogenetic technology allows study of these cells, utilizing light to activate receptors temporally and spatially in lieu of adrenergic ligands. T cells were genetically modified to express a chimeric fusion of the β2-adrenergic receptor and bovine rhodopsin. Optogenetic activation was verified to activate intracellular pathways, and modulate T cell cytokine responses. This tool will allow further study into the role of immune cells as part of neural pathways, and could provide new treatment modalities.

Understanding the interactions of these two systems is vital to the newly-developing field of bioelectronic medicine, which promises to treat disease by modulating electrical signals of the nerves throughout the body. The examples provided herein are important pieces of the overall puzzle that will provide new therapeutic interventions.

Preface

“A person who never made a mistake never tried anything new.”

-Albert Einstein

“The science of today is the technology of tomorrow.”

-Edward Teller

Table of Contents

List of Figures

List of Abbreviations

α7 nAChR	α7 nicotinic acetylcholine receptors
ACh	Acetylcholine
AChE	Acetylcholinesterase
ACK	Ammonium-Chloride-Potassium
ANOVA	Analysis of variance
APC	Antigen presenting cell
B2AR	Beta-2 adrenergic receptor
BCR	B cell receptor
cAMP	Cyclic adenosine monophosphate
CCR	C-C chemokine receptor
CD	Cluster of differentiation
CGRP	Calcitonin gene-related protein (CGRP
ChAT	Choline acetyltransferase
ChR2	Channelrhodopsin 2
CTLA-4	Cytotoxic T-lymphocyte-associated protein 4
CXCR	C-X-C chemokine receptor
DNA	Deoxyribonucleic acid
DRG	Dorsal Root Ganglion
eGFP	Enhanced green fluorescent protein
ELISA	Enzyme-linked immunosorbent assay
eNOS	Endothelial nitric oxide synthase

FcR	Fc receptor
GAD65	Glutamate decarboxylase 65
HR	Heart rate
IAA	Insulin autoantibodies
IACUC	Institutional Animal Care and Use Committee
IgE	Immunoglobulin E
IgG	Immunoglobulin G
IgM	Immunoglobulin M
IFN	Interferon
I.I.	Integrated Intensity
IL	Interleukin
ITAM	Immunoreceptor tyrosine-based activation motif
ITIM	Immunoreceptor tyrosine-based inhibitory motif
KLH	Keyhole-limpet hemocyanin
KO	Knockout
JT_{ChAT}	ChAT-overexpressing Jurkat T cells
L-NAME	L-NG-Nitroarginine methyl ester
L-NMMA	L-NG-monomethyl arginine citrate
LPS	Lipopolysaccharide
MAC	Membrane attack complex
MAP	Mean arterial pressure
MBP	Myelin basic protein
MCP-1	Monocyte chemotactic protein 1
MHC	Major-histocompatibility complex
MOG	Myelin oligodendrocyte glycoprotein

mRNA	Messenger ribonucleic acid
NIH	National Institutes of Health
NO	Nitric oxide
NOD	Non-obese diabetic
OVA	Ovalbumin
PAMPS	Pathogen-associated molecular patterns
PBS	Phosphate-buffered saline
PFC	Plaque-forming cell
PGP9.5	Protein gene product 9.5
PRR	Pattern recognition receptors
SEM	Standard error of the mean
sIgG	Specific immunoglobulin G
TCR	T cell receptor
T_{FH}	T follicular helper cell
TGF-β	Transforming growth factor beta
Th	T helper cell
TLR	Toll-Like Receptor
TNF	Tumor necrosis factor
TRPV1	Transient receptor potential cation channel subfamily V member 1
Wt	Wildtype
ZnT8	Zinc transporter protein

Acknowledgments

I would like to thank Kevin Tracey for his wisdom and guidance through my graduate studies. In addition, I would like to thank my committee for their time and effort.

I wish to thank the following people for their assistance in these studies:

Peder Olofsson, LaQueta Hudson, Tea Tsaava, Mahendar Ochani, Yaakov Levine, Jesse Roth, Yehuda Tamari, Andrew Stiegler, Sébastien Talbot, Maud A. Pascal, Simmie Foster, Clifford Woolf, and Sangeeta Chavan.

I would also like to thank Gary Janssen and Elena Koustova for their early mentorship in my scientific studies.

Vita, Publications and Field of Study

1. William M. Hanes, Peder S. Olofsson, Sébastien Talbot, Tea Tsaava, Mahendar Ochani, Gavin Imperato, Manojkumar Gunasekaran, Yaakov A. Levine, Jesse Roth, Maud A. Pascal, Simmie L. Foster, Ping Wang, Clifford Woolf , Sangeeta S. Chavan, Kevin J. Tracey (2015). **"**Neuronal circuits modulate antigen flow through lymph nodes." (manuscript submitted for publication).

2. Peder S Olofsson, William Hanes, Benjamin E. Steinberg, Michaela Oswald, Mohamed N. Ahmed, Ferenc Szekeres, Maureen A. Cox, Andrea Introini, Cecilia Lövdahl, Shu Fang Liu, Nichol E. Holodick, Thomas L. Rothstein, Sangeeta S. Chavan, Kristina Broliden, Ulf Andersson, Huan Yang, Valentin A. Pavlov, Betty Diamond, Edmund J. Miller, Anders Arner, Peter K. Gregersen, Tak W. Mak and Kevin J. Tracey (2015). "Choline Acetyltransferase+ CD4+ Lymphocytes Are Essential Regulators of Blood Pressure." (manuscript under revision).

3. Hanes, W. M., P. S. Olofsson, K. Kwan, L. K. Hudson, S. S. Chavan, V. A. Pavlov and K. J. Tracey (2015). "Galantamine Attenuates Type 1 Diabetes and Inhibits Anti-Insulin Antibodies in Non-Obese Diabetic Mice." Mol Med. E-pub ahead of print. doi: 10.2119/molmed.2015.00142.

4. Hanes, W. (2007). "Rejection of the Need for Informed Consent in Prostate Tissue Sample Research." Cardozo JL & Gender 14: 401.

5. Koustova, E., P. Rhee, T. Hancock, H. Chen, R. Inocencio, A. Jaskille, W. Hanes, C. R. Valeri and H. B. Alam (2003). "Ketone and pyruvate Ringer's solutions decrease pulmonary apoptosis in a rat model of severe hemorrhagic shock and resuscitation." Surgery 134(2): 267-274.

6. Jaskille, A., H. B. Alam, P. Rhee, W. Hanes, J. R. Kirkpatrick and E. Koustova (2004). "D-lactate increases pulmonary apoptosis by restricting phosphorylation of bad and eNOS in a rat model of hemorrhagic shock." J Trauma 57(2): 262-269.

Chapter 1 – Introduction

For most of history, the link between the nervous and immune systems has been poorly understood, and therefore, largely unexplored. The disciplines of immunology and neuroscience both developed roots in the beginning of the 20th century. Golgi and Ramón y Cajal shared the Nobel Prize in Physiology or Medicine in 1906 for their extensive observation, description, and categorization of neurons throughout the brain. Ilya Mechnikov and Paul Ehrlich shared the same Nobel Prize in 1908 for identifying the cellular and humoral basis of immunity. Since then, both fields developed in parallel, with very little overlap.

Early anatomical studies, beginning with Tonkoff's first description of the presence of nerves in lymphoid organs in 1899 [1]* and continued in the 1960's [2-4], suggested a correlation between the two systems. Synapses were described in close apposition to immune cells, which express receptors for several different neurotransmitters. Finally, in 1995, Linda Watkins established a direct connection between the two systems with the discovery that induction of fever in rodents through administration of intra-abdominal IL-1β requires an intact vagus nerve [5]. Cutting the vagus nerve would lead to an incomplete immune response and no fever. Since this discovery, numerous other examples of immune-nervous interactions have been described [See [6] and below for review].

With further understanding of the complex interactions between the two systems, the complexities of the individual fields may be more fully described. Herein, I reveal novel mechanisms in nervous system regulation of responses to antigen, both in context of antibody production in type I diabetes and antigen

*References are found under Cited Literature, beginning on page 104

trafficking during bacterial infection. I also describe our findings related to a special subset of immune cells serving as interneurons in blood pressure regulation, and a new tool to discover further functions of the subset of T cells.

Introduction to the Immune System

The principal role of the immune system is to prevent and eradicate infections. The immune system consists of two complementary branches; innate and adaptive immunity. Innate immunity refers to host defenses that are constitutively present in healthy individuals, and mediate early responses to block and eliminate microbes. Adaptive immunity responds to specific cues from microbes, and participates in immunological memory, helping to clear recurring infections, and is the basis for vaccination. The following is a brief primer on the immune system; for an in-depth review see [7] or [8].

Innate Immunity

The innate immune system is evolutionarily ancient and provides an initial defensive role against pathogens. It co-evolved along with microbes to protect all manner of multicellular organisms, including plants, worms, and insects. Adaptive immunity did not appear until the jawed invertebrates.

The first line of defense against invading microbes is the barrier established by epithelial cells, such as the skin and mucosal linings. This barrier prevents the entry of bacteria by establishing a physical wall. At the same time, microbes encounter antibodies and enzymes, such as lysozyme and peroxidase, which actively trap and kill the microbes. If microbes do penetrate the initial

defenses, phagocytes, such as neutrophils, macrophages and dendritic cells, and complement proteins serve as the next line of defense.

Phagocytic cells respond to molecular markers of classes of microbes, pathogen-associated molecular patterns (PAMPS) using receptors known as pattern recognition receptors (PRR). When these PAMPS activate receptors on phagocytic cells, they respond by engulfing the microbe (phagocytosis), by secreting proteins, such as defensins and lysozymes that actively kill microbes, and by releasing chemical messengers, such as cytokines and chemokines, that alert and modulate the responses of other cells to the presence of the invading microbes.

A prototypical example of PRRs is the Toll-Like Receptor (TLR) family. Each class of TLR recognizes different types of PAMPs, which allows the cell to respond to different invasive microbes in different manners depending on the activated receptors. For example, TLR-2 binds to the peptidoglycan of Gram-positive bacteria such as streptococci and staphylococci; TLR-3 binds to double-stranded RNA; TLR-4 is activated by lipopolysaccharide. Binding of the pathogen to the TLR initiates signaling pathways which activate transcription factors that then initiate production of proinflammatory cytokines, such as tumor necrosis factor (TNF) and interleukin-1β (IL-1β).

In addition to PRRs, phagocytic cells also respond to antibody-antigen complexes. A surface-bound Fc receptor (FcR) binds to the Fc region of antibodies, which is the non-antigen binding portion. When many of these antibodies are bound to the same antigen, the numerous Fc regions bring together several Fc receptors and enhance intracellular signaling. There are two functionally different classes of FcRs: the activating and inhibitory receptors [9]. For example, FcγRIIB functions as an inhibitory receptor whereas FcγRI positively regulates immune responses. Positive Fc receptor signaling is

propagated by immunoreceptor tyrosine-based activation motifs (ITAM), which are phosphorylated by tyrosine kinases. FcγRI uses an adapter protein, the Fcγ subunit, which possesses this ITAM. This activation can lead to induction of phagocytosis, or release of mediators, such as cytokines and histamine [10]. Negative signaling is mediated by immunoreceptor tyrosine-based inhibitory motifs (ITIM), which utilize phosphatases such as SHIP-1 [11].

Phagocytic cells also serve an important role as antigen-presenting cells. Once pathogens have been phagocytosed, the cell migrates through the lymphatic system to the lymph node. For example, a special class of dendritic cell, the Langerhans cell, resides in the skin, where they take up and process microbial antigens, then travel to the lymph nodes to interact with T cells. Alternatively, some antigen-presenting cells reside in the lymph nodes and capture soluble antigen that travels with the lymph. The antigen-presenting cells degrade the antigen and present it in the context of a membrane bound major-histocompatibility complex (MHC). T cells recognize antigen in these receptors, and become activated, proliferating and releasing cytokines that coactivate other immune cells.

The complement system comprises a group of serum proteins that initiate a cascade effect once activated by binding directly to bacteria or to antibody-antigen complexes. The initiation of this cascade leads to the cleavage or aggregation of several of the proteins in the group. The cleavage products can serve as signaling molecules, drawing immune cells to the site of infection, and enhance phagocytic clearing of microbes. The aggregation products form a membrane attack complex (MAC) which punches holes in the outer membrane of bacteria and virus-infected cells, leading to their destruction.

Adaptive Immunity

The adaptive immune arm complements innate responses and produces specific responses to specific antigens. Adaptive immunity refers to cellular and humoral immune responses to specific antigens. The term antigen refers to a molecule that produces a specific immunological response, as opposed to the generalized responses of the innate system. The adaptive immune system develops specific memories that temper responses to future exposures of the same antigen. The adaptive immune system consists of lymphocytes, including T and B cells and their antibody products.

T lymphocytes play a variety of roles in augmenting and effecting immune responses. T cell responses are driven by activation of the T cell Receptor (TCR), which recognizes antigen presented in the context of MHC. The MHC–bound antigen is the product of intracellular lysis of antigen, and subsequent surface presentation of the MHC-antigen combination. The TCR recognizes a cognate antigen in this context, which initiates intracellular signaling cascades, followed by a subsequent response and clonal expansion. T cell responses are segregated broadly into two separate classes according to the T cell class type; helper and cytotoxic T cells.

Helper T cells express the cluster of differentiation (CD) surface marker CD4. These cells coactivate macrophages to eliminate engulfed microbes, release proinflammatory cytokines like interferon-γ (IFN-γ) and coactivating cytokines that help B cells produce antibodies, including interleukin-4 and -5 (IL4, IL-5). Cytotoxic T cells express CD8, and kill cells that need to be eliminated, such as cells infected with intracellular pathogen and tumor cells. They release cytotoxins

such as perforin, granzymes, and granulysin, which punch holes in plasma membranes and induce caspase cascade that lead to apoptosis.

B cells produce antibodies, which are secreted into the circulation and the mucosa. There, these antibodies can neutralize microbes and microbial toxins, as well as tag the microbes for phagocytosis. The B cell receptor (BCR) bound to the surface of the B cell recognizes specific antigens. When the BCR comes in contact with its cognate antigen, the cell begins to multiply and prepare to make antibodies specific to the antigen that activated the BCR. B cells reorganize their genetic material on the genome level to enhance specificity of the antibodies they produce. In the final stage of differentiation, B cells are known as plasma cells, and release vast amounts of highly specific antibodies.

Immunological memory refers to the acquired immunity after initial exposure to an antigen. Active immunity arises after direct exposure to an antigen through infection or vaccination. Passive immunity arises after transfer of cells or antibodies from an actively immunized individual. The advantage of this immunity is the broad diversity and specificity of responses. The system is able to differentiate between millions of different antigens.

Memory arises after elimination of invading microbes. When a microbe is encountered a second time, there is an accelerated immunological response. Antibodies are formed in only 1-2 days as opposed to the 7-14 days of an initial response. These antibodies are also more specific due to the selection process the B cells underwent. Some of the B and T cells that were activated become long-lived memory cells. When these cells are activated in the future, they respond more rapidly and more specifically than naïve cells. Some plasma cells relocate to the bone marrow and continue secreting antibodies. This is the basis of vaccination and the rapid clearing of infections when the actual microbe was never encountered. This memory process is illustrated in Figure 1 [12].

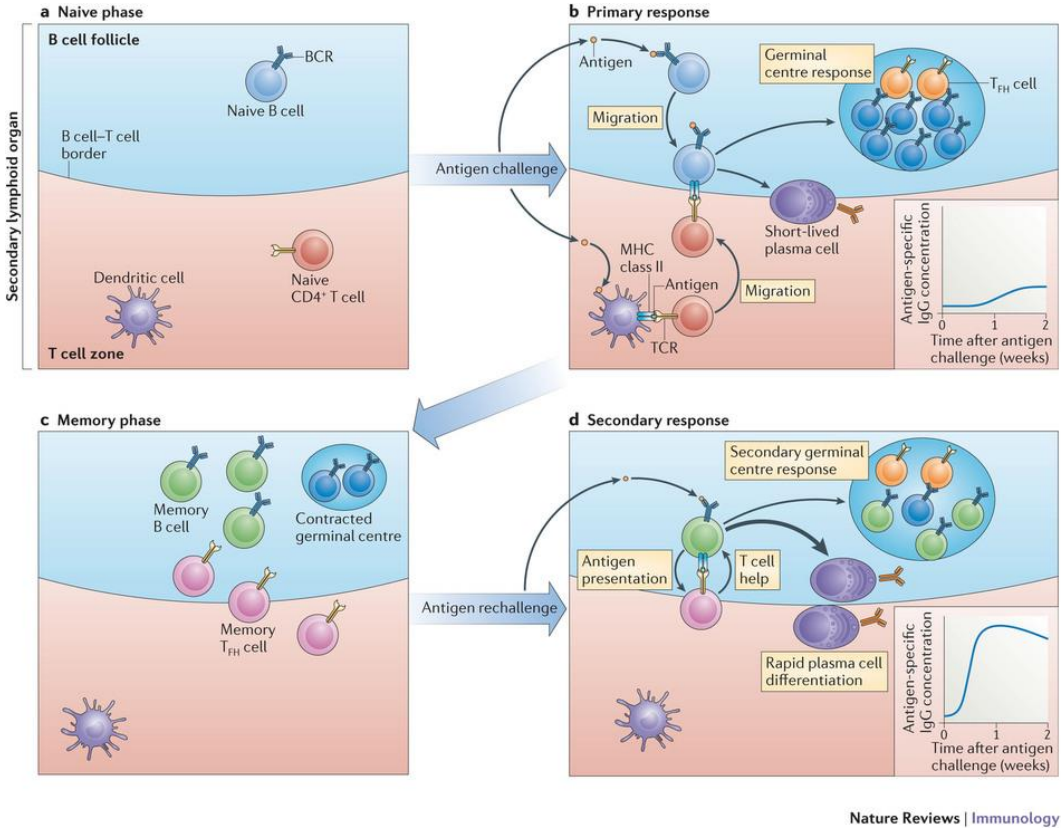

Figure 1 - The memory response in lymph nodes

A) Before antigen challenge, naïve B cells are located in the follicle while T cells are in the paracortical T cell zone. B) After challenge, dendritic cells activate antigen specific T cells, which then migrate toward the B cell follicle. Antigen-specific B cells that encounter antigen also migrate to the border of the T cell zone. There, an interaction between cognate B cells and T cell is formed. From there, some of the activated B cells differentiate into short-lived plasma cells and others develop a germinal center with help from T follicular helper cells (T_{FH} cells). Low levels of antigen-specific IgG antibodies are produced by one week. C) Once antigen is cleared, antigen-specific memory T cells and memory B cells are generated. D) Following antigen rechallenge, memory B cells function as antigen-presenting cells to efficiently present antigens to cognate memory T cells. These memory B cells rapidly differentiate into plasma cells produce high levels of antigen-specific IgG antibodies within a few days.
(Reproduced under license number 3762840509026.)

Lymphatics and Lymph Nodes

Antigens are normally encountered by the immune system in specialized organs called lymph nodes. Antigen is transported to these nodes through the lymphatic system. Fluid from the tissue space in areas such as the skin and parenchymal organs drains into lymphatic capillaries. This interstitial fluid originates from plasma exudate near bed capillary beds and becomes lymph when it enters the lymphatic capillaries. These lymphatic capillaries combine in ever larger lymphatic vessels. Eventually, these vessels reach a lymph node a wherein the lymph enters the subcapsular sinus. The lymph percolates through the lymph node, providing an opportunity for immune surveillance of the tissue microenvironment, as sampled by the draining lymph. The lymph then continues to travel through the lymphatics and through other lymph nodes in a chain. Eventually, the lymphatics come together in the thoracic duct and empty into the bloodstream at the subclavian vein. This system is illustrated in Figure 2.

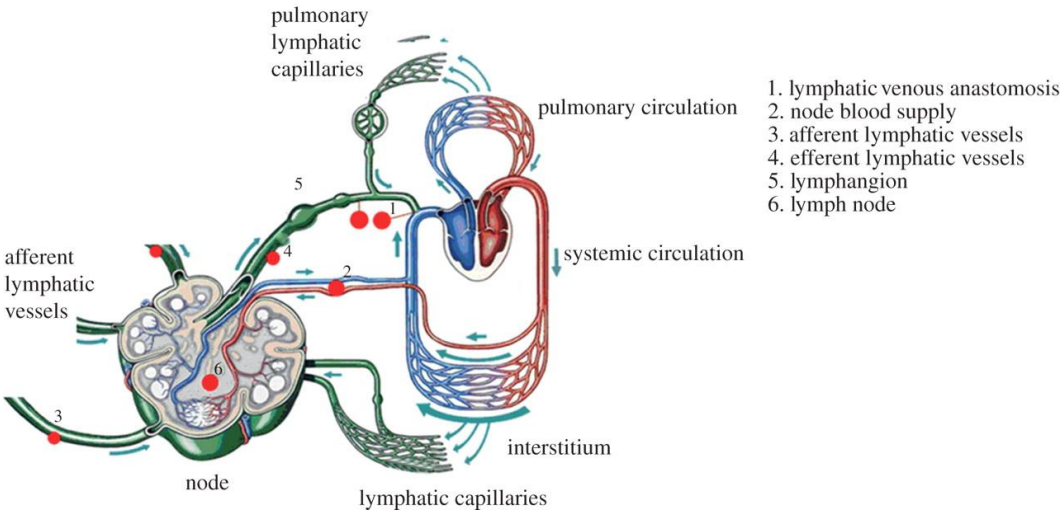

Figure 2 – The lymphatic system

[13] Reproduced under Creative Commons Attribution 4.0 license.

Soluble antigens can enter the lymphatics directly, where they travel with the lymph and can be encountered by immune cells. Alternatively, larger antigens and microbes are ingested by local phagocytic cells, which digest and present the antigen after traveling to the lymph node. Additionally, cytokine markers of inflammation can travel through the lymphatics, alerting distant cells to infection.

Lymph nodes are organized into cell-specific regions. A series of conduits directs lymph throughout the node and is lined with dendritic cells. These dendritic cells constantly sample the lymph and present antigen to T cells. B and T lymphocytes are located in the outer cortex. B cells are found in follicles and form germinal centers after clonal expansion of memory B cells. T cell are found in the cortex as well, but more centrally. Most of these cells are CD4+ve helper T cells that augment responses of B cells and phagocytic cells. Macrophages and plasma cells are found in the inner medulla. The localization of these cells is controlled by local chemokines, which attract different cell types to different regions.

Regulation of the flow of antigen through the lymphatic system has implications in many diseases [14, 15]. In cancer, lymph nodes draining tumor-containing regions are known as sentinel lymph nodes and can be the immune system's first exposure to cancer-related antigens, leading to activation of tumor-killing cytotoxic T-cells [16]. Tumors can also invade the lymphatic system to metastasize to distant locations in the body [16]. In allergy, plasma cells in draining lymph nodes produce IgE, which binds to FcεRI on mast cells. When antigen binding crosslinks these receptors, mast cells degranulate and release histamine, leading to allergic reactions [17]. In autoimmune diseases, antigen again drains to the lymph nodes, and may activate auto-reactive T-helper or B-cells to induce attacks against host tissues. In type I diabetes, self-antigens, such as insulin and glutamate decarboxylase 65 (GAD65) drain from the pancreas to

lymph nodes where autoimmunity is initiated; removal of the pancreatic lymph nodes prevents diabetes in animal models [18]. In rheumatoid arthritis the onset of arthritic flare has been suggested to be related to altered lymphatic flow and volume [19].

Immune System Response Regulation

It is essential that immune responses be tempered to maintain homeostasis. Too little activation can lead to immunosuppression and infection. Too much activation leads to autoimmunity and inflammatory disease. The immune system maintains a series of checks and balances that prevent excessive activation and allow return to base state after an infection is cleared.

A first mechanism of regulation is a series of positive and negative selection steps during lymphocyte development. B and T cells both undergo randomization of the genetic material that encodes their respective receptors. During the maturation process, these cells are tested with antigens while developing in the bone marrow. Cells that respond weakly continue to mature, while cells that activate too strongly, or fail to respond at all, die off. To prevent autoimmunity, cells are then tested with self-antigens in the bone marrow and thymus; any cells that respond to these self-antigens are also killed off.

Another mechanism is the use of costimulatory molecules. When the TCR is activated by MHC-bound antigen, the presence of other costimulatory molecules, such as CD28 binding to B7-1/-2, is necessary. When CD28 is activated, it activates additional signaling pathways within the cell. If CD28 is not activated, the T cell will become anergic and undergo apoptosis. This prevents random activation of circulating T cells.

Self-reactive lymphocytes are also regulated by a class of T cells known as regulatory T cells. These T cells have TCRs that can be self-reactive, and either arise from activation in the thymus or in the periphery. They are characterized by

expression of the transcription factor, FoxP3. When activated, they secrete immunosuppressive signals, such as interleukin-10 (IL-10) and transforming growth factor (TGF-β), which inhibit activation of T cells and macrophages.

When an infection has been resolved, and microbes cleared, the immune system must enter a contraction phase. The antigen that had previously activated the immune system is no longer present, so many of the cells undergo apoptosis and die off. Additionally, cells begin to express coregulatory molecules, such as cytotoxic T-lymphocyte-associated protein 4 (CTLA-4), which competes for CD28 activation. Cells will also express Fas receptor, which induces cell death when its cognate ligand is bound. The cells of the innate system require regular stimulation by PAMPs to maintain activation as well. Once the pathogens are cleared, intracellular signaling mechanisms degrade and return the cells to a basal state.

Neural Regulation of Inflammation

The nervous system regulates mammalian homeostasis by monitoring and modulating organ function. Increasing data have revealed an important role for neural circuits in regulation of the immune system [6, 20-24]. Multiple anatomic connections permit communication between the central nervous system and the immune system [25-27]. Immune cells express a range of receptors for neurotransmitters, including dopamine, ACh, and norepinephrine, which regulate activity and differentiation [28-36].

A prototypical and well-characterized neuronal circuit that controls immune responses is the inflammatory reflex [6, 23, 37]. Invasion and tissue injury are detected by sensory nerves, whereupon immunomodulatory signals originate in the central nervous system and travel through the vagus nerve [38, 39]. These signals travel to the celiac ganglion, then through adrenergic neurons to the spleen, where they terminate adjacent to acetylcholine-producing T cells regulated by β2-adrenergic receptors (β2-AR) [34, 40, 41]. This adrenergic signaling induces acetylcholine release from these T cells, which binds to α7 nicotinic acetylcholine receptors (α7 nAChR) on macrophages [42]. This down-regulates inflammatory cytokine production by Nf-κB signaling suppression [26]. In addition, acetylcholine translocates into the cytoplasm of immune cells during inflammation, where activation of mitochondrial α7 nAchR prevents release of mitochondrial DNA, an NLRP3 ligand, inhibiting inflammasome activation [43].

In addition to the vagus nerve circuit described above, several additional examples of immune control have been described. Vagus nerve stimulation can

modulate and reduce B cell migration and production of antibodies in response to blood-borne streptococci [44] and in type 1 diabetes [45]. Similarly, adrenergic stimulation of the lymph nodes can restrict T cell mobility and suppress inflammation [20]. Nerves have also been shown to respond directly to bacteria, modulating pain and immune responses [46]. Additionally, sensory neurons express functional receptors for antibody-antigen complexes (FcγRI and FcεRI), although their role in physiology has not yet been elucidated [47-50].

The relative paucity of examples of known regulation of immunity is staggering when we consider how much we know about nervous control of all other aspects of physiology. With additional knowledge of neural pathways that regulate immunity, novel therapeutic interventions will be possible.

In Chapter 2, a novel neural reflex circuit is revealed, which regulates antigen flow through peripheral lymph nodes based on immunization status, and offers a potential role for neuronal Fc receptors.

In Chapter 3, a centrally-acting acetylcholine-esterase inhibitor, galantamine, is shown to delay the onset of type 1 diabetes, an autoimmune disease.

Chapter 4 reviews work describing a novel role for acetylcholine-producing T cells in regulation of blood pressure homeostasis.

Chapter 5 describes an optogenetic tool developed to further study the role of β2-AR signaling in acetylcholine-producing T cells.

Chapter 2 – Neuronal Circuits Modulate Antigen Flow through Lymph Nodes

Abstract

After a break in the skin, bacteria can enter and initiate an infection. These bacteria can pass through the lymphatic system, into the bloodstream leading to systemic infection. Depending on immunization status, bacteria are trapped in the initial lymph nodes, or pass through the lymphatics into the bloodstream. Here we describe a role for neurons in the restriction of antigen. Antigen injected into the dorsum of the mouse hind paw flows through the lymphatics to the popliteal lymph node, then to the sciatic node, through the lymphatics to eventually reach the bloodstream. When immunized, flow of fluorescent Keyhole-Limpet Hemocyanin (KLH), through lymph nodes was restricted. Imaging after antigen administration revealed a significant decrease in sciatic KLH levels of immunized mice (naïve 54.34 ± 8.840 versus, immunized 9.730 ± 3.715 $p<0.001$). Blocking neuronal activity with the local anesthetic bupivacaine at the lymph nodes of immunized animals resulted in restoration of antigen flow (saline 31.45 ± 3.759 versus bupivacaine 45.65 ± 5.350, $p<0.05$). Depletion of NaV1.8-sensory neuron populations, induced a similar loss of antigen restriction (control 15.41 ± 3.526 versus NaV1.8-DTA 35.56 ± 6.035, $p<0.05$). Conversely, direct activation of nerve fibers by noninvasive magnetic stimulation resulted in a significant decrease of antigen trafficking compared to

*References are found under Cited Literature, beginning on page 104

sham controls (sham 55.99 ± 4.993 versus magnet 30.87 ± 4.169, $p<0.001$). Skin samples from injection sites of immunized animals showed colocalization of PGP9.5-expressing nerve fiber terminals, FcγRI receptors, and antigen. Additionally, an FcγRI/FcεRI knockout phenotype fails to restrict antigen. Together, these studies reveal a novel neuronal circuit that modulates antigen trafficking through a pathway involving antigen interaction with Fc receptors.

Introduction

The lymphatic system is a series of lymph nodes arranged in a chain, connected by lymphatic vessels. Interstitial fluid from the tissue space drains into the end of these vessels and becomes lymph. This lymph carries substances from the extracellular tissue space to the lymph nodes, where the immune system surveys it and determines whether there are any threats. After a break in the epidermal layer of the skin, bacteria can enter the tissue and initiate an infection. From there, the bacteria multiply and enter the lymphatic system. Lymph ascends into the thoracic duct, providing a conduit for pathogens into the bloodstream, and systemic spread [51-55]. Invading pathogens in lymph nodes are recognized by the host and initiate an immune response.

Antigens from the skin drain into the lymphatic through the lymph, or they are actively transported to the lymph node by dendritic cells after phagocytosis [56]. Soluble antigen traveling with the lymph to the lymph node is captured by antigen-presenting cells (APC) in the node, such as B cells and dendritic cells [57]. These cells line the system of reticular fibers that form conduits [58], which extend into the follicular regions and mediate delivery of small, soluble antigen [59]. APCs then degrade the pathogen and display fragments of antigen to T cells in the context of major-histocompatibility complex II (MHC II) on their surface membrane [60, 61], initiating an antigen-specific T cell activation [62]. While T cells are activated in the by antigen in the context of MHC II, B cells are able to recognize antigen in its native, unprocessed form via their B cell receptor (BCR), a surface-bound immunoglobulin (Ig) receptor [63].

In 1966-67, Nossal, Ada and their colleagues described changes in antigen localization in lymphatic tissue based on immunization status [64-66]. When an animal is immunized, whether by active vaccination or injection of antibodies from an immunized animal, antigen is trapped in the lymph nodes draining the site of injection. If an animal is not immune to the antigen, it moves through the lymphatic system, and from there enters the blood, liver, and spleen [64-66].

Infection is normally accompanied by lymph node swelling and pain, which is driven by neural input. Lymph nodes are innervated by a combination of sympathetic and peptidergic sensory neurons [67]. Tonkoff first described the presence of nerves innervating lymph nodes in 1899 [1]. In the 1980's, several groups utilized electron microscopy to confirm the presence of partially myelinated axons entering the node at the hilar region, as well as potential sensory nerve terminals branching into cortical and paracortical regions, terminating among T lymphocyte regions [25, 27, 68-71]. Noradrenergic fibers enter at the hilus with the vasculature and continue to innervate small vessels, particularly in the medullary region [25]. These fibers also innervate the cortical and paracortical regions, as well as the capsule and associated trabeculae, but not the germinal centers [25]. Dopamine β-hydroxylase-expressing neurons can be detected, but remain mostly with the vasculature [71]. Acetylcholinesterase staining fibers have been detected in lymph nodes, but there is no evidence yet that these fibers are cholinergic [72]. Many neuropeptides have also been detected in lymph nodes, including neuropeptide Y, vasoactive intestinal polypeptide, substance P, and calcitonin gene-related protein (CGRP) [73]. The presence of sensory nerves was first suggested when electron microscopy revealed bundled myelinated axons entering at the hilus in mouse lymph nodes [69]. Characterization of these neurons in canine mesenteric lymph nodes revealed that CGRP binding sites are expressed by trabeculae, arterioles, venules

and 25% of the germinal centers, while substance P receptor binding sites are localized at arterioles and venules in the T cell regions and 25-30% of the germinal centers [27]. Vasoactive intestinal polypeptide binding sites are found at the T cell regions, medullary cords, and 10-20% of germinal centers [27].

Immune cell responses are modulated by the neurotransmitters released by the peripheral terminals of these neurons [6, 28, 44]. Depletion of norepinephrine from lymph nodes with 6-hydroxydopamine resulted in a diminished plaque-forming cell (PFC) response in draining lymph nodes following subcutaneous injection of sheep red blood cells [25]. Activation of lymphocyte β-adrenergic receptors suppresses interleukin 2 receptors T cells, leading to suppressed activation and reduction of proliferation [74]. Activation of β-adrenergic receptors suppresses lipopolysaccharide-induced tumor necrosis factor secretion [75]. Stress-induced epinephrine increases the number of natural killer cells in circulation by reducing adhesion to fibronectin [76]. Activation of lymphocyte β-adrenergic receptors on Th1 cells before activation inhibited IFN-gamma production subsequent IgG2a production by B cells; mouse Th2 cells lack a β-adrenergic receptors [77]. Electrical activation of the vagus nerve reduces B cell antibody production while arresting migration [44]. In T cells, the β2-adrenergic receptor interacts with the chemokine receptors CCR7 and CXCR4, increasing lymph node retention [20]. CGRP stimulates dendritic cells to shift immunity towards type 2 responses immunity [78, 79].

Emerging data uncover a role for sensory neurons in the detection of peripheral pathogenic bacteria and modulation of the subsequent immune response [20, 80]. In *Caenorhabditis elegans*, a nervous system signal regulates epidermal immunity against pathogens by induction of a signal that induces the expression of antimicrobial peptides [80, 81]. In higher mammals, Clifford Woolf and his group demonstrated that neurons in mice can respond directly to bacterial

products, initiating action potentials and inducing pain hypersensitivity while downregulating immune responses.

Neurons express the molecular receptors able to detect antibody-antigen complexes, Fc receptors [82], which could contribute to the detection of immunized antigen. Andoh and Kuraishi first described the high affinity IgG receptor FcγRI, but not the low affinity receptors FcγRII and FcγRIII, on mouse lumbar DRG neurons [47, 83]. Since then, Receptors specific to both IgG (FcγRI) [47] and IgE (FcεRI) [48] have been further described. These functional neuronal Fc receptors induce action potentials and calcium flux in response to antigen-antibody complexes [47-50]. Antigen or antibody alone fail to trigger calcium flux, indicating that only the intact antigen-antibody complex is capable of activating FcγRI on primary sensory neurons[83]. FcγRI is present on both the somata and axons of DRG neurons,[83] and the mRNA expression level of FcγRI observed in superior cervical ganglion neurons is higher than in the bone marrow derived mouse mast cells [49]. The role of these receptors on neurons has been largely undetermined, but it has been speculated that the may play a role in immune complex-mediated pain [50].

Evidence suggests that neuronal input regulates lymph flow and lymphatic contraction [84, 85]. In sheep, both mean arterial pressure and lymphatic flow are increased by a cerebral ischemic response evoked by air injection into the common carotid artery; this effect was blocked by administration of phentolamine, an alpha-adrenergic antagonist [85]. Additionally, lymphatic flow and contraction frequency are increased by injection of intravenous epinephrine and norepinephrine [86], as well as by electrical stimulation of the lumbar sympathetic chain [84].

Recent work has focused on specific cellular interactions with antigen within an individual lymph node [52, 59, 87-90]. Despite the important finding of

a nerve-mediated regulation of lymphocyte cell trafficking [20, 76], whether the nerve fibers innervating the lymph node regulate the trafficking of antigen through the lymphatic system is unknown. Here, we explore this and show that sensory and motor nerves do regulate antigen trafficking through distal to proximal lymph nodes. This neuronal control of alteration of lymphatic trafficking provides a new way for bioelectronic intervention to modulate immune function.

Methods

Animals

Balb/c, B6.129P2-Gt(ROSA)26Sor$^{tm1(DTA)Lky}$ **(**DTA), B6.129-Trpv1$^{tm1(cre)Bbm}$ (TRPV1-cre), and B6;129P2-Fcer1g^{tm1Rav} (FcR KO) mice were obtained from Jackson Laboratories. Nav1.8-Cre [91] mice were a gift to Dr. Woolf from R. Kuner (University of Heidelberg). Nav1.8-Cre$^{+/-}$ mice were bred with C57BL/6 DTA$^{+/+}$ mice to generate nociceptor-deficient Nav1.8-Cre$^{+/-}$/DTA$^{+/-}$ and control littermates (Nav1.8-Cre$^{-/-}$/DTA$^{+/-}$). TRPV1-Cre$^{+/-}$ mice were bred with C57BL/6 DTA$^{+/+}$ mice to generate TRPV1-Cre$^{+/-}$/DTA$^{+/-}$ and control littermates (TRPV1-Cre$^{-/-}$/DTA$^{+/-}$). Food and water were available ad libitum. Mice were used in subsequent experiments after at least a 14 day-adaptation period. All procedures were performed in accordance with the National Institutes of Health (NIH) Guidelines [92] under protocols approved by the Institutional Animal Care and Use Committee (IACUC) of the Feinstein Institute for Medical Research.

Antigen Labeling

Keyhole limpet hemocyanin (KLH, Calbiochem) or ovalbumin (OVA, Sigma-Aldrich) were diluted to 1 mg/mL with phosphate-buffered saline (PBS), then potassium phosphate, dibasic, pH 9.0 was added to 0.1M final concentration. 0.5 mg IrDye (800CW-NHS ester or 680LT-NHS ester, Licor) or Alexa Fluor® 647 NHS Ester (A647, Thermo Fisher Scientific) was added for each 25 mg protein. 1 mL aliquots were incubated at 20C with 300 RPM shaking for 2 hours.

Free label was separated by centrifugation through PBS-washed Zeba spin desalting columns (Thermo Fisher Scientific). Dye-labeled antigens were concentrated with 100K (KLH) or 30K MWCO (OVA) spin columns (Millipore).

Gel Electrophoresis

Labeled antigens were loaded on NuPAGE 4-12% Bis-Tris Gels (Invitrogen) with NuPAGE MOPS SDS Running Buffer and run according to manufacturer's instructions, 50 minutes at 200 constant volts. Gels were extracted from cassettes and imaged directly on an Odyssey infrared imager (Licor).

In situ Antigen Imaging

20 ul of 100 ug labeled antigen was injected subcutaneously into the dorsum of the hind paw with an insulin syringe. After the predetermined time, the animal was euthanized using carbon dioxide, the skin over the area of interest was removed, and the animal was placed in a supine position in an Odyssey infrared imager. To image lymph node antigen content, sciatic and popliteal lymph nodes were surgically removed and placed into black, clear-bottomed 96-well plates filled with T-per (Thermo Fisher Scientific). These plates were imaged on the Odyssey imager. Images were analyzed using Image Studio software (Licor). All units reported as Antigen Signal are equivalent to the normalized Integrated Intensity (I.I.) reported by the software.

Immunization

Unlabeled antigen (100ug) and 50% Imject alum (Thermo Fisher Scientific) in 200 ul 0.9% saline was injected intraperitoneally. Two weeks later, animals were injected again with the same solution as a booster. Two weeks after the booster injection, animals were used for experiments. Control animals received injections of 50% alum in saline.

Antigen-specific Antibody Titer

High-binding 96-well microplates (Corning) were coated using 20ug/mL KLH in phosphate-buffered saline (PBS), and incubated overnight at room temperature. The following day, the plates were washed with PBS + 0.01% Tween20 and blocked with 1 mg/mL bovine serum albumin in PBS. Serum from immunized animals was obtained by cardiac puncture followed by centrifugation at 2,000 x g for 10 minutes. Serum was diluted 1:100-1:10,000 with PBS and 100 ul per sample added to washed and blocked plates. Plates were incubated for 2 hours followed by incubation with 1:2000 sheep-derived anti-mouse IgM-HRP (BD) or anti-mouse IgG (Amersham) for 2 hours. Plates were washed a final time, developed using Opt-EIA (BD), and the reaction stopped with H_2SO_4.

Nerve Block

Mice were immunized with 100ug antigen and 50% Imject alum in 200 ul saline injected intraperitoneally twice, two weeks apart. Two weeks after the second injections, 25 ul bupivacaine (0.375%, APP Pharmaceuticals) or 0.9% saline was injected at the sciatic nerve and the femoral nerve of the hind leg. 20 minutes after the initial injection, animals were injected with labeled antigen in

the dorsum of the hind paw. After one hour, animals were euthanized and imaged.

Electrical Nerve Stimulation

Mice were anesthetized using isoflurane in a prone position. A 28 gauge, uncoated grounding electrode (Technomed) was placed subcutaneously at the top of the thigh, and a coated needle electrode (Alpine Biomed) was inserted by the popliteal lymph node. Stimulation delivered by a Biopac stimulation module controlled with AcqKnowledge 4.1 software. Parameters were -5V constant, 0.75 msec pulse duration, 20 Hz (50 msec period). Stimulation was applied for five minutes; after the first minute, KLH-800CW was injected into the dorsum of the hind paw. Mice were allowed to awake, then euthanized and imaged after one hour.

Magnetic Nerve Stimulation

Mice were anesthetized using isoflurane in a prone position. Magnetic stimulation administered using an MC-B35 butterfly coil driven by a MagPro stimulator (Magventure) aimed at the popliteal and sciatic lymph nodes. The parameters used were: 50% power, 120 pulses (2 Hz, 60 s) train 1, 1 s train interval. Control animals were anesthetized and the magnetic coil was positioned, but no current applied. Immediately after stimulation, mice removed from the table, then KLH-800CW was injected into the dorsum of the hind paw. Mice were allowed to awake, then euthanized and imaged after one hour.

Passive Immunization

Naïve Balb/c mice were injected intraperitoneally with 100 ug rabbit polyclonal anti-ovalbumin antibody (Millipore). After 24 hours, mice were injected with OVA-800CW or KLH-800CW subcutaneously in the dorsum of the hind paw. After one hour, mice were euthanized and imaged.

Tissue Staining

Mice were immunized with 100ug antigen and 50% Imject alum in 200 ul saline injected intraperitoneally twice, two weeks apart. Two weeks after the second injection, mice were injected with KLH-A647 in the dorsum of the hind paw. After one hour, skin around the injection site was excised, frozen in optimal cutting temperature (OCT) media (Tissue-Tek), sliced at 10 μm, and mounted on Superfrost/Plus slides (Fisher Scientific). Sections were blocked with 5% goat serum, and rat anti-CD16/CD32 (BD Biosciences). Sections were then stained for 1 hour with rabbit anti-PGP9.5 (EMD Millipore) and mouse anti-CD64 (Biolegend, clone X54-5/7.1). Secondary antibodies were goat anti-mouse IgG-Dylight 550 and goat anti-rabbit IgG-Dylight 488 (Thermo Fisher Scientific). Images were obtained on a FluoView FV300 laser-scanning confocal microscope (Olympus).

Statistics

Antigen concentration compared to fluorescence and *in situ* compared to in plate fluorescence were analyzed by linear regression. Control and experimental popliteal and sciatic lymph node signals were individually analyzed by unpaired student's *t*-test. Antigen concentration curves and Control-TRPV1-$Na_V1.8$lymph node fluorescence were analyzed by one-way ANOVA followed by Bonferroni post-test. All tests with a *P* value of less than .05 were considered

statistically significant. Statistical analyses were performed using Graphpad Prism 6 software. Unless otherwise stated, all numbers are given as average ± standard error of the mean. 'n' represents the number of mice used in each group. In graphs, "*" indicates $p<0.05$, "**" indicates $p<0.01$, "***" indicates $p<0.001$, and "****" indicates $p<0.0001$.

Results

Antigen flow through the lymphatic chain can be monitored with infrared fluorescent dye-labeled antigen.

To monitor antigen localization and concentration in the peripheral lymphatic tissue, we utilized antigens linked to near infrared fluorescent dyes. This allowed imaging of whole animals using a Licor Odyssey flatbed imager with low background and relatively high resolution, *in situ*, giving a view of the involved lymphatic system as a whole. To validate this method, we first ran a range of concentrations of dye-labelled antigen on a polyacrylamide gel. After imaging the gel on a Licor Odyssey infrared plate imager, a linear correlation between antigen concentration and fluorescent signal was found (Figure 3A-B). When a range of concentrations of labeled antigen was injected in the dorsum of the hind paw of a mouse, a dose-dependent fluorescent antigen signal could be detected from the foot, to the popliteal lymph node (Figure 3C), to the sciatic lymph node (Figure 3D), then up the rest of the chain of lymph nodes (not shown). The lymph nodes were extracted and imaged in a 96-well plate, and a similar dose-dependent fluorescent signal was observed in the popliteal (Figure 1E) and sciatic lymph nodes (Figure 3F). A linear correlation with an R-squared value of 0.7634 was found between the *in situ* fluorescent signal and the signal in the 96-well plate (Figure 3G). These data indicate that fluorescently labeled antigens can be used to monitor the localization and concentration of an immunized antigen in the lymphatic system.

Antigen flow through peripheral lymph nodes is restricted in immunized animals

To determine the effects of vaccination on antigen trafficking, unlabeled antigen with alum as an adjuvant was injected intraperitoneally into mice, twice, two weeks apart to immunize the animals to the antigen. Two weeks after the second injection, KLH-800CW was injected into the dorsum of the hind paw. In mice immunized to the antigen, the flow of that antigen was restricted. Specifically, the fluorescent antigen signal was significantly reduced in the sciatic lymph node (naïve, 54.34 ± 8.840, n=5 versus KLH-immunized, 9.730 ± 3.715, n=5, $p<0.001$ by t-test) (Figure 4A-B). This indicates a restriction of antigen flow through the lymphatic system.

Next, we assessed the specificity of antigen restriction by subjecting KLH immunized mice to OVA-680LT challenge. In animals immunized against KLH, OVA was not restricted (Figure 4C, third panel, OVA in red), but immunization with OVA led to subsequent restriction of OVA (Figure 4C, fourth panel, OVA in red). Therefore, an antigen-specific "memory" leads to the subsequent restriction of the same antigen. To determine the durability of the "memory," mice were injected with labeled antigen at various times after the booster injection, up to 17 weeks later. We observed that the amount of antigen in the sciatic lymph node remained lower in immunized animals for at least 17 weeks after a booster (Figure 4D).

Antigen flow restriction is dependent on sensory neural innervation of the lymph node.

Lymph nodes are innervated by a variety of neural fibers. To investigate if neuronal input from the lymph node contributes to the restriction of antigen, neuronal activity was blocked using bupivacaine, a sodium channel blocker that

inhibits action potentials. Animals were immunized with intraperitoneal injections of KLH with 50% alum twice, two weeks apart. Two weeks after the second injection, bupivacaine was injected in close proximity to the sciatic and femoral nerves, the main nerves innervating the leg. In control animals, the same volume of saline was injected at each location. Blocking of the nerves in immunized mice was sufficient to increase antigen signal in the sciatic lymph node (Figure 5A-B) (saline, 31.45 ± 3.759, n=10, and bupivacaine, 45.65 ± 5.350, n=9, $p<0.05$ by t-test).

Bupivacaine has a short half-life and may incompletely penetrate the thick sciatic and femoral nerve bundles at the doses given. Therefore, to complement these findings we used utilized a genetically-driven sensory neuron-depletion model. $Na_V1.8$-expressing nociceptive neurons mediate neurogenic inflammation [22] and neuronal responses to bacterial infections [46]. In the $Na_V1.8$-cre/DTA mouse, Nav1.8-expressing cells also express diphtheria toxin (DTA), effectively ablating the $Na_V1.8$ population [46, 93]. $Na_V1.8$-Cre/DTA and littermate controls were immunized with KLH as described above, and when KLH-800CW was injected into the dorsum of the hind paw, increased amounts of antigen were observed compared with control mice in the sciatic lymph nodes (Figure 5C-D) (control, 15.41 ± 3.526, n=13 versus $Na_V1.8$-DTA, 35.56 ± 6.035, n=16, $p<0.05$ by t-test). No difference was observed in naïve $Na_V1.8$-DTA mice, compared with controls (data not shown). Additionally, serum IgG and IgM levels against KLH were similar in $Na_V1.8$ and control mice, suggesting that these animals were not merely immunocompromised (Figure 6). These data collectively suggest that sensory neurons contribute to the observed restriction of immunized antigen flow.

A subset of $Na_V1.8$-expressing nociceptive neurons also express transient receptor potential channel vanilloid 1 (TRPV1), which mediates the pain and sensations associated with capsaicin and heat. These capsaicin-sensitive neurons

have been implicated in neuronal responses to infectious bacteria [46]. To determine the contribution of TRPV1-expressing neurons to immunized-antigen restriction, these neurons were depleted by generating mice that express DTA in TRPV1+ neurons. After TRPV1-depleted mice were immunized with KLH and alum, KLH-800CW was injected in the dorsum of the hind paw and the mice were imaged after one hour. $Na_V1.8$-DTA and littermate controls were also included as controls. Surprisingly, the increase in antigen seen in $Na_V1.8$-DTA mice was not recapitulated in TRPV1-DTA mice in the sciatic lymph node (Figure 5E) (control, 6.783 ± 1.290, n=9; TRPV1-DTA, 6.345 ± 1.547, n=10; and $Na_V1.8$-DTA, 43.93 ± 15.57, n=6, $p<0.001$ by one-way ANOVA Bonferroni post-test). This suggests that a $TRPV1^{neg}$ $Na_V1.8$+ population is required for antigen restriction.

Induction of neuronal activity initiates a reduction in antigen flow

To determine the role of nerve fibers innervating the lymph nodes in restriction of antigen flow, the femoral and sciatic nerves were electrically stimulated in the popliteal fossa. A monopolar needle electrode was inserted adjacent to the popliteal lymph node of anesthetized animals and electrical current (-5V constant, 0.75 msec pulse duration, 20 Hz) was applied to stimulate the local neurons. In sham animals, a needle electrode and grounding electrode were inserted, but no current applied. After stimulation, KLH-800CW was injected into the dorsum of the hind paw. In electrically stimulated animals, lower levels of antigen were seen in the sciatic lymph nodes (sham, 114.1 ± 16.17, n=5 versus electrically stimulated, 56.76 ± 14.38, n=5, $p<0.05$ by t-test) (Figure 7A-B).

Next we stimulated the nerve fibers in the adjacent to the popliteal lymph node noninvasively. We administered a time-varying magnetic field with an electromagnetic coil directed to the hind leg of anesthetized naïve mice, followed

by injection of KLH-800CW. Sham animals were anesthetized and the coil positioned, but no current applied. In magnetically stimulated animals, lower levels of antigen were seen in the sciatic lymph nodes compared to sham stimulated animals (sham stimulated, 55.99 ± 4.993, n=10, versus magnetically stimulated, 30.87 ± 4.169, n=12, $p<0.001$ by t-test) (Figure 7C-D).

Together, these findings indicate that activation of neuronal signals is sufficient to regulate antigen flow.

Neuronal Fc receptors play a role in antigen restriction.

When an animal is immunized against an antigen, this results in production of antibodies specific to this antigen. Because antigen restriction occurs only when an animal has been immunized against an antigen, it is plausible that antibody-antigen interactions may underlie the restriction mechanism. To determine whether the presence of antibodies alone would be sufficient to activate restriction of antigen, passive immunization model was utilized. Polyclonal anti-OVA antibodies from rabbit was injected intraperitoneally into naïve mice, and 24 hours later OVA-800CW or KLH-800CW was injected in the dorsum of the hind paw. The amount of OVA antigen in the sciatic lymph nodes was significantly decreased compared to KLH (KLH, 32.95 ± 7.741, n=10 versus OVA, 6.483 ± 1.461, n=9) (Figure 8A).

To determine the role of Fc receptors in antigen restriction in immunized mice, naïve and KLH immunized Balb/c and FcR KO mice were injected subcutaneously in the hind paw with KLH-800CW. No difference was seen in antigen signals of naïve Balb/c and FcR KO mice in the sciatic lymph node (Balb/c, 62.50 ± 5.614, n=8 versus FcR KO, 71.48 ± 8.197, n=6) (Figure 9). When mice were immunized, more antigen was seen in the lymph nodes of FcR

KO mice in sciatic lymph nodes (Balb/c, 15.76 ± 2.721, n=10 versus FcR KO, 44.29 ± 6.500, n=11, $p<0.001$ by t-test) (Figure 8B). Moreover, in mice immunized with KLH, antigen and Fc receptors colocalize on PGP9.5+ve nerve fibers at the site of injection. (Figure 8C).

These data suggest that Fc receptors are a necessary component of the restriction of immunized antigen and this may be mediated by expression of the receptors on nerve fibers.

Discussion

In the present study, we have generated evidence for neuronal involvement in the regulation of antigen flow through peripheral lymph nodes (Figure 10). In this novel neural circuit, immunized antigen is distinguished from naïve antigen by TRPV1^{neg} $Na_V1.8$+ neurons, which generate a response signal, leading to restriction of antigen flow from lymph node A to lymph node B (e.g., popliteal to sciatic lymph node). The restriction of antigen can be reduced by nerve blockade and activated by nerve stimulation.

From an evolutionary standpoint, this circuit provides a way for the nervous system to rapidly detect invading microorganisms, discern which may be pathogenic, and limit their spread through the lymphatic system by quarantining the offensive organism to the site of invasion. The nervous system may also mediate additional actions that activate the immune system, perhaps increasing circulation of neutrophils and memory lymphocytes such that they would be more likely to encounter their respective antigens. Trapping of the antigen in the draining lymph nodes also provides additional opportunity for antigen presentation to circulating lymphocytes, increasing the chances of effective immune activation.

The mechanism for restriction of the antigen at a molecular level remains to be elucidated. Control of lymphocyte egress from lymph nodes has been shown to be modulated by lymphocytic β_2-adrenergic receptor signaling [20]. Additionally, neutrophils have been described as trafficking to lymph nodes

in response to infection [94-96]; and a neuronal control may be involved in this phenomenon

Once bacteria enter the broken skin, they can travel through the lymphatic system, eventually becoming a systemic infection. As small molecules such as KLH and OVA can be stopped from progressing through the lymphatics after neuronal stimulation, it plausible that bacteria could also be halted and this now needs to be examined. If so, electrical stimulation of the innervating nerve fibers of the draining lymph node soon after a penetrating injury may prevent bacteremia and sepsis.

Cancers, especially carcinomas, can metastasize to new locations through the lymphatic systems [97-99]. Many therapeutic courses involve lymphatic mapping to determine the lymph nodes draining the site of a primary tumor [100-104]. These lymph nodes are then monitored for development of new micrometastases. It will be interesting to see if trafficking of these micrometastases could also be halted through neuronal stimulation, halting the spread of secondary tumors.

This antigen-restriction neuronal circuit we define opens therefore, additional important areas of study. While expression of the Fc receptor on neurons has been described and its activation is capable of inducing action potentials and calcium flux, little is known about the mechanisms connecting the initial activation of the receptor and any downstream membrane potential changes. Molecular analysis of the components of this pathway could provide important insight into the role of neurons in the modulation of immune responses. Additionally, the exclusion of TRPV1+ve neurons as essential in this pathway is somewhat surprising, as this nociceptor subset comprises the vast majority of the NaV1.8+ve neurons, and is well-characterized. This nevertheless provides

incentive to study the role and function of the TRPV1negNav1.8+ve population, about which less is known.

The discovery and characterization of a novel neural circuit where sensory nerve fibers regulate antigen trafficking through distal to proximal lymph nodes provides additional insight into the complex and dynamic interplay between the nervous and immune systems. Much work remains to be done regarding the characterization of the sensory signal, the mechanism of the restriction and its implications for pathogen spread, and raises the question what other effects the nervous system may impose on the immune system in response to detection of dangerous antigens.

This chapter has focused on a newly discovered neural circuit capable of modulating antigen trafficking, and has been the focus of much of my work. The following chapters outline other examples of neural control of immune responses that I have investigated. These include the use of a neuromodulatory drug to delay the onset of type 1 diabetes in a mouse model, a new role for T cells as interneurons in the regulation of blood pressure, and a tool for studying the temporal and locational effect of neurotransmitters on T cell responses.

Figures

A

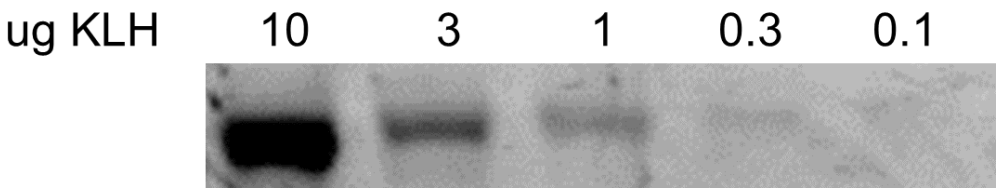
ug KLH
10
3
1
0.3
0.1

B

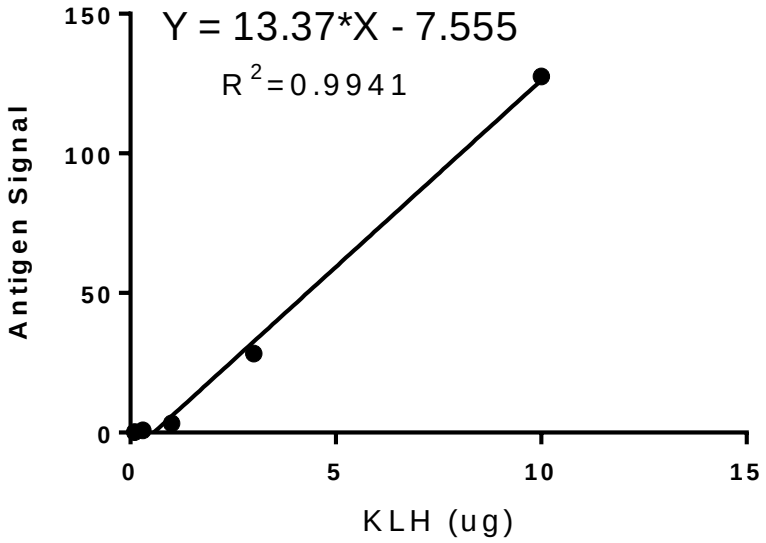
Y = 13.37*X - 7.555
R 2=0.9941
Antigen Signal
150
100
50
0
0
5
10
15
KLH (ug)

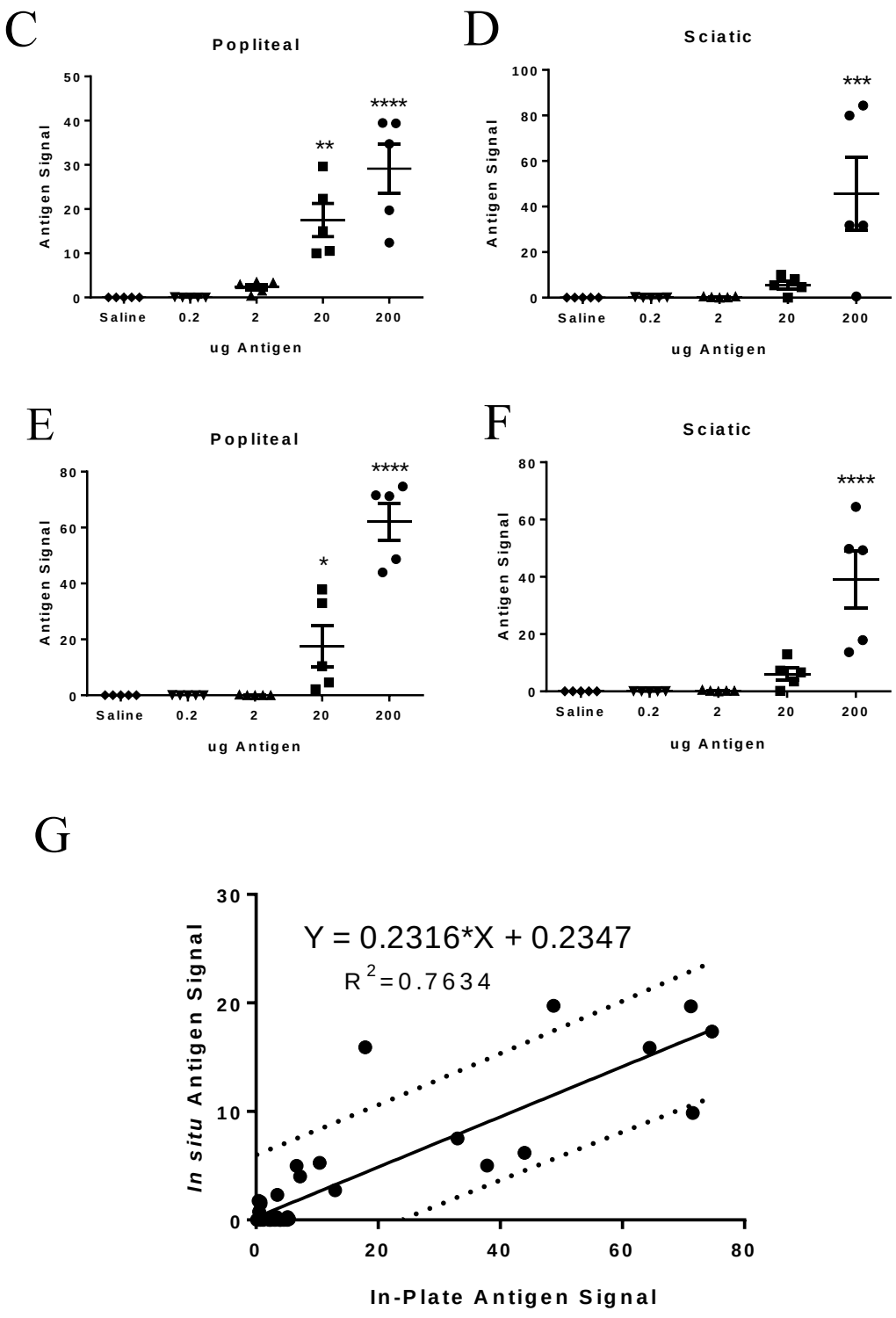
C
Popliteal
Antigen Signal
50
40
30
20
10
0
**
****
Saline
0.2
2
20
200
ug Antigen
D
Sciatic
Antigen Signal
100
80
60
40
20
0
***
Saline
0.2
2
20
200
ug Antigen
E
Popliteal
Antigen Signal
80
60
40
20
0
*
****
Saline
0.2
2
20
200
ug Antigen
F
Sciatic
Antigen Signal
80
60
40
20
0
****
Saline
0.2
2
20
200
ug Antigen
G
Y = 0.2316*X + 0.2347
R 2=0.7634
In situ Antigen Signal
30
20
10
0
0
20
40
60
80
In-Plate Antigen Signal

Figure 3 - Antigen flow through the lymphatic chain can be monitored with infrared fluorescent dye-labeled antigen.

Keyhole limpet hemocyanin (KLH) was labeled with 800CW infrared fluorescent dye (KLH-800). A) Decreasing amounts of KLH-800 were electrophoretically run on a polyacrylamide gel, then imaged on an Odyssey infrared imaging system. Image is a representative gel of two separate experiments. B) A linear correlation was found between amount of KLH-800 and the measured fluorescent signal intensity. C-D) Increasing amounts of KLH-800 were injected into the subcutaneous dorsum of the hind foot of a Balb/c mouse. When the whole mouse was imaged after one hour, increasing amounts of KLH-800 correlated with an increasing fluorescent signal located at both the popliteal (C) and sciatic (D) lymph nodes, as well as the ratio of sciatic to popliteal signal, an approximation of flow. Data represent means ± SEM, n=5 per concentration. A similar increase in signal was observed in E) popliteal and F) sciatic lymph nodes extracted from mice injected with increasing amounts of KLH-800 and minced into T-Per. Data represent means ± SEM, n=5 per concentration. G) A linear correlation was found between *in situ* signal and in-plate signal with an R-squared value of 0.7634. The dotted line indicates the 95% prediction band.

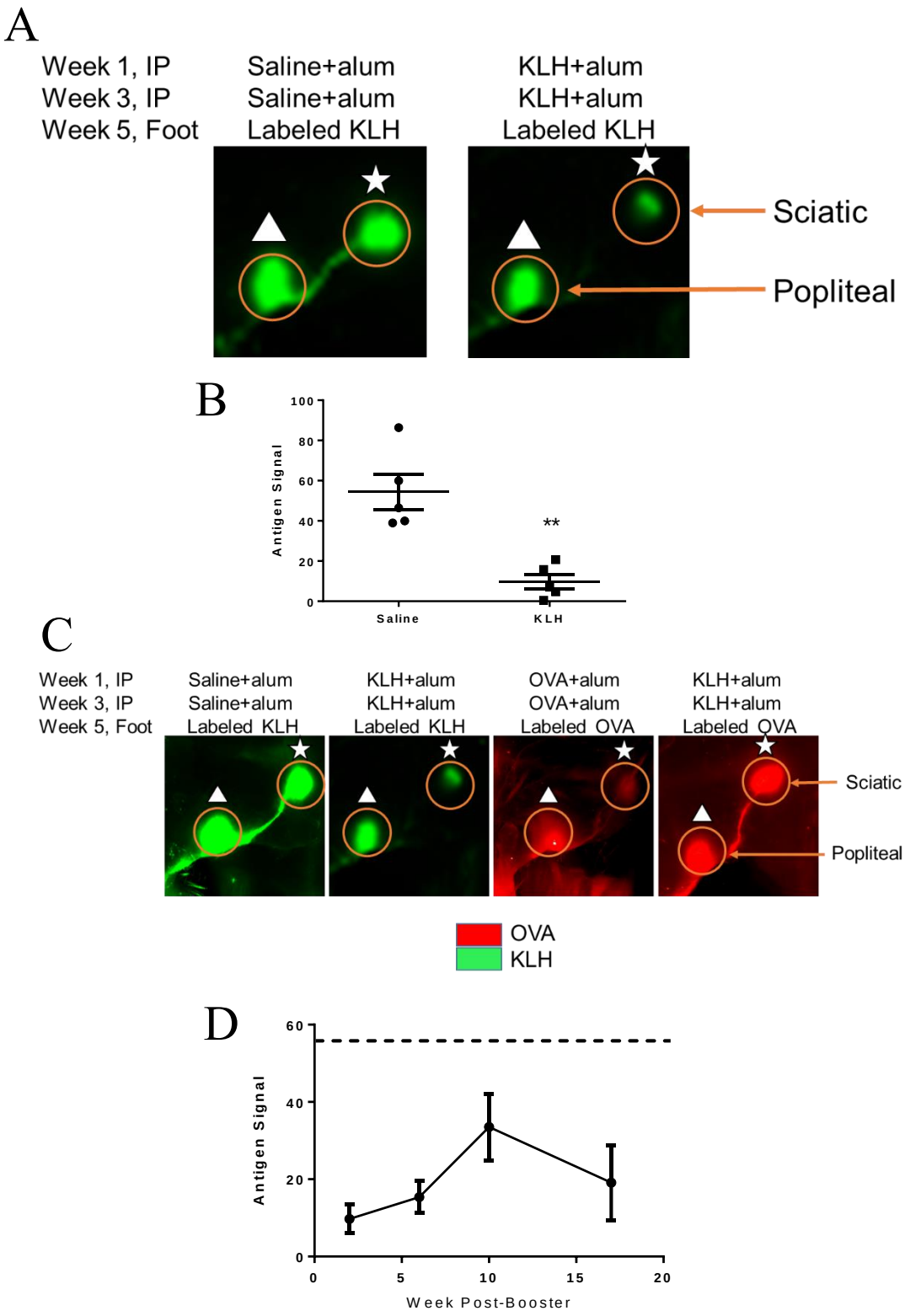
A
Week 1, IP
Week 3, IP
Week 5, Foot
Saline+alum
Saline+alum
Labeled KLH
KLH+alum
KLH+alum
Labeled KLH
Sciatic
Popliteal
B
Antigen Signal
100
80
60
40
20
0
**
Saline
KLH
C
Week 1, IP
Week 3, IP
Week 5, Foot
Saline+alum
Saline+alum
Labeled KLH
KLH+alum
KLH+alum
Labeled KLH
OVA+alum
OVA+alum
Labeled OVA
KLH+alum
KLH+alum
Labeled OVA
Sciatic
Popliteal
OVA
KLH
D
Antigen Signal
60
40
20
0
0
5
10
15
20
Week Post-Booster

Figure 4 - Antigen flow is restricted in mice immunized to the antigen.

A-B) Mice were immunized biweekly with intraperitoneal injections of KLH and alum or saline and alum. Two weeks after the second injection, 200 ug of KLH-800CW was injected into the subcutaneous dorsum of the foot. When the whole mouse was imaged after one hour (A), a lower antigen signal was observed in the sciatic lymph node of KLH-immunized mice compared to naïve mice (B) (naïve, 54.34 ± 8.840, n=5 versus KLH-immunized, 9.730 ± 3.715, n=5, $p<0.001$ by t-test) A) Images are representative; triangles indicate popliteal lymph nodes while stars represent sciatic lymph nodes. B) Data shown are individual values. C) This effect was specific to the immunized antigen, as OVA signal injected in a mouse immunized to KLH was not reduced, but OVA injected into OVA-immunized mice was reduced. Images are representative of five animals per group. D) Antigen signal in the sciatic lymph node remained lower in mice injected in the foot for at least 17 weeks after booster injection. Data represent means ± SEM. Dotted line indicates average naïve mouse antigen signal. n=5 to 8.

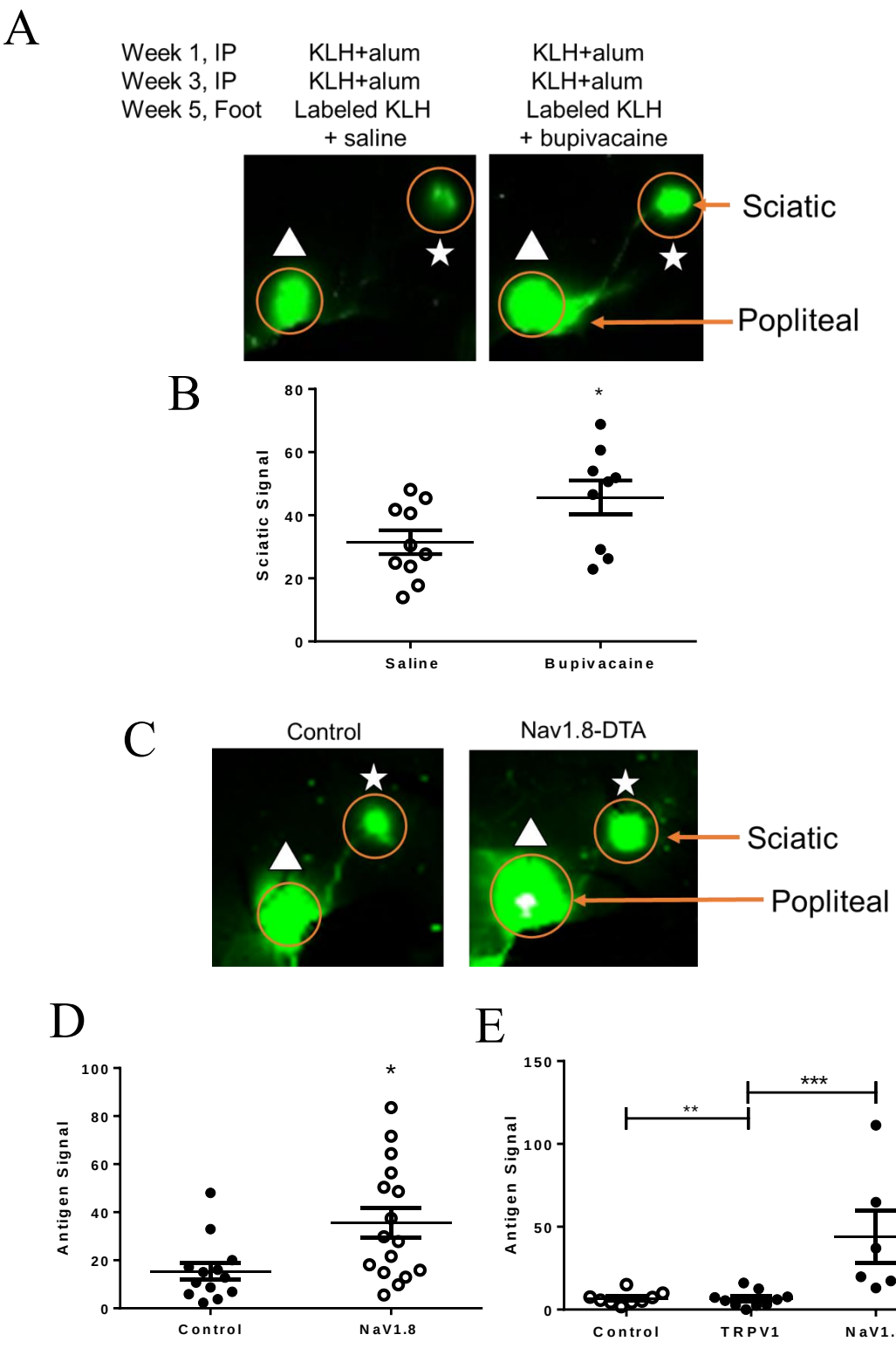
A
Week 1, IP
Week 3, IP
Week 5, Foot
KLH+alum
KLH+alum
Labeled KLH
+ saline
KLH+alum
KLH+alum
Labeled KLH
+ bupivacaine
Sciatic
Popliteal
B
Sciatic Signal
80
60
40
20
0
*
Saline
Bupivacaine
C
Control
Nav1.8-DTA
Sciatic
Popliteal
D
Antigen Signal
100
80
60
40
20
0
*
Control
NaV1.8
E
Antigen Signal
150
100
50
0
**
***
Control
TRPV1
NaV1.8

Figure 5 - Antigen flow restriction is dependent on neural input.

A-B) Mice immunized with KLH were injected with bupivacaine at the femoral and sciatic nerves. When mice were imaged (A), an increase in antigen signal was seen in (B) in the sciatic lymph nodes of mice administered a nerve block (saline, 31.45 ± 3.759, n=10, and bupivacaine, 45.65 ± 5.350, n=9, $p<0.05$ by t-test). A) Images are representative; triangles indicate popliteal lymph nodes while stars represent sciatic lymph nodes. B) Data shown are individual values. C-D) $Na_V1.8$-DTA mice were immunized with KLH. When compared to littermate controls (C), higher levels of KLH-800CW were found in the sciatic lymph nodes (D) (control, 15.41 ± 3.526, n=13 and $Na_V1.8$-DTA, 35.56 ± 6.035, n=16, $p<0.05$ by t-test). C) Images are representative; triangles indicate popliteal lymph nodes while stars represent sciatic lymph nodes. D) Data shown are individual values. E) Immunized TRPV1-DTA, $Na_V1.8$-DTA and littermate control mice were injected with KLH-800CW in the hind paw. The increase in antigen seen in $Na_V1.8$–DTA mice was not recapitulated in TRPV1-DTA mice in the sciatic lymph node (control, 6.783 ±1.290, n=9; TRPV1-DTA, 6.345 ± 1.547, n=10, and $Na_V1.8$-DTA, 43.93±15.57, n=6, $p<0.001$ by one-way ANOVA Bonferroni post-test). Data represent individual values and means ± SEM.

A

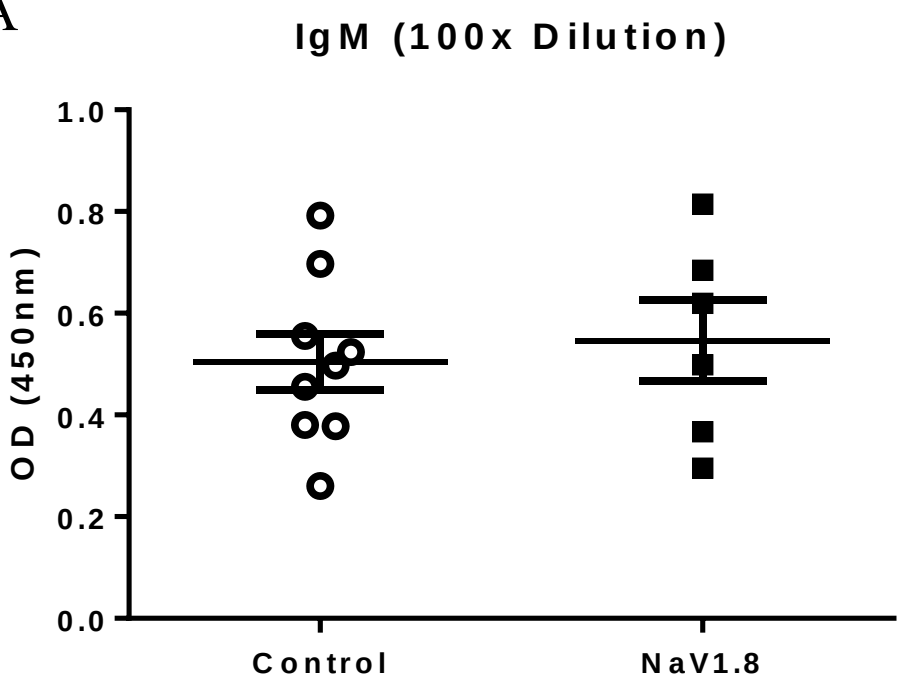
IgM (100x Dilution)
OD (450nm)
1.0
0.8
0.6
0.4
0.2
0.0
Control
NaV1.8

B

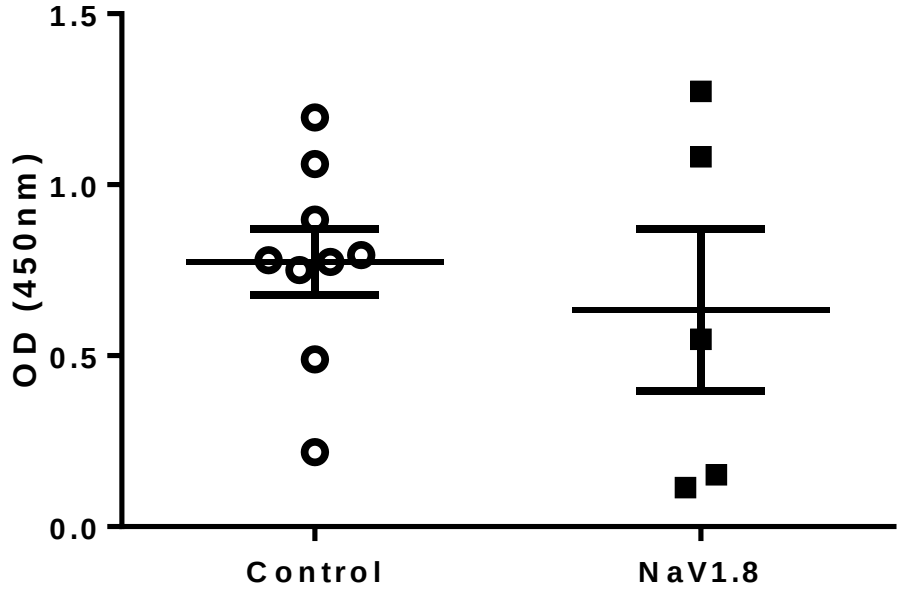
IgG (10,000x Dilution)
OD (450nm)
1.5
1.0
0.5
0.0
Control
NaV1.8

Figure 6 - Nav1.8-depleted mice produce normal levels of antigen specific antibodies.

Mice were immunized biweekly with intraperitoneal injections of KLH and alum. Two weeks after the booster injection, serum was obtained after cardiac puncture and immunoglobulin titers measured by ELISA. A) IgM and B) IgG titers were similar between Nav1.8-depleted mice and littermate controls (IgM, Nav1.8-depleted, 0.5044 ± 0.05477, n=9 versus control, 0.5466 ± 0.08038, n=6) (IgG, Nav1.8-depleted, 0.7737 ± 0.09626, n=9 versus control, 0.6340 ± 0.2365, n=5).

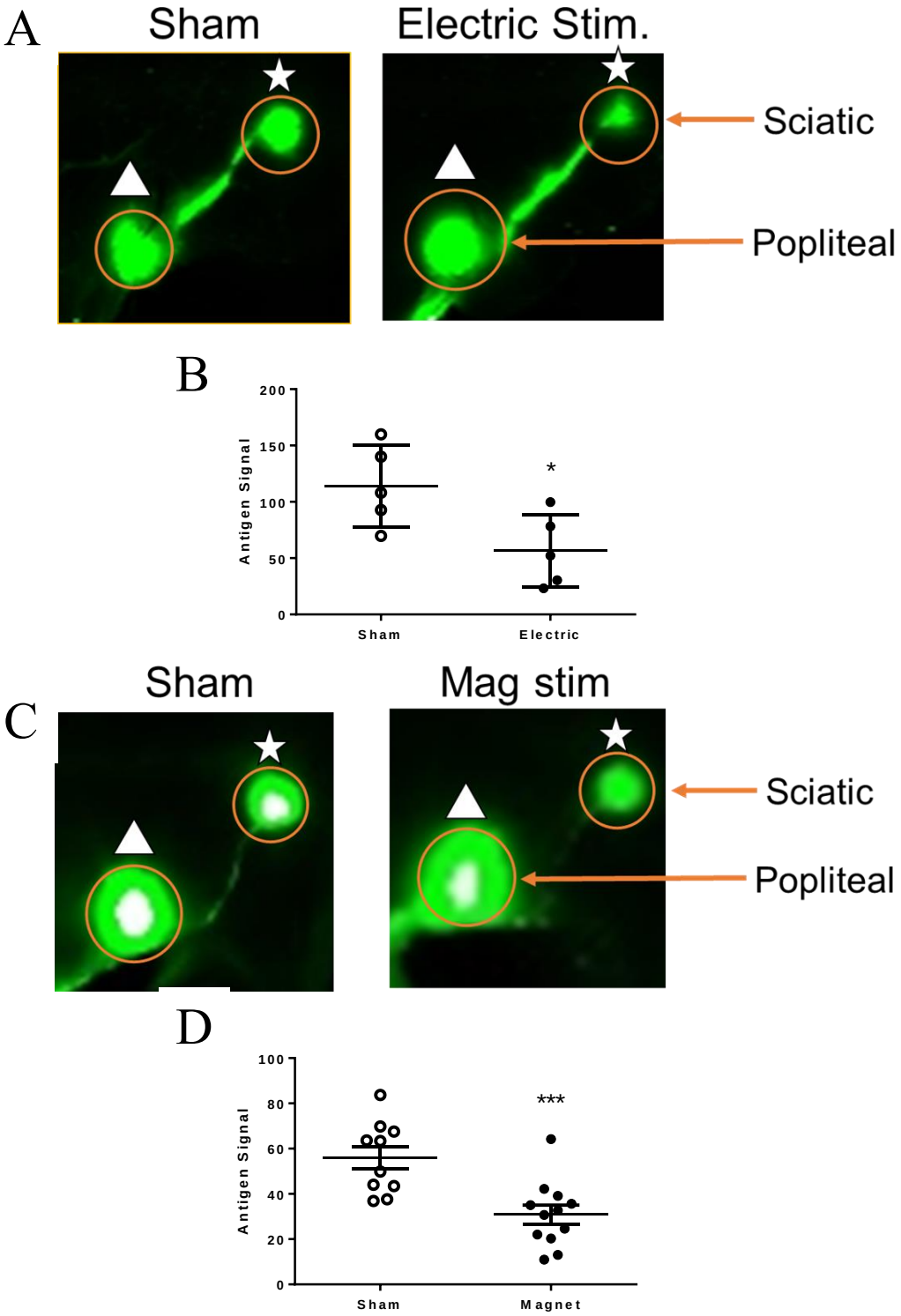
A
Sham
Electric Stim.
Sciatic
Popliteal
B
Antigen Signal
200
150
100
50
0
*
Sham
Electric
C
Sham
Mag stim
Sciatic
Popliteal
D
Antigen Signal
100
80
60
40
20
0
***
Sham
Magnet

Figure 7 - Induction of neuronal activity initiates reduction antigen flow.

A-B) Nerves by the popliteal lymph node were stimulated by application of an electrical current applied through a monopolar needle electrode, followed by injection of KLH-800CW and imaging after one hour. In electrically stimulated animals, lower levels of antigen were observed in the sciatic lymph nodes (sham, 114.1 ± 16.17, n=5 versus electrically stimulated, 56.76 ± 14.38, n=5, $p<0.05$ by t-test). A) Images are representative. B) Data shown are individual values. C-D) A noninvasive magnetic field was applied to the hind leg of naïve mice to induce nerve activity, followed by injection of KLH-800CW. In magnetically stimulated animals, lower levels of antigen were observed in the sciatic lymph nodes (sham, 55.99 ± 4.993, n=10, versus magnetically stimulated, 30.87 ± 4.169, n=12, $p<0.001$ by t-test). C) Images are representative; triangles indicate popliteal lymph nodes while stars represent sciatic lymph nodes. D) Data shown are individual values.

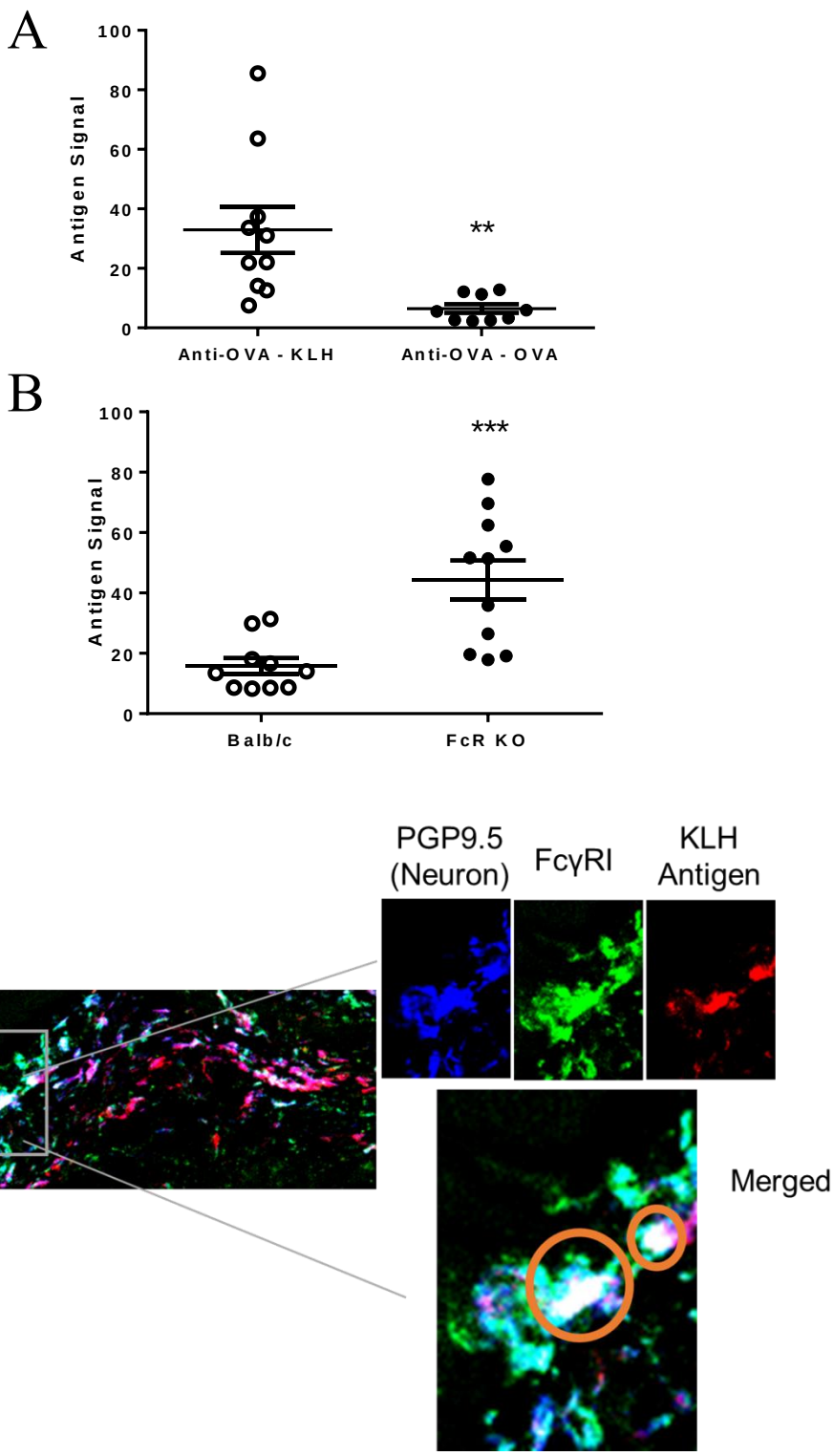
A
100
80
60
40
20
0
Antigen Signal
**
Anti-OVA - KLH
Anti-OVA - OVA
B
100
80
60
40
20
0
Antigen Signal
***
Balb/c
FcR KO
C
PGP9.5
(Neuron)
FcγRI
KLH
Antigen
Merged

Figure 8 - Neuronal Fc receptors play a role in antigen restriction.

A) Naïve mice were injected intraperitoneally with polyclonal anti-OVA antibodies from rabbit. 24 hours later OVA-800CW or KLH-800CW was injected in the dorsum of the hind paw. The amount of OVA antigen was significantly decreased compared to KLH in the sciatic lymph nodes (KLH, 32.95 ± 7.741, n=10 versus OVA, 6.483 ± 1.461, n=9). B) Immunized Balb/c and FcR KO mice were injected subcutaneously in the hind paw with KLH-800CW. More antigen was seen in the sciatic lymph nodes of FCR KO (Balb/c, 15.76 ± 2.721, n=10 versus FCR KO, 44.29 ± 6.500, n=11, $p<0.001$ by t-test). D) Mice immunized with KLH were injected with KLH-A647 in the dorsum of the hind paw. After one hour, skin around the injection site was excised, frozen in OCT media and sliced at 10 μm. After mounting tissue slices on slides, they were stained with antibodies against PGP9.5 and FcγRI. Images were obtained on a laser-scanning confocal microscope. Images shown are representative of slices from three different animals. Blue indicates PGP9.5, green indicates FcγRI, red indicates signal from KLH-A647, and white in the merged image indicates colocalization of all three signals. Orange circles indicate regions of interest.

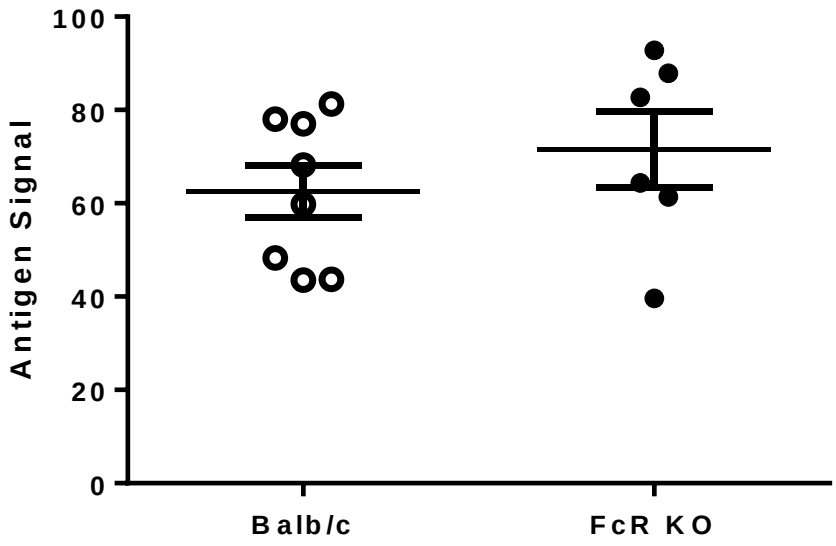
100
80
60
40
20
0
Antigen Signal
Balb/c
FcR KO

Figure 9 - Antigen trafficking is not different in naïve mice.

Naïve Balb/c and FcR KO mice were injected subcutaneously in the hind paw with KLH-800CW. No difference was seen in antigen signals of naïve Balb/c and FcR KO mice in the sciatic lymph node (Balb/c, 62.50 ± 5.614, n=8 versus FCR KO, 71.48 ± 8.197, n=6).

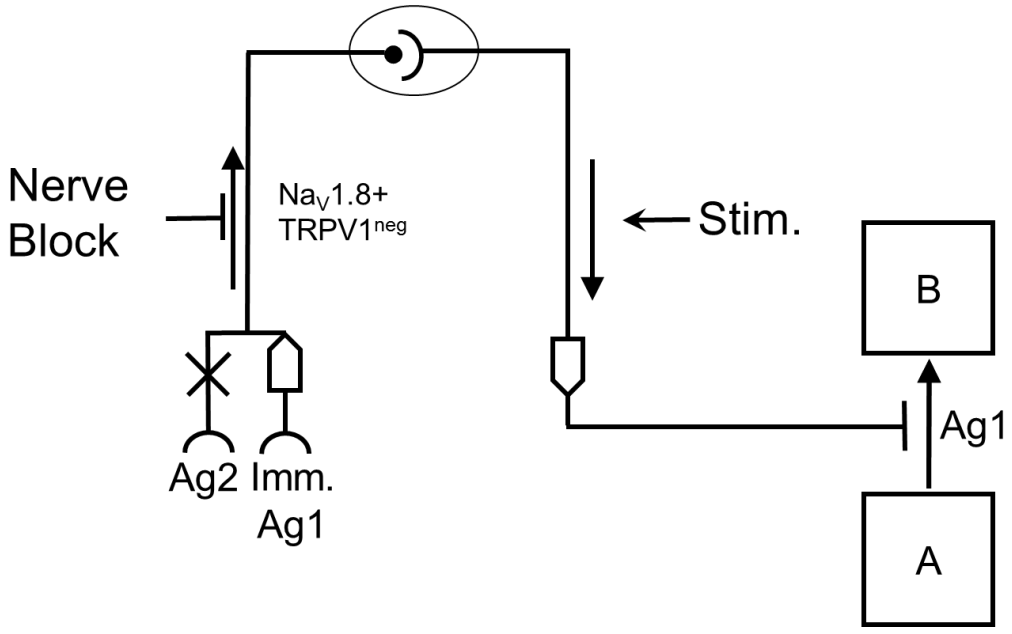
Nerve
Block
$Na_V1.8+$
$TRPV1^{neg}$
Stim.
B
Ag1
A
Ag2 Imm.
Ag1

Figure 10 - A model diagram illustrating the immunized-antigen reflex response.

A neuronal pathway distinguishes between novel and immunized antigens, sending a nerve signal through $Na_V1.8+$,TRPV1- neurons which is transmuted into a motor signal leading to restriction of antigen flow from lymph node A to lymph node B (e.g., popliteal to sciatic lymph node).

Acknowledgements

I would like to thank Clifford Woolf and his group at Harvard Medical School for their collaboration and providing mice in the neuronal depletion experiments.

Chapter 3 – Galantamine Attenuates Type 1 Diabetes and Inhibits Anti-Insulin Antibodies in Non-Obese Diabetic Mice

Abstract

Type 1 diabetes in mice is characterized by autoimmune destruction of insulin-producing pancreatic β cells. Disease pathogenesis involves invasion of pancreatic islets by immune cells, including macrophages and T cells, and production of antibodies to self-antigens, including insulin. Activation of the inflammatory reflex, the neural circuit that inhibits inflammation, culminates on cholinergic receptor signals on immune cells to attenuate cytokine release and inhibit B cell antibody production. Here, we show that galantamine, a centrally acting acetylcholinesterase inhibitor and an activator of the inflammatory reflex, attenuates murine experimental type 1 diabetes. Administration of galantamine to animals immunized with keyhole limpet hemocyanin (KLH) significantly suppressed splenocyte release of immunoglobulin G (IgG), interleukin-4 and -6 (IL-4 and IL-6) during KLH-challenge *ex vivo*. Administration of galantamine beginning at one month of age in non-obese diabetic (NOD) mice significantly delayed the onset of hyperglycemia, attenuated immune cell infiltration in pancreatic islets and decreased anti-insulin antibodies in serum. These observations indicate that galantamine attenuates experimental type 1 diabetes in mice and suggest that activation of the inflammatory reflex should be further studied as a potential therapeutic approach.

*References are found under Cited Literature, beginning on page 104

Introduction

Type 1 diabetes is associated with substantially increased rates of morbidity and mortality, accounting for costs exceeding $14.9 billion in healthcare costs in the U.S. each year [105-115]. It is characterized by decreased insulin secretion and severe hyperglycemia, which can lead to ketoacidosis, coma, and death. The disease pathogenesis is attributed to immune-mediated destruction of the insulin-producing β cells of pancreatic islets. Histopathological findings in type 1 diabetes includes inflammation and destruction of pancreatic islets with infiltration of macrophages, T cells and other immune cells [116-123]. Titers of auto-reactive antibodies are significantly increased in patients suffering from type 1 diabetes, including antibodies specific for insulin (IAA), glutamic acid decarboxylase (GAD), protein tyrosine phosphatase (ICA512 or IA2A), and zinc transporter protein (ZnT8) [124-127]. There are currently no effective treatments for type 1 diabetes. Anti-B cell antibodies (rituximab), anti-CD3 antibodies (otelixizumab and teplizumab) targeting T-cells, and the Diamyd vaccine (GAD immunotherapy) have all failed to meet endpoints in recent clinical trials [128-134].

Recent advances in understanding neural control of innate immunity reveal that neural reflexes, including the inflammatory reflex and the cholinergic anti-inflammatory pathway, control cytokine release and inflammation [6, 23, 37, 135-140]. The cholinergic anti-inflammatory pathway is defined as a vagus nerve signal that culminates on T cell acetylcholine release and activation of α7nAChR on splenic macrophages, which inhibits pro-inflammatory cytokine release [40,

42, 141-143]. Nerve stimulation and administration of α7 receptor agonists are in clinical development for treatment of inflammatory diseases [6, 144-146]. Recent evidence also links activation of the cholinergic anti-inflammatory pathway to a reduction in antibody production in spleen, specifically lower antibody titers and B cell activity during *Streptococcus pneumoniae infection* [44]. Here we reasoned that the cholinergic anti-inflammatory pathway would attenuate inflammation and serum antibody titers in murine type 1 diabetes.

Galantamine, a centrally acting acetylcholinesterase (AChE) inhibitor and clinically approved to treat Alzheimer's disease [147, 148], is an activator of the cholinergic anti-inflammatory pathway [138, 149]. We recently reported that galantamine treatment of mice with high fat diet-induced obesity significantly alleviates weigh gain, obesity-associated inflammation, hyperglycemia, and insulin resistance [150]. The NOD mouse is a model of type 1 diabetes, spontaneously developing antibodies against self-antigens, with islet infiltration starting at 3-4 weeks, leading to later islet destruction and hyperglycemia around 16-18 weeks [121]. In addition, similar antibodies as observed in humans have been described in the non-obese diabetic (NOD) mouse model of type 1 diabetes [151-153]. Accordingly here we administered galantamine to NOD mice beginning at a preclinical stage and measured blood glucose and serum antibodies. We found that galantamine administration attenuates type 1 diabetes-associated hyperglycemia, confers protection against islet inflammation, and decreases serum titers of diabetes-related autoimmune antibodies.

Methods

Animals

Non-obese diabetic (NOD) (4-5 weeks old) and Balb/c (6-8 weeks old) were obtained from Jackson Laboratories. Food and water were available *ad libitum*. Mice were used in subsequent experiments after at least a 14 day-adaptation period. All procedures were performed in accordance with the National Institutes of Health (NIH) Guidelines [92] under protocols approved by the Institutional Animal Care and Use Committee (IACUC) of the Feinstein Institute for Medical Research.

Cytokine and Antibody Determination

Balb/c mice were injected intraperitoneally (IP) with 100 ug keyhole limpet hemocyanin (KLH) (Calbiochem) + 50% Imject Alum (Thermo Fisher Scientific) in 200 ul saline two times, two weeks apart. Two weeks after the second injection, 4 mg/kg galantamine was injected IP. Splenocytes were harvested 4 hours later, erythrocytes lysed with Red Blood Cell Lysis Buffer (Sigma-Aldrich), and cultured in RPMI, HEPES, Penicillin/Streptomycin, L-glutamine, 1% Nonessential Amino Acids, and Beta-mercaptoethanol. Cells were exposed to increasing concentrations of KLH for 48 hours and media analyzed for cytokine and antibody content. Cytokines were measured by multiplex ELISA (Quansys) and IgG antibodies were measured by ELISA. Briefly, plates were coated with 20 ug/mL KLH antigen in phosphate buffered saline (PBS, Life Technologies) overnight followed by blocking with 1% bovine serum albumin

(BSA) in PBS for two hours. Plates were washed with PBS + 0.01% Tween-20 (PBST) three times. Blood collected by capillary tube from nicked mouse tail was spun at 5000xg, then serum was extracted and diluted 1:1000-1:10000 in PBS+BSA. 100 ul of diluted serum was incubated on coated plates for one hour at room temperature, then washed three times with PBST. A 1:2000 dilution of horseradish peroxidase-conjugated sheep anti-mouse IgG (GE Healthcare) was added to the plates for one hour at room temperature, then washed again. Plates were then developed using OptEIA TMB substrate (BD) and optical density at 450 nm was measured. Total IgE levels were determined by ELISA with rat anti-mouse IgE (BD Biosciences) coated plates, probed with biotinylated rat anti-mouse IgE antibody, followed by horseradish peroxidase-conjugated streptavidin.

Drug Administration

Five-week-old female NOD/ShiLtj mice were injected intraperitoneally with 1 mg/kg galantamine (Calbiochem) or vehicle control in 200 µl normal saline, daily, until the end of the experiment. Blood glucose was measured once weekly using a Freestyle Freedom Lite meter (Abbott). Mice were deemed diabetic after two consecutive blood glucose readings >200 mg/dL. For therapeutic experiments, NOD/ShiLtJ mice with overt diabetes (blood glucose >200 mg/dl for two weeks in a row, 16-22 weeks of age) were injected intraperitoneally with 1 mg/kg galantamine or saline, daily, with monitored blood glucose. At the end of the experiment, mice were euthanized with CO_2, and pancreas, spleen, and serum collected and processed for further analyses.

Tissue Processing and Insulitis Scores

Mice were euthanized at 17 weeks, and pancreas fresh frozen in optimal cutting temperature (O.C.T.) medium. Diabetic and nondiabetic mice were both included in the analysis of insulitis. 5-7 μm slices were obtained by cryostat sectioning, mounted and fixed in acetone, allowed to dry at room temperature, and stained with Mayer's haematoxylin for five minutes. Insulitis was scored using a bright field microscope in double-blinded manner (blinded to both treatment groups and diabetic state). At least 50 islets from at least three disparate sections of each mouse pancreas were then scored as follows: 0 – no insulitis, 1 – peri-insulitis, 2 – moderate (<70%) insulitis, 3 – complete (>70%) insulitis (Figure 14A).

Antibody Determination

Plates were coated with antigens including: insulin (human insulin, Sigma), histone II-A (from calf thymus, Sigma), myelin basic protein (MBP, from mouse, Sigma), myelin oligodendrocyte glycoprotein (MOG, immunodominant epitope of mouse MOG, Sigma), and deoxyribonucleic acid (DNA, from calf thymus, Sigma). IgG levels were determined by ELISA as previously described using plates coated with each respective antigen.

Statistics

Blood glucose, KLH antibody responses and cytokine responses were analyzed by two-way ANOVA followed by Bonferroni post-test. Diabetes onset survival curves were analyzed by log-rank (Mantel-Cox). Islet scores were analyzed by Chi-square. All tests with a *P* value of less than .05 were considered statistically significant. Statistical analyses were performed using Graphpad

Prism 6 software. Unless otherwise stated, all numbers are given as average ± standard error of the mean.

Results

Galantamine attenuates antibody release by splenocytes

We first examined the effect of galantamine administration on splenocyte antibody release. Mice were immunized intraperitoneally with keyhole limpet hemocyanin in alum twice, two weeks apart. Fourteen days after the second immunization, mice were injected with galantamine (4 mg/kg) or saline intraperitoneally 4 hours prior to euthanasia, and isolated splenocytes were cultured in the presence of KLH *in vitro* for up to 7 days. Splenocytes from mice administered galantamine produced less KLH-specific IgG, while producing more total IgE (Figure 11A). In addition, galantamine administration resulted in reduced IL4 and IL6, but not IL2, release by splenocytes (Figure 12). No changes in cell numbers were observed.

Galantamine delays hyperglycemia and diabetes onset

To study the preventative effects of galantamine in type 1 diabetes, 4-5-week-old NOD mice were administered 1 mg/kg galantamine (n=11) or saline (n=10) intraperitoneally, 200uL daily for 20 weeks. Blood glucose was monitored weekly to determine the onset of hyperglycemia, defined as glucose >200 mg/dL. Mice administered galantamine did not develop hyperglycemia until week 19, while almost all mice administered saline rapidly developed hyperglycemia by week 14 (Figure 13A). The average glucose levels in saline-administered animals was 226.6 ± 60.3mg/dl by week 14; similar levels were not reached in galantamine-administered animals until week 19 (227.8 ± 52.3mg/dl)

(Figure 13A). Additionally, the prevalence of diabetes (two consecutive blood glucose levels >200mg/dl), in mice administered galantamine was lower (Figure 13B, $p<0.05$). Galantamine-administered mice that did develop diabetes rapidly progressed to high levels of blood glucose (data not shown).

To determine galantamine's efficacy in treating established diabetes, NOD mice with two consecutive weeks of blood glucose >200 mg/dl were administered 1 mg/kg galantamine daily. Galantamine treatment did not significantly alter blood glucose levels as compared to vehicle treatment. Together, these results indicate that galantamine in the context of preclinical type I diabetes at relatively early stages of disease progression is efficacious in delaying onset of hyperglycemia.

Galantamine attenuates pancreatic islet inflammation.

To determine to effect of galantamine on immune cell infiltration in pancreatic islets, pancreata from 17-week-old female NOD mice administered 1 mg/kg galantamine or saline IP daily were investigated using histochemical methods. 7 um sections were obtained from throughout the pancreas, at least 100 um apart. Insulitis was scored from 0-3 as indicated in Figure 14A. Administration of galantamine reduced the severity of insulitis (Figure 14B) and improved the overall insulitis score in galantamine-administered animals (Figure 14C, Chi-square $p<0.0005$).

Galantamine reduces serum levels of anti-insulin antibodies in NOD mice

NOD mice produce elevated levels of auto-antibodies [152]. To investigate the effect of galantamine on serum antibody levels, titers of anti-insulin, anti-histone, anti-DNA, anti-MOG and anti-MBP antibodies were measured in galantamine-administered and control NOD mice. IgG antibodies specific to insulin were significantly reduced in galantamine-administered animals (Figure 15A), while antibodies directed against histone, DNA, MOG and MBP were unaffected (Figure 15B-E). These results indicate a selective suppressive effect of galantamine administration on insulin-specific antibody production in this model.

Discussion

Here, we show that administration of the acetylcholinesterase inhibitor galantamine, [138, 149, 154] delays elevation of blood glucose levels and onset of diabetes in the NOD model. In this disease model, galantamine reduces pancreatic islet inflammation and lowers disease-specific antibody levels without reducing levels of other tested IgG antibodies. Furthermore, splenocytes derived from galantamine- administered mice released less IL-4, IL-6 and IgG in response to antigen re-exposure *in vitro*.

The observation that splenocytes derived from galantamine-administered mice released less IgG and higher IgE levels in response to immunized antigen *in vitro* suggests that galantamine stimulates class-switching of B cells from IgG to IgE. In addition, the lower IL-4 and IL-6 secretion by splenocytes from galantamine- administered animals after antigen exposure suggests an environment less supportive of B cells antibody release, including suppression of Th2 helper T cells. These findings highlight a previously unrecognized anti-inflammatory effect of galantamine in preclinical type I diabetes.

Autoimmunity in NOD mice is initiated in the pancreatic lymph nodes, but not in the spleen, at 2-3 weeks of age [155]. Treatment starting from 5 weeks of age could influence a mechanism that slows the progression of insulitis and ultimately the onset of clinical diabetes separate from the initial priming for autoimmunity to islet autoantigens. We examined cytokine content by ELISA from pancreatic samples at 12 weeks of age after 8 weeks of galantamine administration. The lysate of these samples included embedded pancreatic lymph

nodes. We found no difference in levels of interferon gamma (IFNγ), interleukin 17 (IL-17), monocyte chemotactic protein 1 (MCP-1), or interleukin 1β (IL-1β) (data not shown).

Changes in cellular populations could be an important component of galantamine's anti-inflammatory effects. To examine changes in populations, we obtained single cell isolates from both spleen and total pancreas, including lymph nodes, taken from mice administered galantamine for 8 weeks. We examined CD3+CD4+, CD3+CD4+FoxP3+, and CD3+CD8+ populations by flow cytometry. We observed no difference in percentages of these populations in treated animals compared to vehicle control in both spleen and pancreas (data not shown). Fewer cells were observed in the pancreata of galantamine-treated animals (data not shown). It is plausible that galantamine may suppress the inflammatory activity of the immune cells, but does not alter the immune cell composition. The specific effect of galantamine on cellular function remains to be elucidated, and additional analyses would provide useful data.

Galantamine has previously been shown to exert anti-inflammatory effects through brain-mediated and vagus nerve-dependent signaling [138, 149]. The vagus nerve innervates the pancreas and vagus nerve cholinergic output controls pancreatic endocrine and exocrine secretion [156-158]. A role for the vagus nerve has also been shown in suppressing pancreatic inflammation; surgical transection of the vagus nerve (vagotomy) results in exacerbated murine pancreatitis, thus indicating a tonic anti-inflammatory role of these innervations [159]. The vagus nerve also innervates the liver and it is known that vagus nerve-mediated signaling suppresses hepatic glucose production [160-162] – one of the main determinants of fasting blood glucose levels. We suggest that galantamine-mediated activation of the vagus nerve reduces pancreatic inflammation and delays onset of diabetes. In this context, it is possible that metabolic effects of

vagus nerve activation on hepatic glucose release may also play a role [163]. Future studies should address the role of these and other mechanisms in mediating galantamine efficacy in type I diabetes.

Galantamine is in clinical use for treatment of Alzheimer's disease patients in the United States, and has been used for decades in Europe in treating myasthenia gravis and Alzheimer's disease and in children with autism spectrum disorders [147, 148, 164]. This abundant clinical experience in adult and pediatric populations should facilitate potential experimental use of galantamine in the treatment of type I diabetes. Other therapeutic approaches, including beta cell transplantation or beta cell regeneration have been explored [165-172]. In light of our current findings, it would be interesting to further study whether galantamine treatment in combination with islet restoration would improve clinical outcomes in established type 1 diabetes.

Figures

A

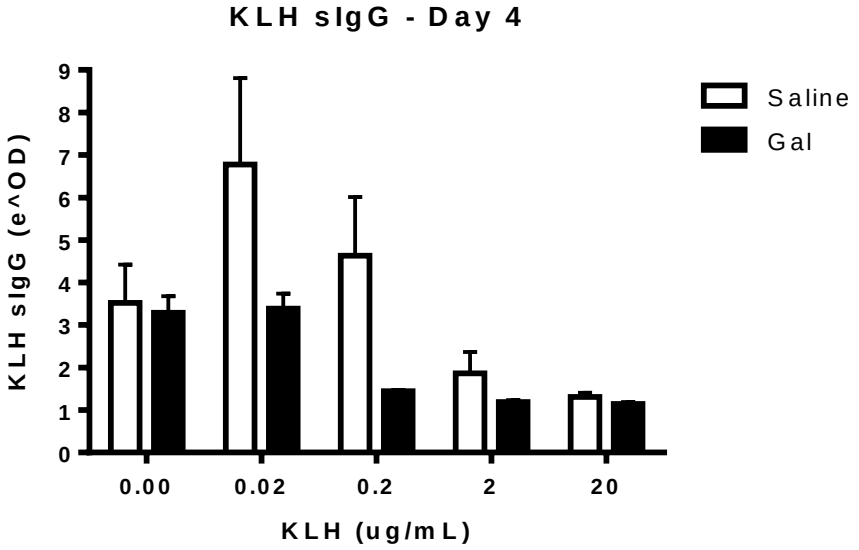
KLH sIgG - Day 4
KLH sIgG (e^OD)
9
8
7
6
5
4
3
2
1
0
0.00
0.02
0.2
2
20
KLH (ug/mL)
Saline
Gal

B

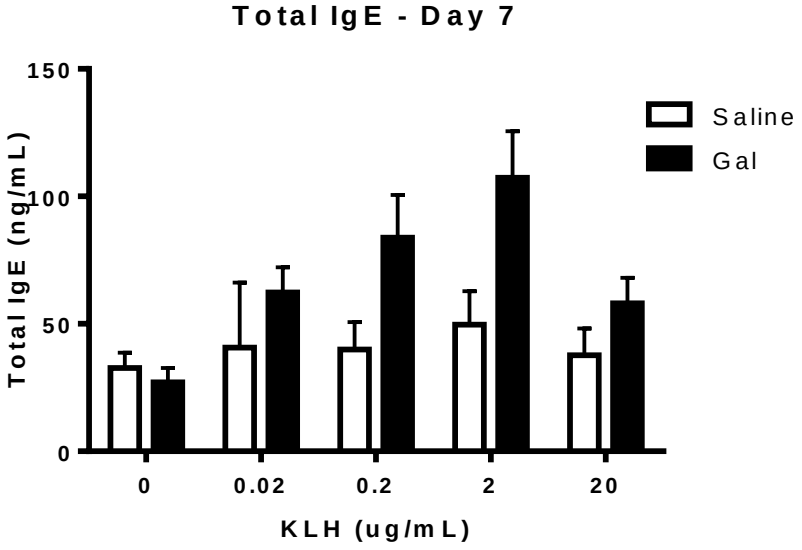
Total IgE - Day 7
Total IgE (ng/mL)
150
100
50
0
0
0.02
0.2
2
20
KLH (ug/mL)
Saline
Gal

Figure 11 - Galantamine alters antibody responses in immunized mice.

KLH immunized mice were administered galantamine (4 mg/kg) or saline 4 hours before sacrifice. Splenocytes were extracted, plated at 2 *10^5 in 96-well plates, and incubated with indicated ug/well KLH. A) KLH-specific IgG and B) Total IgE was determined by ELISA. Galantamine affected antibody levels (IgG $P<0.05$, IgE $p<0.01$ by two-way ANOVA;*=$p<0.05$ by Bonferroni post-test).

A

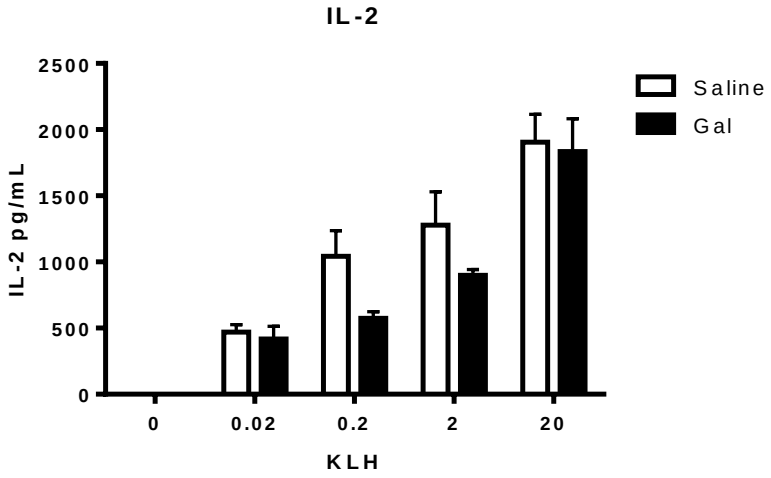
IL-2
2500
2000
1500
1000
500
0
IL-2 pg/mL
0
0.02
0.2
2
20
KLH
Saline
Gal

B

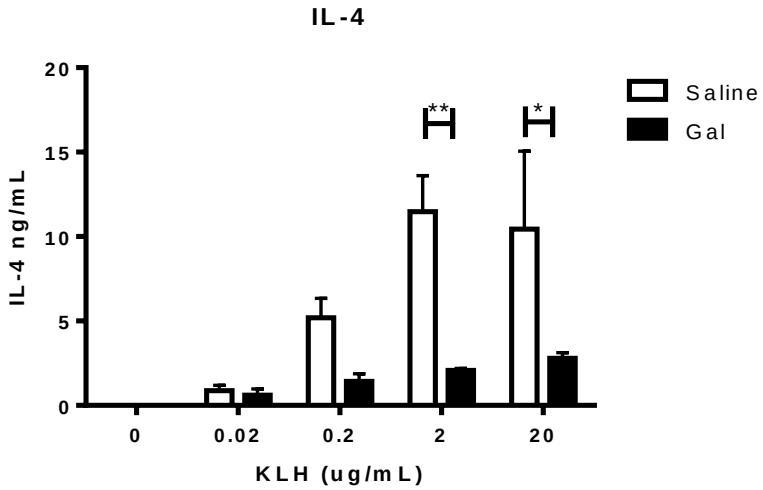
IL-4
20
15
10
5
0
IL-4 ng/mL
**
*
0
0.02
0.2
2
20
KLH (ug/mL)
Saline
Gal

C

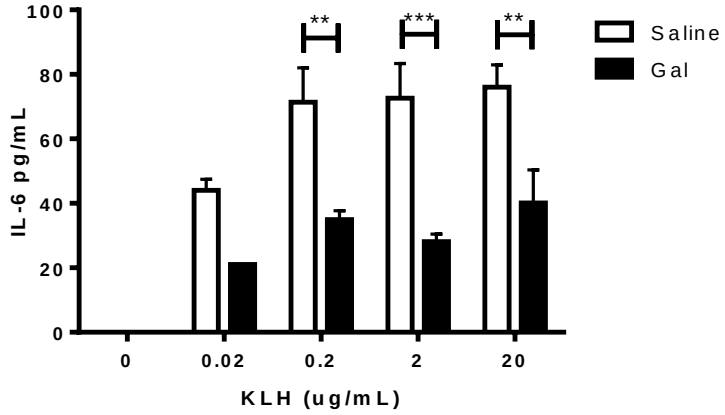
IL-6
100
80
60
40
20
0
IL-6 pg/mL
**
***
**
0
0.02
0.2
2
20
KLH (ug/mL)
Saline
Gal

Figure 12 - Galantamine alters cytokine responses in immunized mice.

KLH immunized mice were administered galantamine (4 mg/kg) or saline 4 hours before sacrifice. Splenocytes were extracted, plated at 2 *10^5 in 96-well plates, and incubated with indicated ug/well KLH. Cytokines were determined on Day 7 by Quansys multiplex ELISA. A) Galantamine did not significantly affect IL-2. B) IL-4 ($p<0.001$) and IL-6 ($p<0.0001$) were significantly different in galantamine-treated animals (Two-way ANOVA;*=$p<0.05$, **=$p<0.01$, ***=$p<0.001$ by Bonferroni post-test).

A

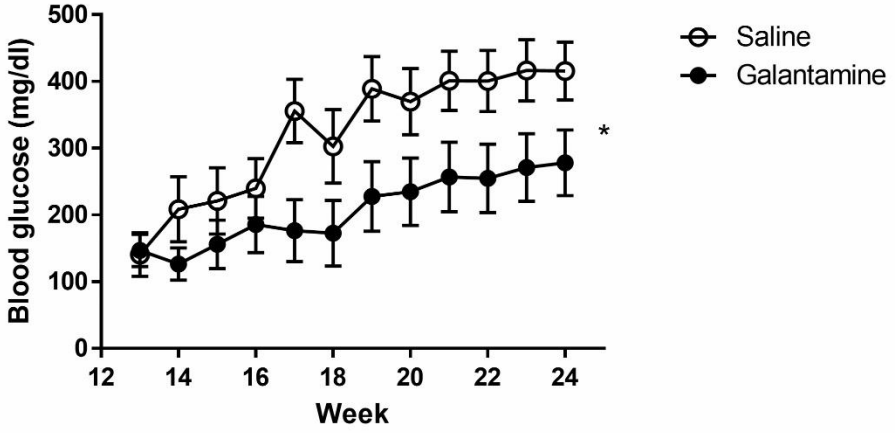
Blood glucose (mg/dl)
500
400
300
200
100
0
12
14
16
18
20
22
24
Week
*
Saline
Galantamine

B

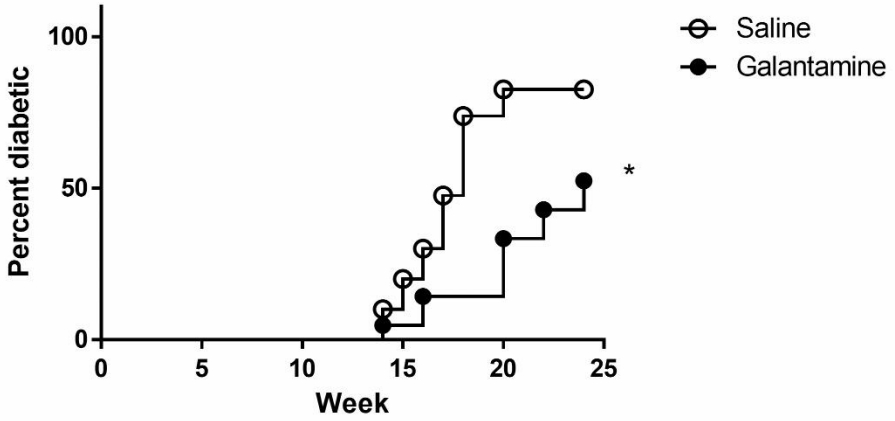
Percent diabetic
100
50
0
0
5
10
15
20
25
Week
*
Saline
Galantamine

Figure 13 - Galantamine delays the onset of hyperglycemia and diabetes.

1 mg/kg galantamine (n=11) or saline (n=10) was administered IP daily to NOD mice beginning at 5 weeks of age. Blood glucose levels were measured weekly, with two successive weeks of blood glucose >199 mg/dl indicating onset of diabetes. Administration of galantamine A) significantly reduced the average blood glucose over time ($p<0.05$, Two-way ANOVA), and B) significantly delayed onset of diabetes ($p<0.05$, Mantel-Cox, results of two combined experiments).

A

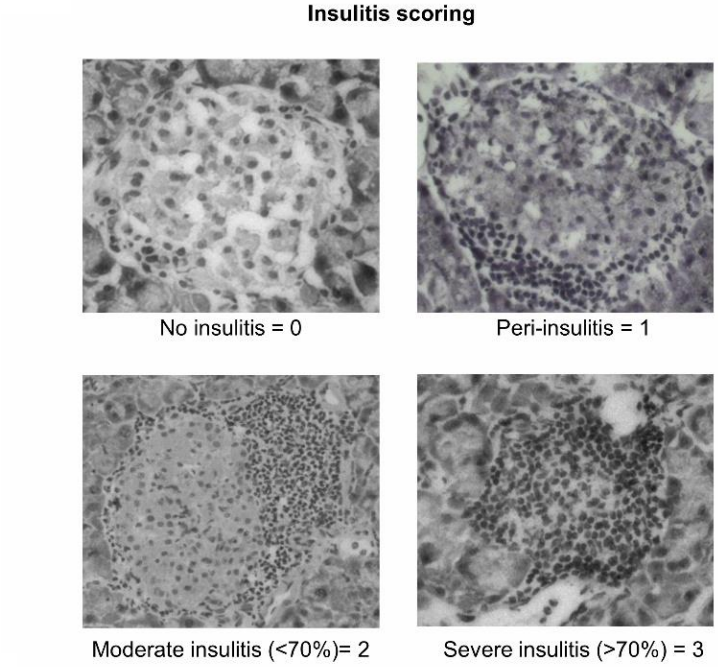
Insulitis scoring
No insulitis = 0
Peri-insulitis = 1
Moderate insulitis (<70%)= 2
Severe insulitis (>70%) = 3

B

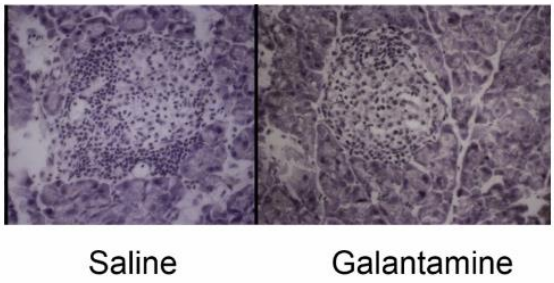
Saline
Galantamine

C

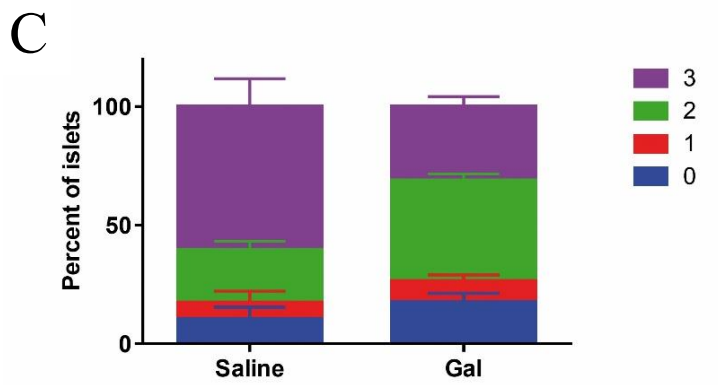
Percent of islets
100
50
0
Saline
Gal
3
2
1
0

Figure 14 - Daily administration of galantamine decreases islet infiltration by immune cells

Islets with no infiltrating mononuclear cells were scored as 0, peri-islet inflammation only = 1, moderate intra-islet inflammation occupying <70% of the islet = 2, severe-complete intra-islet inflammation occupying >70% of the islet = 3. B-C) Pancreata from 16 week-old NOD mice injected IP with saline or galantamine from 5 weeks of age were isolated and frozen in OCT media, then sliced at 10 um. At least 50 total islets from 3 disparate areas of each pancreas were scored blindly. Administration of galantamine B) reduced the severity of insulitis in NOD mice (representative images), as well as C) improved the overall level of insulitis in the pancreas (n=5, Chi-square $p<0.0005$).

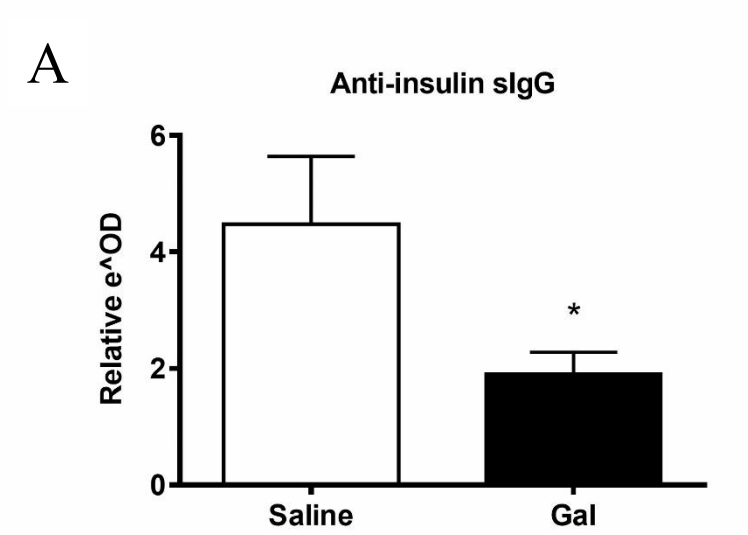
A
Anti-insulin sIgG
Relative e^OD
6
4
2
0
*
Saline
Gal

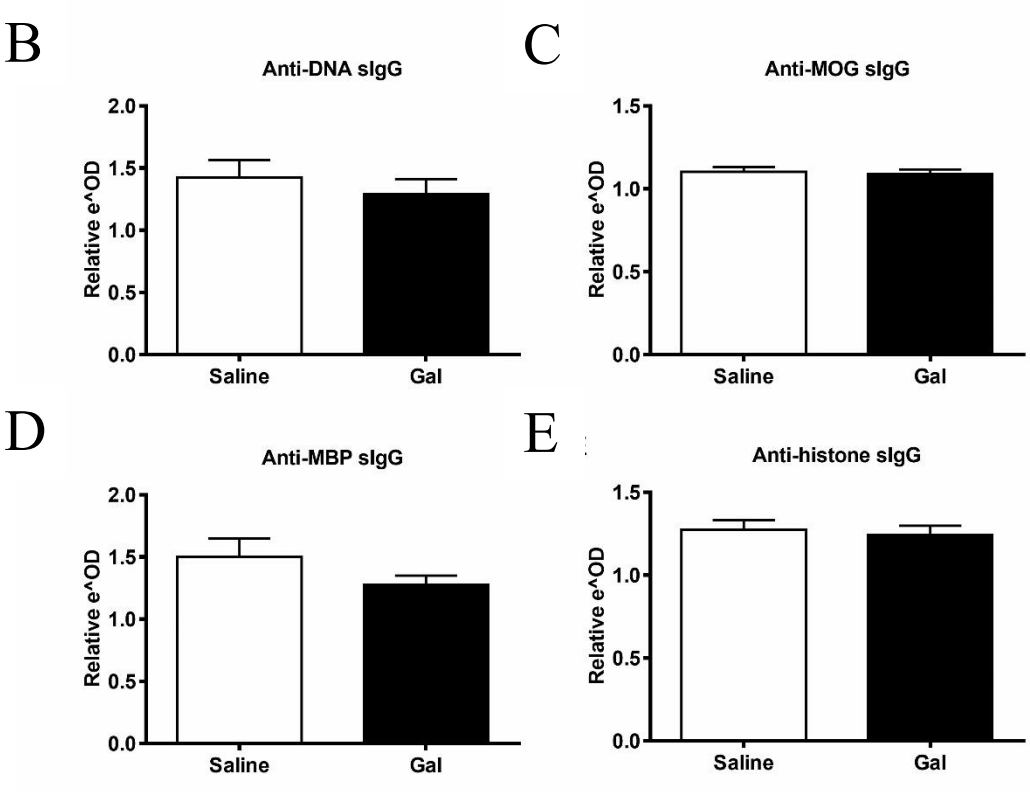
B
Anti-DNA sIgG
Relative e^OD
2.0
1.5
1.0
0.5
0.0
Saline
Gal
C
Anti-MOG sIgG
Relative e^OD
1.5
1.0
0.5
0.0
Saline
Gal
D
Anti-MBP sIgG
Relative e^OD
2.0
1.5
1.0
0.5
0.0
Saline
Gal
E
Anti-histone sIgG
Relative e^OD
1.5
1.0
0.5
0.0
Saline
Gal

Figure 15 - Galantamine administration reduces levels of circulating pathogenic anti-insulin antibodies.

Serum from galantamine- or saline-administered was applied to ELISA plates coated with antigens, then probed with anti-mouse antibodies. Serum anti-insulin antibodies were reduced in animals administered galantamine (A) ($p>0.05$), but other common NOD autoantibodies were not affected (B-E).

Acknowledgements

This work was supported by a grant from the Juvenile Diabetes Research Fund and the following grants from the National Institute of General Medical Sciences, National Institutes of Health: R01GM057226 (to KJ Tracey) and R01GM089807 (to KJ Tracey and VA Pavlov).

This work has been accepted for publication in Molecular Medicine, and is available by e-publication ahead of print [45].

Chapter 4 – Choline Acetyltransferase+ CD4+ Lymphocytes Are Essential Regulators of Blood Pressure

Abstract

Hypertension, a chronic increase in resting blood pressure, is a major risk factor for cardiovascular morbidity and mortality. Acetylcholine, an evolutionarily ancient signaling molecule produced by neurons and lymphocytes, mediates decreases in blood pressure by stimulating endothelial cell production of nitric oxide (NO), a potent vasodilator. However, the cellular source for acetylcholine in the vasculature is currently unknown. We reasoned that subset of CD4+ T lymphocytes expresses choline acetyltransferase (ChAT), the enzyme that catalyzes the biosynthesis of acetylcholine, are anatomically positioned to provide this acetylcholine. Accordingly, we term these CD4+ ChAT+ T cells "TChAT." Genetic ablation of ChAT in CD4+ cells (CD4+ TChAT-/-) in mice significantly increases mean arterial blood pressure as compared to littermate mice expressing ChAT in CD4+ cells (CD4+ TChAT+/+). Blood pressure is significantly decreased in mice receiving Jurkat T cells genetically engineered to overexpress ChAT (JTChAT). Administration of atropine, a muscarinic receptor antagonist, or L-NG-Nitroarginine methyl ester (L-NAME), a nitric oxide synthase inhibitor, significantly attenuates this development of hypotension in

*References are found under Cited Literature, beginning on page 104

mice receiving JTChAT. Thus, acetylcholine-releasing CD4 TChAT lymphocytes are essential for blood pressure homeostasis by providing a vasodilatory signal through NO-dependent relaxation of blood vessels.

Introduction

Current treatment of clinical hypertension is mostly empirical, because the pathogenesis is unknown in about 90% of cases. Interactions between genetic and environmental factors that result in endothelial dysfunction, inflammation, and vascular remodeling have been proposed to underlie long-term disease development [173]. Although the causes of hypertension are largely unclear, many aspects of the physiology of blood pressure regulation are well understood. Therapeutic approaches to date, however, have primarily focused on reducing vascular tone by interfering in adrenergic signaling and the renin-angiotensin-aldosterone systems, rather than directly promoting vasodilatation.

Acetylcholine is a neurotransmitter known to promote vasodilatation and reduce blood pressure [174]. The underlying mechanism involves activation of cholinergic receptors on vascular endothelial cells and stimulation of endothelial nitric oxide synthase (eNOS), the rate limiting enzyme in the biosynthesis of nitric oxide (NO) [175]. Endothelium-derived NO diffuses to adjacent smooth muscle cells in the vascular wall, where it stimulates guanylate cyclase. This relaxes the vascular smooth muscle cells, producing vasodilation which in turn decreases blood pressure. Paradoxically, although this mechanism of blood pressure control is well established, endothelial cells do not receive direct input from neurons that secrete acetylcholine.

A subset of T cells express choline acetyltransferase (ChAT), the rate limiting enzyme for the biosynthesis of acetylcholine [40, 143, 176]. These acetylcholine-producing T cells are integral components of a neural information

system that reflexively controls innate immune responses. These cells constitute <10% of the $CD4^{+}$ $CD44^{high}$ $CD62L^{low}$ population in spleen [40]. Because lymphocytes can produce acetylcholine, we reasoned that they may provide an important vasodilatory signal in the regulation of blood pressure.

Methods

Animals

Choline acetyltransferase (ChAT)-GFP (B6.Cg-Tg(RP23-268L19-EGFP)2Mik/J), ChAT-floxed (B6.129-Chattm1Jrs/J), and mice expressing Cre recombinase under the control of the endogenous CD4 promoter (CD4-Cre) were purchased from Jackson Laboratories (Bar Harbor, ME, USA). ChAT-floxed and CD4-Cre mice were crossed to generate mice genetically devoid of ChAT in the $CD4^+$ population. Food and water were available *ad libitum*. Mice were used in subsequent experiments after at least a 14 day-adaptation period. All procedures were performed in accordance with the National Institutes of Health (NIH) Guidelines [92] under protocols approved by the Institutional Animal Care and Use Committee (IACUC) of the Feinstein Institute for Medical Research.

Isolation of Primary ChAT-expressing T Cells

ChAT-$eGFP^+$ and ChAT-$eGFP^-$ cells were isolated from spleens of B6.Cg-Tg(RP23-268L19-eGFP)2Mik/J reporter mice by MACS cell negative selection for $CD4^+$ T cells (Miltenyi Biotec) followed by cell sorting by flow cytometry using a FACSAria of the $CD4^+$ $CD44^{hi}$ $CD62L^{low}$ population (BD Biosciences) into $eGFP^+$ and $eGFP^-$ subsets as previously described [40].

Formation of Stable Chat-Jurkats

Jurkat lymphocytes were stably transfected with the pCMV6-mChAT vector (Origene, Rockville, MD). Briefly, the cells were transformed with the vector using FuGene HD (Promega) according to the manufacturer's directions. After 48 hours, transformed cells were selected by incubation with 600 ug/mL G418 (InvivoGen). Antibiotic pressure was maintained for 2 weeks, and monoclonal colonies were obtained by picking single cells. ChAT expression was confirmed by western blot using anti-choline acetyltransferase antibody (Abcam).

Endothelial Cell Response

Primary $ChAT^+$ lymphocytes or transfected, $ChAT^+$ Jurkat T lymphocytes (JT_{ChAT} lymphocytes) were co-cultured with either murine endothelial cells or human endothelial cells derived from pulmonary microcirculation (HPMEC-ST1.6R) [177, 178]. Endothelial cells were loaded with Fluo-4 (Life Technologies, Carlsbad, CA) and fluorescence observed in a microscope or endothelial cell lysates were analyzed by Western blot for phospho-eNOS. Media nitrate+nitrite was analyzed by nitrate/nitrite colorimetric assay kit

Blood Pressure Measurement

Primary $ChAT^+$ lymphocytes or transfected, $ChAT^+$ Jurkat T lymphocytes (JT_{ChAT}) were injected into the left ventricle of the heart. Blood pressure was measured 1) through a 26 G needle placed in the left ventricle and recorded using a Biopac Systems Inc., a TSD104A transducer, and AcqKnowledge 4.1 software, 2) using the CODA NIBP tail-cuff device (Kent Scientific Corp., Torrington, CT, USA) as per the manufacturer's instructions or 3) using a saline filled catheter

inserted in the left carotid artery and an AD-instruments recording system. L-NG-monomethyl arginine citrate (L-NMMA) and L-N^G-Nitroarginine methyl ester (L-NAME) were used as an NOS inhibitors. Atropine was used as a muscarinic receptor blocker.

Results

ChAT^{+} leukocytes modulate blood pressure

Earlier work indicated that mammalian leukocytes express ChAT, and release acetylcholine in blood [179], but whether ChAT^{+} leukocytes modulate blood pressure was unknown. Accordingly, tail vein blood samples were collected from ChAT-eGFP mice and analyzed by FACS. We observed that ChAT-eGFP^{+} represent 1.1% of total circulating T lymphocytes (median 95% confidence interval: 0.5%-2%) (Figure 16A). To study whether this small fraction of lymphocytes modulates blood pressure, we utilized Cre-lox recombination in mice to selectively ablate ChAT in CD4^{+} cells. Mice expressing Cre recombinase under the control of the endogenous CD4 promoter (CD4-Cre) were crossed with ChAT-floxed mice to generate CD4^{+} ChAT deficient offspring (CD4^{+} ChAT$^{-/-}$). We observed that blood pressure in six-week-old CD4^{+} ChAT$^{-/-}$ mice (mean arterial pressure (MAP) 113 ± 3 mmHg, n = 23) is significantly increased as compared to littermate mice expressing ChAT in CD4^{+} cells (CD4^{+} ChAT$^{+/+}$) (MAP 103 ± 4 mmHg, n = 17, p=0.028) (Figure 16B). Measurement of blood pressure in these animals for at least 12 weeks revealed persistent hypertension in the CD4^{+} ChAT$^{-/-}$ as compared to the CD4^{+} ChAT$^{+/+}$ (Figure 16C). Thus, despite the relative paucity of these cells in blood, genetic evidence establishes a physiological role of CD4 T_{ChAT} in regulation of blood pressure.

T cell-derived acetylcholine modulates blood pressure

To study T cell derived acetylcholine in acute regulation of blood pressure, Jurkat T lymphocytes were stably transfected with the pCMV6-mChAT vector engineered to express ChAT. These transfected T lymphocytes (JT_{ChAT}) constitutively produce acetylcholine, whereas non-transfected Jurkat T cells (JT) did not produce detectable levels of acetylcholine. Blood pressure was measured in mice following insertion of a catheter (PE10) into the left carotid artery. Infusion of JT_{ChAT} significantly reduced mean arterial pressure within minutes, producing up to a 10% decrease (Figure 17A). In contrast, administration of saline or JT failed to significantly decrease mean arterial pressure (Figure 17B-C). Administration of the muscarinic receptor blocker atropine, or the NOS inhibitor L-N^G-Nitroarginine methyl ester (L-NAME) significantly attenuates JT_{ChAT}-mediated decreases in blood pressure (Figure 17D-E).

$ChAT^+$ lymphocytes activate nitric oxide synthase in vascular endothelial cells

Acetylcholine mediates vasodilation and hypotension by increasing intracellular Ca^{2+}-levels, and activating endothelial nitric oxide synthase (eNOS) by phosphorylation of serine 1177 (Ser1177) to catalyze biosynthesis of NO from L-arginine [180]. To investigate this mechanism here, endothelial cells were pre-loaded with the calcium-responsive Fluo-4 dye and co-cultured with JT_{ChAT}. We observed that co-culture of $2x10^6$ JT_{ChAT} cells with endothelial cells triggered a transient increase in endothelial Ca^{2+}-levels as measured by time-lapse fluorescent microscopy, whereas JT failed to significantly increase endothelial intracellular Ca^{2+}-levels (Figure 18A). Co-culture of primary $ChAT^+$ lymphocytes derived from ChAT-eGFP reporter mice or JT_{ChAT} with endothelial cells stimulated

Ser1177 phosphorylation (Figure 18B-C). This eNOS phosphorylation is attenuated by atropine (Figure 18C). Addition of JT_{ChAT} to endothelial cultures significantly increased production of nitrate and nitrite in medium, indicating enhanced production of NO (Figure 18D).

Discussion

This study defines CD4 T_{ChAT} as a discrete T cell subset capable of releasing acetylcholine and decreasing blood pressure. The observation that genetic ablation of CD4 ChAT in mice causes hypertension indicates that hematopoietic cells provide essential regulation of blood pressure. Not surprisingly, infusion of ChAT-expressing Jurkat T cells reduces blood pressure, an effect that is attenuated by blocking muscarinic receptors or nitric oxide synthase. Together, these findings indicate that acetylcholine released from these luminal T lymphocytes in proximity of the vascular endothelial cell lining directly mediates endothelial-dependent arterial relaxation.

The identification of $ChAT^+$ lymphocytes in regulation of eNOS activity and blood pressure here presents a new mechanism for understanding how specific lymphocyte subsets mediate cardiovascular responses. Previously, CD4 T_{ChAT} had been implicated in the neural control of immune responses [40, 145]. The finding here of bloodborne CD4 T_{ChAT} provides a means for delivery of acetylcholine to cells devoid of direct cholinergic innervation. This includes vascular endothelial cells, which respond to acetylcholine to mediate NO-dependent vasodilation. Because of the physical constraints of 20-40 um arterioles [181], circulating ~10 um CD4 T_{ChAT} are likely to appear frequently within micrometers of arteriolar endothelial cells. This proximity should be sufficient for delivery of acetylcholine to vascular endothelial cells in blood-pressure regulating arterioles. Significantly decreased lymphocyte expression of ChAT in hypertensive rats as compared to normotensive rats has been reported

[182], and treatment with inhibitors of acetylcholinesterase can attenuate pathological cardiovascular changes in spontaneously hypertensive rats [183].

The underlying pathophysiology of hypertension is unclear in approx. 90% of patients, and analysis of ChAT, acetylcholine, and plasma cholinesterase in blood may provide a novel opportunity to identify a treatable cause of hypertension in some individuals, maybe even before it manifests clinically. Perhaps it will be possible to alleviate disease in these individuals by promoting an increased number of $ChAT^+$ lymphocytes and ChAT activity in blood by pharmacological means or by other immunomodulating therapy. It may even be possible to engineer T cells for adoptive transfer [184] to release acetylcholine at specific locations in the vasculature to therapeutically regulate local blood flow and blood pressure. Since CD4 T_{ChAT} are controlled by neural signals in spleen [40], it is conceivable that modulation of neural signals by implanted nerve stimulators [185, 186] can control the activity also of blood pressure-regulating $ChAT^+$ lymphocytes. Furthermore, in future studies, it will be important to clarify whether therapies that reduce the $ChAT^+$ lymphocyte population cause hypertension.

T cells may also participate in the development of hypertension through mechanisms that involve chronic inflammation in the vasculature [187, 188]. Effector T subsets promote vascular infiltration of immune cells and vascular remodeling, and cause chronic increase in blood pressure, whereas regulatory T cells attenuate development of hypertension by reducing vascular inflammation [189, 190]. The isolation and characterization of CD4 ChAT now enables direct analysis of T cell subsets in mediating hypotension and hypertension. It is interesting to consider the function for different subsets of T cells in this context, and it has hitherto not been possible to assess the role of T_{ChAT} in this response [191, 192].

The findings in this study indicate that a deficiency in CD4 T_{ChAT} promotes hypertension and that bloodborne acetylcholine-releasing T cells lower blood pressure. In light of this discovery, it is now conceivable to consider whether acetylcholine-releasing cells can be manipulated in future therapeutic modalities for hypertension.

Figures

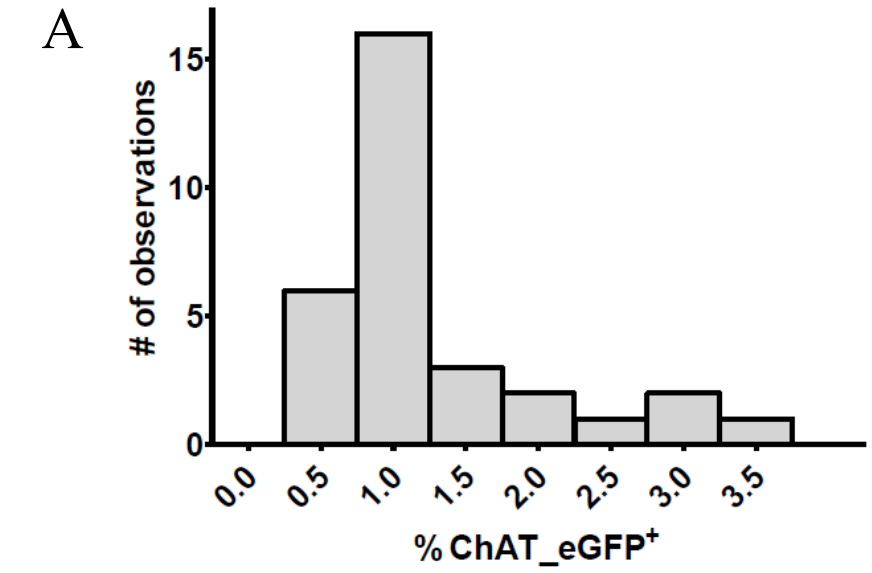
A
# of observations
15
10
5
0
0.0
0.5
1.0
1.5
2.0
2.5
3.0
3.5
% ChAT_eGFP+

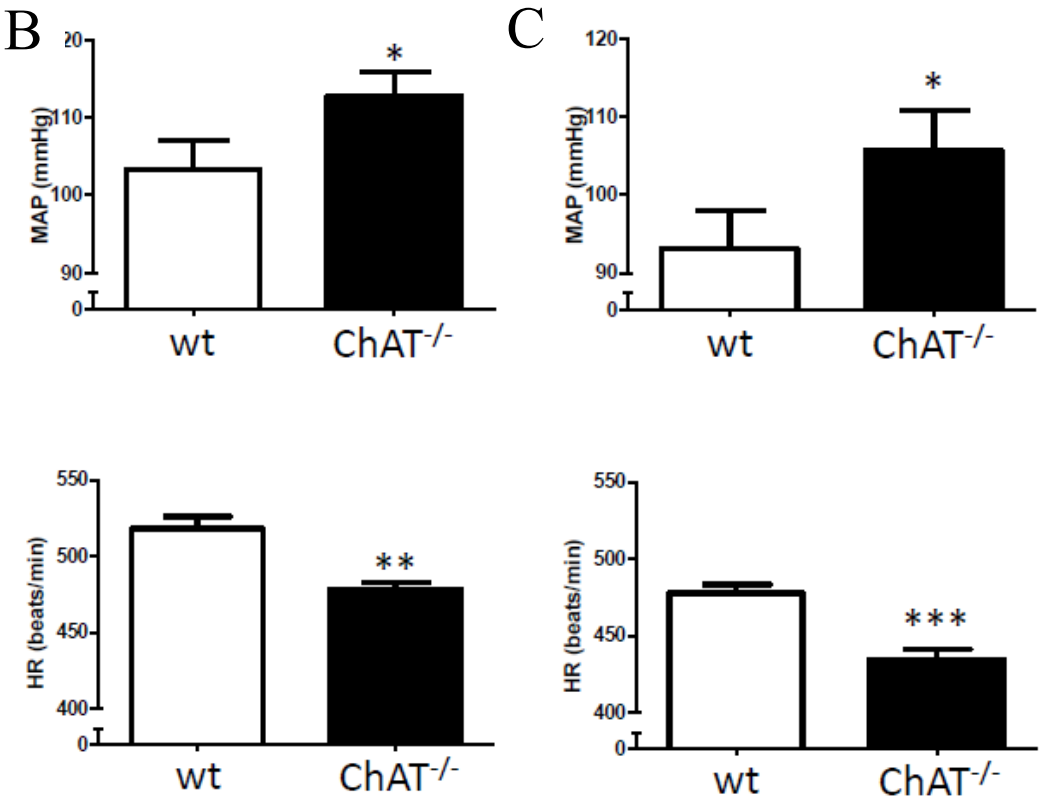
B
C
MAP (mmHg)
120
110
100
90
0
*
wt
ChAT-/-
HR (beats/min)
550
500
450
400
**
***

Figure 16 - Increased blood pressure in mice with genetic ablation of choline acetyltransferase+ $CD4^+$ cells.

A) Blood from ChAT-eGFP reporter mice 6-12 weeks of age obtained by tail bleed was analyzed by flow cytometry to determine the fraction of ChAT-$eGFP^+$ cells of $CD3^+$ cells. A histogram of the compiled data is plotted. B-C) Mean arterial blood pressure (MAP) and heart rate (HR) was measured using a tail cuff system in ChAT-deficient CD4-$Cre^{+/0}$ x $ChAT^{loxP/loxP}$ ($ChAT^{-/-}$) and their CD4-$Cre^{0/0}$ x $ChAT^{loxP/loxP}$ ($ChAT^{+/+}$) littermate controls at (B) six weeks of age (n=25 ChAT-deficient and 17 controls) and (C) 12 weeks of age (n=17 ChAT-deficient and 13 controls). Bars show mean ± SEM * - $P < 0.05$, ** - $P < 0.01$ (one-tailed Student's t test).

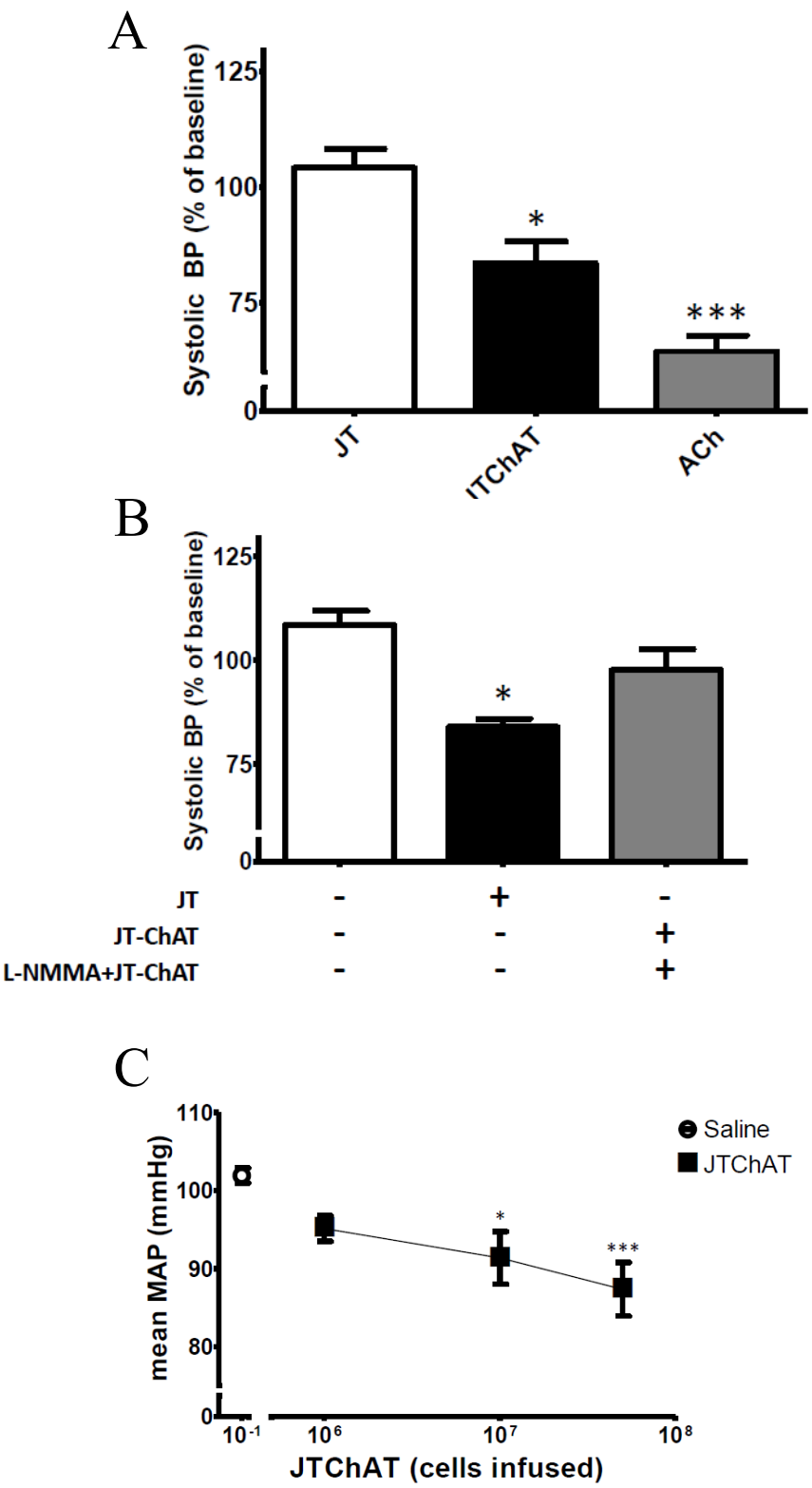
A
Systolic BP (% of baseline)
125
100
75
0
*
***
JT
JTChAT
ACh
B
Systolic BP (% of baseline)
125
100
75
0
*
JT - + -
JT-ChAT - - +
L-NMMA+JT-ChAT - - +
C
mean MAP (mmHg)
110
100
90
80
0
Saline
JTChAT
*
***
10-1
10⁶
10⁷
10⁸
JTChAT (cells infused)

D

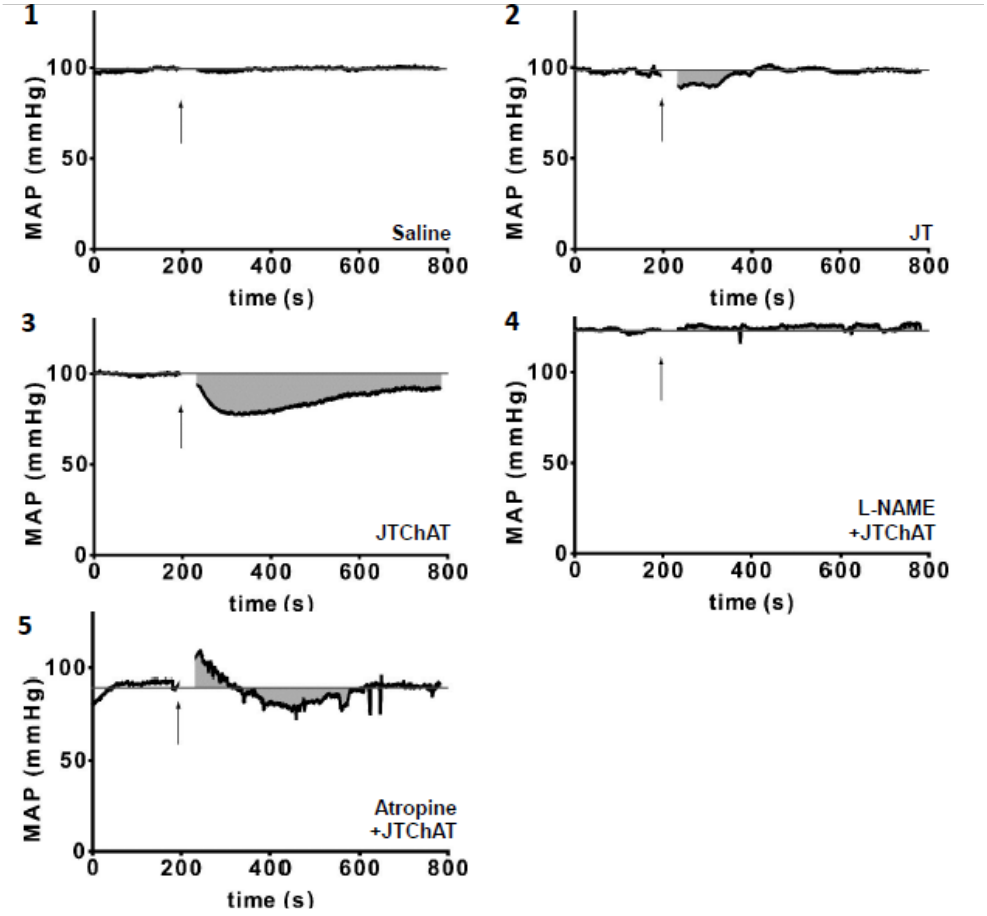
1
2
3
4
5
MAP (mmHg)
time (s)
Saline
JT
JTChAT
L-NAME
+JTChAT
Atropine
+JTChAT

E

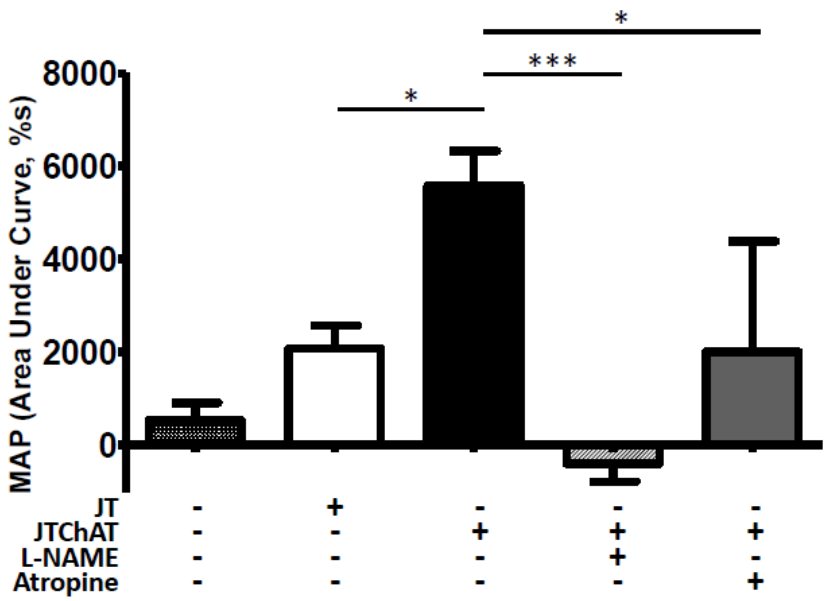
MAP (Area Under Curve, %s)
8000
6000
4000
2000
0
*
***
*
JT
JTChAT
L-NAME
Atropine

Figure 17 - Infusion of JT_{ChAT} lymphocytes lowers blood pressure.

A) Left ventricular blood pressure was monitored in anesthetized wild type mice and 2-3x106 Jurkat T lymphocytes (JT) (n=4), pCMV6-mChAT vector-transfected Jurkat T lymphocytes (JTChAT) (n=4) or 100 umol/kg acetylcholine (ACh)(n=3) injected into the left cardiac ventricle. The relative change in mean systolic blood pressure from baseline at 10-20 s after injection was plotted. B) Left cardiac ventricular blood pressure was monitored in anesthetized wild type mice. JT lymphocytes (n=2) or JTChAT lymphocytes were injected into the left cardiac ventricle without (n=6) or after (n=6) administration of L-NG-monomethyl arginine citrate (L-NMMA). The relative change in mean systolic blood pressure from baseline at 10 -20 s after injection was plotted. * - $p<0.05$, *** - $p<0.001$. "Systolic BP" denotes "mean systolic left ventricular end-systolic pressure". C-E) Mean arterial blood pressure was measured over time in a catheter inserted in the left carotid artery in anesthetized wild-type C57Bl/6 mice. C) Mean MAP over ~9 min. after infusion of JTChAT lymphocytes or saline. Open circle – saline (n=14). Closed squares - JTChAT (n=7-13). * - $p<0.05$, *** - $p<0.001$ JTChAT vs Saline by ANOVA followed by Bonferroni post-hoc test. D) Tracings of mean arterial pressure (MAP) over time in mice infused with (1) saline, (2) JT lymphocytes, or (3) JT_{ChAT} lymphocytes, or infusion of JT_{ChAT} lymphocytes after with (4) L-NAME or (5) atropine. Arrows indicate the time for infusion start. The cut in the tracings indicate the period of infusion-related measurement artifacts. E) Mean MAP change from baseline x time expressed as area under the curve ± SEM is shown for mice injected with saline (n=19), JT lymphocytes (n=13) or JT_{ChAT} lymphocytes (n=9). Mice were pre-treated with L-NAME (n=7) or atropine (n=8) as indicated. * - $p<0.05$, *** - $p<0.001$(ANOVA with Bonferroni post-hoc analysis).

A

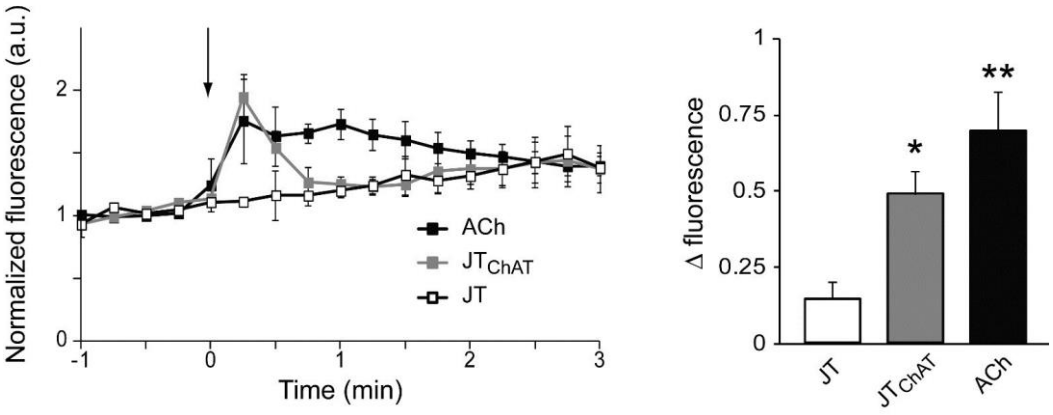
Normalized fluorescence (a.u.)
Time (min)
ACh
JTChAT
JT
Δ fluorescence
JT
JTChAT
ACh
*
**

B

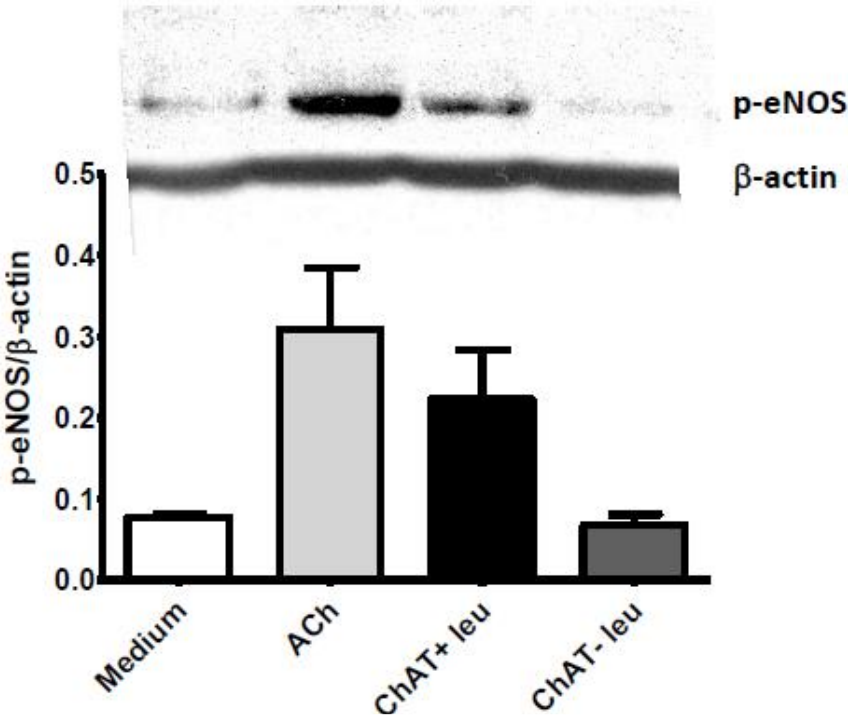
p-eNOS
β-actin
p-eNOS/β-actin
Medium
ACh
ChAT+ leu
ChAT- leu

C

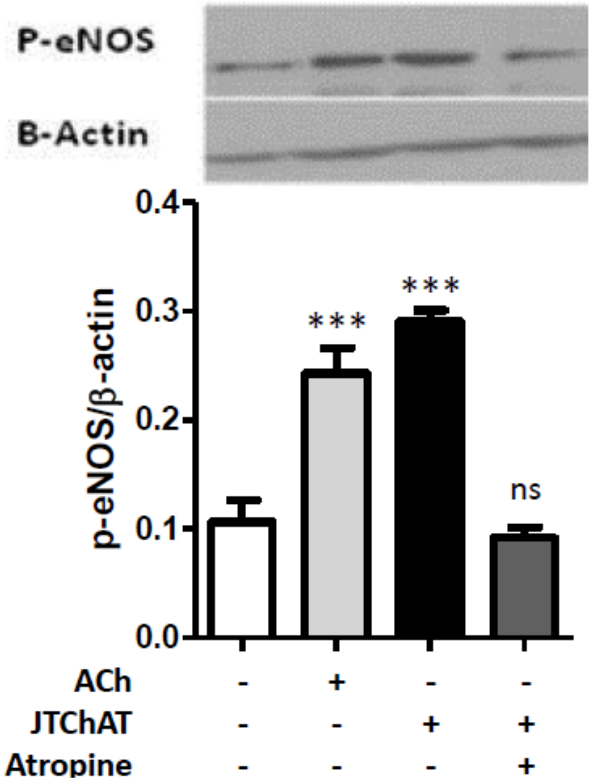
P-eNOS
B-Actin
p-eNOS/β-actin
0.4
0.3
0.2
0.1
0.0
***
***
ns
ACh - + - -
JTChAT - - + +
Atropine - - - +

D

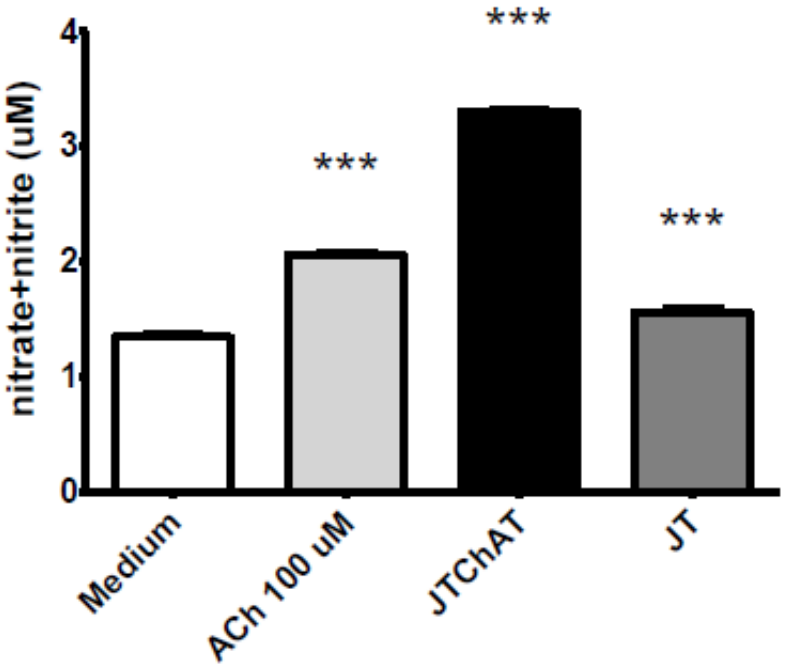
nitrate+nitrite (uM)
4
3
2
1
0
***
***
***
Medium
ACh 100 uM
JTChAT
JT

Figure 18 - $ChAT^+$ lymphocytes activate nitric oxide synthase in vascular endothelial cells.

A) Intracellular calcium levels were monitored in cultured murine primary endothelial cells using the calcium-sensitive fluorophore, Fluo-4. Left: Fluorescence was monitored by time-lapse microscopy, with a single field visualized in each experiment. Following acquisition of baseline fluorescence, cells were exposed to 0.1 mM acetylcholine (black), or co-cultured with 10^6/mL of either untransfected (white) or pCMV6-mChAT vector-transfected (grey) Jurkat T lymphocytes (JT_{ChAT}) at time=0, indicated by the arrow. Intracellular fluorescence normalized to the average baseline value was extracted for each cell contained within the field of view. Individual cell data was then averaged for each experiment. Data is plotted as mean ± SEM for n=3 experiments per condition. Right: To quantify the treatment response, the average fluorescence in the one-minute intervals immediately before and after treatment was calculated. The difference in fluorescence pre- and post-treatment is plotted for each condition, which were significantly different (ANOVA P=0.015). Post-hoc Fisher LSD analysis revealed that the intracellular calcium responses of endothelium either treated with acetylcholine or co-cultured with JT_{ChAT} lymphocytes were significantly greater than endothelium co-cultured with the untransfected Jurkat T lymphocytes (JT) (** $P<0.01$ and * $P<0.05$, respectively). No significant difference was observed between acetylcholine and JT_{ChAT} lymphocytes treatments (P=0.16). B) HPMEC-ST1.6R endothelial cells were exposed in vitro to 0.1 mM acetylcholine, or co-cultured with $ChAT^+$ or $ChAT^-$ leukocytes (leu) isolated from ChAT-eGFP reporter mice by cell sorting. Phosphorylation of Ser1177 eNOS (p-eNOS) was measured by Western blot (insert). Beta-actin-normalized p-eNOS levels are shown in the bar graph as mean ± SEM (n=2). C) HPMEC-ST1.6R endothelial cells were exposed in vitro to 0.1 mM acetylcholine, or co-cultured with JT_{ChAT} lymphocytes in the presence or absence of atropine. Phosphorylation of Ser1177 eNOS (p-eNOS) was measured by Western blot (insert). Beta-actin-normalized p-eNOS levels are shown in the bar graph as mean ± SEM (n=2-3 per group). *** - $p < 0.001$ by one-way ANOVA followed by Dunnet's post-hoc analysis. D) Nitrate and nitrite in medium from HPMEC-ST1.6R endothelial cells exposed to 0.1 mM acetylcholine, or co-cultured with JT or JT_{ChAT} lymphocytes. Mean ± SEM of [nitrate+nitrite] is shown. *** - $p<0.001$ (ANOVA followed by Dunnet's post-hoc test).

Acknowledgements

A manuscript detailing this work was written by Peder S Olofsson.

I contributed to this work by designing and constructing the $ChAT^{+}$ Jurkat T lymphocytes. I also participated in design and analysis of the blood pressure experiments.

Chapter 5 – Optogenetic Control of T Cell Responses

Abstract

During inflammation, the CNS modulates immune responses through vagal nerve signals directed to the spleen through the celiac ganglion, where norepinephrine is released, and inducing acetylcholine release by choline acetyltransferase-expressing T cells, which acts on acetylcholine receptors on macrophages to suppress inflammatory cytokine release. Study of the mechanism for norepinephrine-induced release of acetylcholine by T cells *in vivo* has been hindered by the fact that many immune cells express norepinephrine receptors. Additionally timing of receptor activation relative to T cell activation can have disparate effects. To overcome these challenges, we turned to a novel technique first utilized in the neuroscience field, optogenetics, which uses light-sensitive receptors to modulate intracellular signals. We inserted a fusion of the extracellular portion of bovine rhodopsin and the intracellular portion of the β2-adrenergic receptor into T cells, where we found light-dose sensitive changes in intracellular cAMP. In addition, when stimulated with light, the T cells produced decreased levels of IL-2, and when media conditioned by these cells was added to a macrophage-like cell line, inflammatory cytokine production was inhibited, recapitulating the effects of the native receptor. These data indicate the validity of a novel tool for studying the effects of norepinephrine nerve signals on T cell immune function.

*References are found under Cited Literature, beginning on page 104

Introduction

Neural reflex circuits regulate immune responses and cytokine release to prevent potentially damaging inflammation and maintain homeostasis. The inflammatory reflex modulates inflammation in response to invasion and tissue injury with signals that originate in the central nervous system (CNS) and travel through the vagus nerve [6, 23, 37-39]. CNS signals originate in the nucleus tractus solitarious, which is connected to the dorsal motor nucleus of the vagus (DMN), where the efferent fibers of the vagus originate. Vagal signals travel to the celiac ganglion, then through adrenergic neurons to the spleen. In the spleen, norepinephrine is released at synapses [41]. This release of norepinephrine is associated with β2-adrenergic receptor-mediated reduction in lipopolysaccharide-induced TNF secretion [34]. This reduction in TNF is dependent on the expression of α7 nicotinic acetylcholine receptors (α7 nAChR) on macrophages [42]. The source of β2-adrenergic receptor-mediated acetylcholine remained a mystery until a few years ago when it was discovered that a subset of splenic T cells release acetylcholine in response to β2-adrenergic receptor signaling [40].

Study of the β2-adrenergic receptor signaling pathways and their role in T cell responses *in vivo* and on a temporal scale has been impossible thus far. β2-adrenergic signaling is involved in a variety of immune system functions, making isolation of the effects on specific T cells impossible. β2-adrenergic receptor activation of macrophages can inhibit lipopolysaccharide-induced cytokine expression [193, 194]. Timing of β2-adrenergic signaling in T cell is also important, as activation before activation of the T cell receptor has different cellular effects than activation after [74, 77, 195]. These temporal effects are

difficult to study in a system that relies on delivery of ligands and inherent issues of diffusion and bioavailability.

To enable precise and specific study of $ChAT^{+}$ T cell β2-adrenergic receptor activation, we turned to a novel tool being developed in the neuroscience field: optogenetics. Optogenetics is a technique developed by Karl Deisseroth's group, involving the use of light to activate receptors in genetically modified cells. Application of light induced neuronal activity in cultured primary mouse neurons expressing channelrhodopsin (ChR2), a light-activated cation channel isolated from algae [196, 197]. We utilized this technology to create ChAT-expressing that express a light-responsive β2-adrenergic receptor (opto-B2AR). Opto-B2AR is a fusion of the intracellular portions of the β2-adrenergic receptor and the transmembrane and extracellular portions of bovine rhodopsin [198]. When activated with 505nm (blue-green) light, intracellular cAMP is increased, mimicking activation with β2-adrenergic receptor molecular ligands [198]. Here, the first characterization and use of a light controlled β2-adrenergic receptor in a T lymphocyte population is described.

Methods

Cell culture

Jurkat (ATCC) and ChAT^{Hi} Jurkat cells, discussed in the previous chapter, were cultured at 37C in 5%CO_2 in RPMI supplemented with 5% fetal bovine serum (FBS) and penicillin-streptomycin (Gibco). RAW 264.7 cells (ATCC) were grown in DMEM with 5% fetal bovine serum (FBS) and penicillin-streptomycin.

Primary murine CD4+ T Cell Isolation

Spleens were extracted from 6-8 week-old Balb/c mice and isolated into a single cell suspension by straining through 40 um mesh followed by erythrocyte lysis with ACK Lysing Buffer (Thermo Fisher Scientific). CD4+ T lymphocytes were negatively selected from total splenocytes using a magnetic bead isolation kit (Miltenyi Biotec).

Lentivirus

Plasmids used were pCMVR8.74, pMD2.G, and pLenti-OptoB2AR-IRES-EYFP-WPI (Addgene) 293T cells were grown to 50% confluency, and a mixture of the plasmid and Lipofectamine LTX (Thermo Fisher Scientific) was added to the media. After 24 hours, media was collected and replaced. After an additional 24 hours, media was pooled and spun down by ultracentrifuge to collect vial pellet. Virus was added to 10 million primary CD4 T cells, Jurkat, or ChAT^{Hi}

Jurkat cells in 500 mL media and spun for 2 hours at 2,000 x g at 32C. Media was replaced and fluorescent protein expression was verified by microscopy.

Light stimulation

1X10^6 Opto-B2AR ChAT^{Hi} Jurkat cells in 0.1 mL PBS were placed in an 1.5 mL Eppendorf tube and light stimulation was applied with either 473nm laser (Opto Engine) or 505nm high intensity LED (Thorlabs) as indicated. Max power density of the laser was 200mW/cm^2 and 80mW/cm^2 for the LED.

IL-2 was measured after concanavalin A (10ug/ml) plus light stimulation for 12 hours. Forskolin was utilized as a positive control for increased cAMP. IL-2 levels were determined by ELISA (R&D Systems). cAMP levels were determined by competitive ELISA (R&D Systems) at time points as indicated.

Endotoxin-induced TNF

Opto-B2AR ChAT^{Hi} Jurkat cells were incubated in PBS for 4 hours with 0, 5min. or 4 hours of stimulation starting at time 0. Cells were spun down and media applied to RAW 264.7 cells. After 15 minutes of incubation, 0.1 ng/mL lipopolysaccharide (final concentration) was added to the cells. 4 hours later, media was collected and analyzed for mTNF production by ELISA (R&D Systems).

Statistics

cAMP, IL-2, and mTNF levels were analyzed by one-way ANOVA followed by Tukey post-test. Statistical analyses were performed using Graphpad Prism 6 software. All tests with a *p* value of less than .05 were considered

statistically significant. Unless otherwise stated, all numbers are given as average ± standard error of the mean. In graphs, "*" indicates $p<0.05$, "**" indicates $p<0.01$, "***" indicates $p<0.001$, and "****" indicates $p<0.0001$.

Results

Opto-B2AR expression on T lymphocytes induces light-dependent cAMP production

To determine the effects of optogenetic control of B2-AR signaling, Jurkat T lymphocytes were transduced by lentivirus to express an opto-B2AR chimeric receptor. When these cells were exposed to light, intracellular cAMP levels were increased (Figure 19A). When exposed to increasing powers of light, we found that this increase in cAMP was light dose-dependent (Figure 19B). Intracellular cAMP was also regulated by the time of light exposure with a peak at ≈10 min (Figure 19C).

Activation of beta-2 adrenergic receptors in ChAT+ T lymphocytes modulates IL-2 production

Activation of B2-AR inhibits T cell IL-2 production after activation of the TCR [77, 195, 199]. To ensure that opto-B2AR recapitulates this phenomenon, we stimulated Opto-B2AR Jurkat cells were stimulated with concanavalin A (10ug/ml) and light (80 mW/cm^2, 505 nm) was administered for one minute at time 0 or for the entire 12 hours. Similar inhibition of IL-2 was observed between cells administered forskolin and light (dark, 823.6± 17.68 pg/mL; forskolin, 31.02±2.943 pg/mL; and light, 101.2±3.265, $p< 0.0001$ by one-way ANOVA)

(Figure 20 - Light activation of optoB2AR inhibits IL-2 production). Even a single minute of stimulation at time 0 was sufficient to inhibit IL-2 production (dark, 823.6± 17.68 pg/mL; one minute, 494.6± 7.067pg/mL, $p<0.001$ by Tukey post-test) (Figure 20).

Activation of beta-2 adrenergic receptors in ChAT+ T lymphocytes inhibits endotoxin-induced macrophage TNF release

To investigate the role of β2-AR signaling in suppression of immune responses, opto-B2AR virus-transduced primary CD4+ T cells were light stimulated (80 mW/cm^2, 505 nm) in RPMI for 4 hours and the supernatant was applied to RAW 264.7 cells. LPS was added after 15 minutes hour and media was collected for TNF production analysis 4 hours later. Supernatant from light-exposed cells significantly reduced endotoxin-induced TNF release from RAW cells (dark, 713.6 ± 14.80 pg/mL; 5 minutes light, 354.7 ± 5.98 pg/mL; 4 Hours light 527.9 ± 42.72 pg/mL; $p<0.01$ by one-way ANOVA) (Figure 21).

Discussion

Here, a novel tool for the analysis of B2AR function in T cell responses has been described. The use of a light-responsive receptor allows for temporal and spatial activation of the T cells alone. Previous studies have suggested that B2AR activation can produce different results depending on whether the activation was before or after activation of the T cell receptor [77, 195]. Future studies can now focus on effects of activation timing without the concerns arising from molecular ligands, such as diffusion and inability to completely wash out. In addition, future studies should focus on *in situ* activation within the body. Application of light to a site of injury or inflammation may produce different effects than application at the spleen. This technology allows for discernment of the contribution of local factors that control inflammation progression and restriction.

This tool also provides for future therapeutic applications. Modified T cells could be switched on and off in inflammatory disease as necessary. For example, light could be applied to restrict T cell activation during arthritic flares, and removed to eliminate concerns of immunosuppression. In addition, this would allow targeting of specific organs involved in pathology, while leaving the rest of the body unaffected.

Figures

A

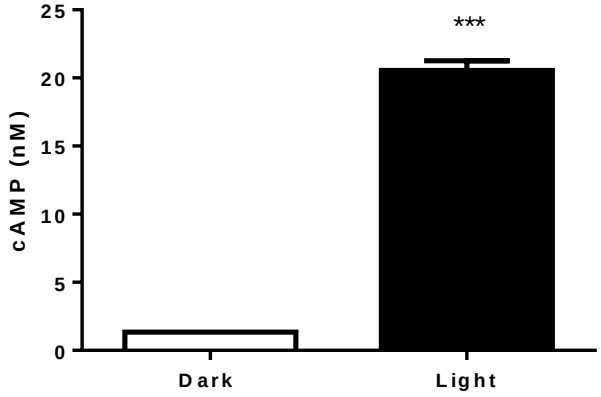
25
20
15
10
5
0
cAMP (nM)
***
Dark
Light

B

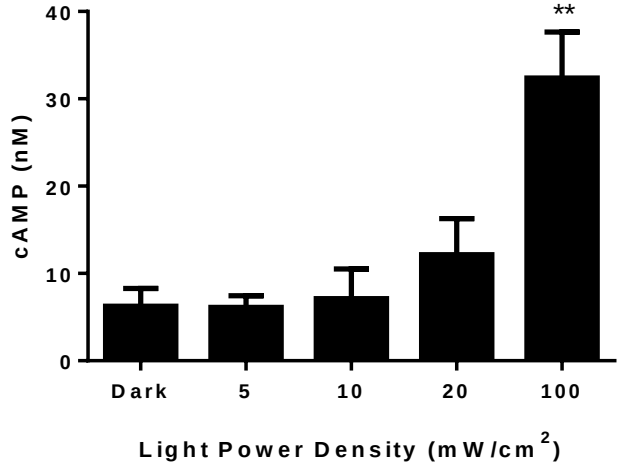
40
30
20
10
0
cAMP (nM)
**
Dark
5
10
20
100
Light Power Density (mW/cm2)

C

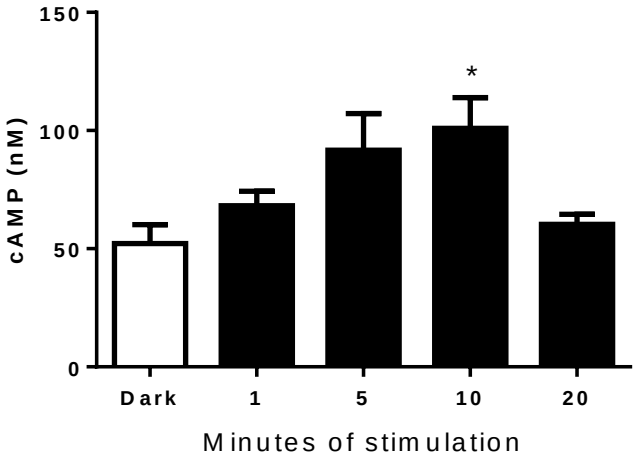
150
100
50
0
cAMP (nM)
*
Dark
1
5
10
20
Minutes of stimulation

Figure 19 - T cell cAMP is increased by light stimulation

Jurkat cells expressing opto-B2AR were exposed to light for one hour, followed by lysis and cAMP analysis. A) Application of 7mW/cm^2 505nm light induced increases in cAMP. B) Application of increasing light power of 473 nm light induced a dose-dependent increase in cAMP. C) cAMP is regulated by light exposure time.

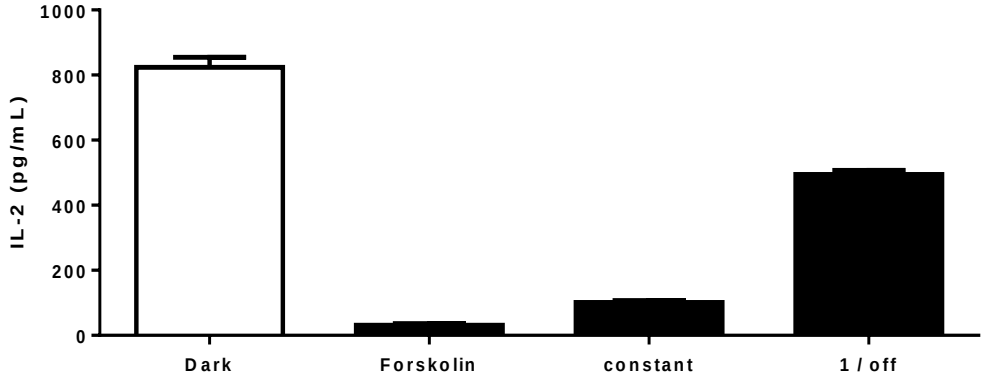
1000
800
600
400
200
0
IL-2 (pg/mL)
Dark
Forskolin
constant
1 / off

Figure 20 - Light activation of optoB2AR inhibits IL-2 production

OptoB2AR Jurkats were activated with concanavalin A (10 ug/mL) and administered light (80 mW/cm^2, 505 nm) for 12 hours. IL-2 production in the supernatant was quantified by ELISA.

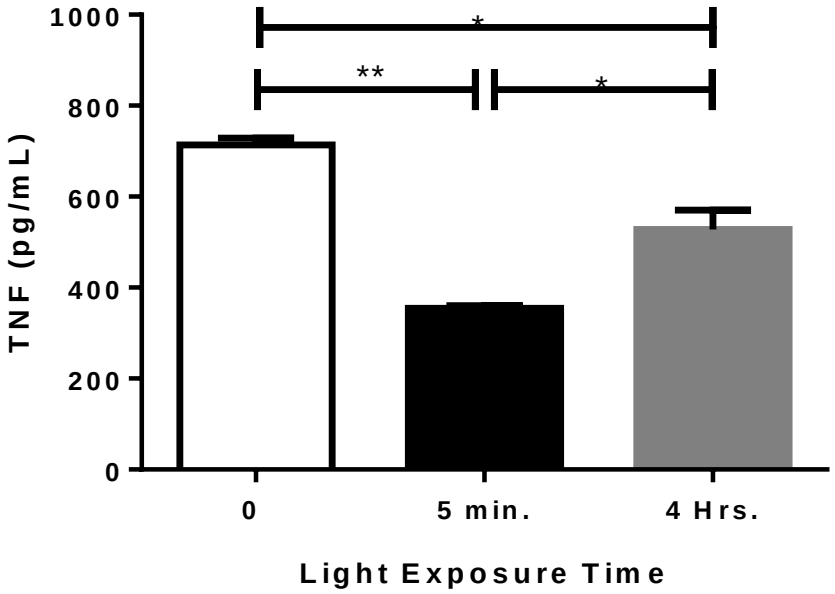
1000
800
600
400
200
0
TNF (pg/mL)
*
**
*
0
5 min.
4 Hrs.
Light Exposure Time

Figure 21 - Activation of opto-B2AR modulates immune responses

Primary CD4+ T cells were transduced with opto-B2AR lentivirus. These cells were incubated with light stimulation and the supernatant was transferred to RAW cells. After 15 minutes of preincubation, LPS was added (0.1 ng/mL) and 4 hours later the supernatant was analyzed for TNF release. Light stimulation of the T cells reduced the amount of TNF released in response to endotoxin.

Acknowledgements

This work was supported by Kevin Kwan, who provided technical assistance with many of the experiments in this chapter. Yehuda Tamari and Andrew Stiegler assisted with construction of LED arrays.

Chapter 6 – Discussion

Within the previous chapters, I have outlined several examples of previously described mechanisms for neural-immune communication, including the well-characterized inflammatory reflex. I have also described novel findings from my own research in interactions between the nervous and immune systems.

Herein, I have revealed the discovery of a novel reflex arc in the nervous system response to immunized antigen. The ability to monitor and control this circuit should provide many therapeutic interventions. In addition, the nervous system is likely to initiate many other responses after detection of antigen to alert the immune system to potential invaders. Future studies should focus on these response mechanisms, as they may provide insights on responses to infections, as well as inappropriate responses, such as allergy.

Use of the pharmaceutical compound galantamine, known to stimulate through the vagus nerve, to delay type 1 diabetes is an example of repurposing well-known drugs for new uses. The fact that the drug inhibited disease-specific immune responses with precision indicates that much remains to be learned about immune responses. Further study should focus on the specific cells that are responding to neuronal input, and the tissue site of interaction, whether spleen, lymph node, or pancreas.

The discovery that T cells could serve as the intermediaries for neuronal-vascular communication. T_{Chat} cells are a novel subset of T cells, first discovered in their role in the inflammatory reflex as translating adrenergic signals into cholinergic to inhibit macrophage TNF production. Their ability to retain,

translate and transmit neuronal signals puts them in a prime location to communicate nervous signals to locations that are not innervated, while providing some checkpoint controls.

While we understand the intracellular mechanisms of β2-AR signaling, it is difficult to study the role of this receptor in the T cell in specific areas of the body and with sufficient temporal resolution. No T cell-specific ligand exists to allow for the study of these cells *in situ*, as any ligand would activate numerous other cells that also express the β2-AR. Use of opto-B2AR allows for temporal and spatial analysis of these populations in health and disease in various tissues of the body. Further research will focus on these aspects, as well as optimization of the signal parameters to more finely control responses.

Bioelectronic medicine aims to treat ailments by controlling the electrical impulses of nerves throughout the body. While this field is still in its infancy, revolutionary advances in understanding and application are already being discovered. The discoveries that I have described herein serve as the framework for much advancement to come.

Cited Literature

1. Tonkoff, W., *Zur Kenntnis der Nerven der Lymphdrüsen.* Anat Anz, 1899. **16**: p. 456-459.

2. Burn, J.H. and M.J. Rand, *Sympathetic postganglionic cholinergic fibres. 1959.* Br J Pharmacol, 1997. **120**(4 Suppl): p. 181-91; discussion 179-80.

3. Crosby, E.C., *Correlative anatomy of the nervous system*. 1962: Macmillan.

4. Ruch, T.C. and J.F. Fulton, *Medical Physiology and biophysics.* Academic Medicine, 1960. **35**(11): p. 1067.

5. Watkins, L.R., et al., *Blockade of interleukin-1 induced hyperthermia by subdiaphragmatic vagotomy: evidence for vagal mediation of immune-brain communication.* Neurosci Lett, 1995. **183**(1-2): p. 27-31.

6. Andersson, U. and K.J. Tracey, *Neural reflexes in inflammation and immunity.* J Exp Med, 2012. **209**(6): p. 1057-68.

7. Abbas, A.K., A.H. Lichtman, and S. Pillai, *Cellular and Molecular Immunology*. 2014: Elsevier Health Sciences.

8. Murphy, K.M., *Janeway's immunobiology*. 2011: Garland Science.

9. Nimmerjahn, F. and J.V. Ravetch, *Fcγ receptors: old friends and new family members.* Immunity, 2006. **24**(1): p. 19-28.

10. Nimmerjahn, F. and J.V. Ravetch, *Fcγ receptors as regulators of immune responses.* Nature Reviews Immunology, 2008. **8**(1): p. 34-47.

11. Huang, Z.-Y., et al., *The effect of phosphatases SHP-1 and SHIP-1 on signaling by the ITIM-and ITAM-containing Fcγ receptors FcγRIIB and FcγRIIA.* Journal of leukocyte biology, 2003. **73**(6): p. 823-829.

12. Kurosaki, T., K. Kometani, and W. Ise, *Memory B cells.* Nat Rev Immunol, 2015. **15**(3): p. 149-159.

13. Margaris, K.N. and R.A. Black, *Modelling the lymphatic system: challenges and opportunities.* Journal of The Royal Society Interface, 2012. **9**(69): p. 601-612.

14. Cueni, L.N. and M. Detmar, *The lymphatic system in health and disease.* Lymphat Res Biol, 2008. **6**(3-4): p. 109-22.

15. Alitalo, K., *The lymphatic vasculature in disease.* Nat Med, 2011. **17**(11): p. 1371-80.

16. Swartz, M.A. and A.W. Lund, *Lymphatic and interstitial flow in the tumour microenvironment: linking mechanobiology with immunity.* Nat Rev Cancer, 2012. **12**(3): p. 210-9.

17. Gould, H.J., et al., *The biology of IgE and the basis of allergic disease.* Annu Rev Immunol, 2003. **21**(1): p. 579-628.

18. Orban, T., et al., *Pancreatic islet autoantibodies as predictors of type 1 diabetes in the Diabetes Prevention Trial-Type 1.* Diabetes Care, 2009. **32**(12): p. 2269-74.

19. Li, J., et al., *Efficacy of B cell depletion therapy for murine joint arthritis flare is associated with increased lymphatic flow.* Arthritis & Rheumatism, 2013. **65**(1): p. 130-138.

20. Nakai, A., et al., *Control of lymphocyte egress from lymph nodes through beta2-adrenergic receptors.* J Exp Med, 2014. **211**(13): p. 2583-98.

21. Steinman, L., *Elaborate interactions between the immune and nervous systems.* Nat Immunol, 2004. **5**(6): p. 575-581.

22. Chiu, I.M., C.A. von Hehn, and C.J. Woolf, *Neurogenic inflammation and the peripheral nervous system in host defense and immunopathology.* Nat Neurosci, 2012. **15**(8): p. 1063-7.

23. Tracey, K.J., *The inflammatory reflex.* Nature, 2002. **420**(6917): p. 853-9.

24. Sundman, E. and P.S. Olofsson, *Neural control of the immune system.* Adv Physiol Educ, 2014. **38**(2): p. 135-9.

25. Felten, D.L., et al., *Sympathetic innervation of lymph nodes in mice.* Brain Res Bull, 1984. **13**(6): p. 693-9.

26. Goehler, L.E., et al., *Vagal immune-to-brain communication: a visceral chemosensory pathway.* Auton Neurosci, 2000. **85**(1-3): p. 49-59.

27. Popper, P., et al., *The localization of sensory nerve fibers and receptor binding sites for sensory neuropeptides in canine mesenteric lymph nodes.* Peptides, 1988. **9**(2): p. 257-67.

28. Elenkov, I.J., et al., *The sympathetic nerve—an integrative interface between two supersystems: the brain and the immune system.* Pharmacological reviews, 2000. **52**(4): p. 595-638.

29. Kipnis, J., et al., *Dopamine, through the extracellular signal-regulated kinase pathway, downregulates CD4+ CD25+ regulatory T-cell activity: implications for neurodegeneration.* The Journal of neuroscience, 2004. **24**(27): p. 6133-6143.

30. Pacheco, R., C. Prado, and F. Contreras, *Cells, molecules and mechanisms involved in the neuro-immune interaction*. 2012: INTECH Open Access Publisher.

31. Prado, C., et al., *Stimulation of dopamine receptor D5 expressed on dendritic cells potentiates Th17-mediated immunity.* J Immunol, 2012. **188**(7): p. 3062-70.

32. Wong, C.H.Y., et al., *Functional innervation of hepatic iNKT cells is immunosuppressive following stroke.* Science, 2011. **334**(6052): p. 101-105.

33. Grebe, K.M., et al., *Sympathetic nervous system control of anti-influenza CD8+ T cell responses.* Proc Natl Acad Sci U S A, 2009. **106**(13): p. 5300-5.

34. Kees, M.G., et al., *Via beta-adrenoceptors, stimulation of extrasplenic sympathetic nerve fibers inhibits lipopolysaccharide-induced TNF secretion in perfused rat spleen.* J Neuroimmunol, 2003. **145**(1-2): p. 77-85.

35. Miura, T., et al., *Effect of 6-hydroxydopamine on host resistance against Listeria monocytogenes infection.* Infect Immun, 2001. **69**(12): p. 7234-41.

36. Straub, R.H., et al., *Neuronally released sympathetic neurotransmitters stimulate splenic interferon-gamma secretion from T cells in early type II collagen-induced arthritis.* Arthritis Rheum, 2008. **58**(11): p. 3450-60.

37. Tracey, K.J., *Physiology and immunology of the cholinergic antiinflammatory pathway.* J Clin Invest, 2007. **117**(2): p. 289-96.

38. Borovikova, L.V., et al., *Role of vagus nerve signaling in CNI-1493-mediated suppression of acute inflammation.* Auton Neurosci, 2000. **85**(1-3): p. 141-7.

39. Borovikova, L.V., et al., *Vagus nerve stimulation attenuates the systemic inflammatory response to endotoxin.* Nature, 2000. **405**(6785): p. 458-62.

40. Rosas-Ballina, M., et al., *Acetylcholine-synthesizing T cells relay neural signals in a vagus nerve circuit.* Science, 2011. **334**(6052): p. 98-101.

41. Felten, S.Y. and J. Olschowka, *Noradrenergic sympathetic innervation of the spleen: II. Tyrosine hydroxylase (TH)-positive nerve terminals form synapticlike contacts on lymphocytes in the splenic white pulp.* J Neurosci Res, 1987. **18**(1): p. 37-48.

42. Wang, H., et al., *Nicotinic acetylcholine receptor α7 subunit is an essential regulator of inflammation.* Nature, 2003. **421**(6921): p. 384-388.

43. Lu, B., et al., *α7 Nicotinic Acetylcholine Receptor Signaling Inhibits Inflammasome Activation by Preventing Mitochondrial DNA Release.* Molecular Medicine, 2014. **20**(1): p. 350-358.

44. Mina-Osorio, P., et al., *Neural signaling in the spleen controls B-cell responses to blood-borne antigen.* Mol Med, 2012. **18**(1): p. 618-27.

45. Hanes, W.M., et al., *Galantamine Attenuates Type 1 Diabetes and Inhibits Anti-Insulin Antibodies in Non-Obese Diabetic Mice.* Mol Med, 2015.

46. Chiu, I.M., et al., *Bacteria activate sensory neurons that modulate pain and inflammation.* Nature, 2013. **501**(7465): p. 52-7.

47. Andoh, T. and Y. Kuraishi, *Direct action of immunoglobulin G on primary sensory neurons through Fc gamma receptor I.* FASEB J, 2004. **18**(1): p. 182-4.

48. Andoh, T. and Y. Kuraishi, *Expression of Fc epsilon receptor I on primary sensory neurons in mice.* Neuroreport, 2004. **15**(13): p. 2029-31.

49. van der Kleij, H., et al., *Evidence for neuronal expression of functional Fc (epsilon and gamma) receptors.* J Allergy Clin Immunol, 2010. **125**(3): p. 757-60.

50. Qu, L., *Neuronal Fc gamma receptor I as a novel mediator for IgG immune complex-induced peripheral sensitization.* Neural Regen Res, 2012. **7**(26): p. 2075-9.

51. Bisno, A.L. and D.L. Stevens, *Streptococcal infections of skin and soft tissues.* N Engl J Med, 1996. **334**(4): p. 240-5.

52. Iannacone, M., et al., *Subcapsular sinus macrophages prevent CNS invasion on peripheral infection with a neurotropic virus.* Nature, 2010. **465**(7301): p. 1079-1083.

53. Cole, J.N., et al., *Molecular insight into invasive group A streptococcal disease.* Nat Rev Microbiol, 2011. **9**(10): p. 724-36.

54. Vindenes, T. and D. McQuillen, *Images in clinical medicine. Acute lymphangitis.* N Engl J Med, 2015. **372**(7): p. 649.

55. Gonzalez, R.J., et al., *Dissemination of a highly virulent pathogen: tracking the early events that define infection.* PLoS pathogens, 2015. **11**(1).

56. Itano, A.A., et al., *Distinct dendritic cell populations sequentially present antigen to CD4 T cells and stimulate different aspects of cell-mediated immunity.* Immunity, 2003. **19**(1): p. 47-57.

57. Sixt, M., et al., *The conduit system transports soluble antigens from the afferent lymph to resident dendritic cells in the T cell area of the lymph node.* Immunity, 2005. **22**(1): p. 19-29.

58. Moe, R.E., *Electron Microscopic Appearance of the Parenchyma of Lymph Nodes.* Am J Anat, 1964. **114**(2): p. 341-69.

59. Roozendaal, R., et al., *Conduits mediate transport of low-molecular-weight antigen to lymph node follicles.* Immunity, 2009. **30**(2): p. 264-76.

60. Inaba, K., et al., *Efficient presentation of phagocytosed cellular fragments on the major histocompatibility complex class II products of dendritic cells.* J Exp Med, 1998. **188**(11): p. 2163-73.

61. Manickasingham, S. and C. Reis e Sousa, *Microbial and T cell-derived stimuli regulate antigen presentation by dendritic cells in vivo.* J Immunol, 2000. **165**(9): p. 5027-34.

62. Germain, R.N., *MHC-dependent antigen processing and peptide presentation: providing ligands for T lymphocyte activation.* Cell, 1994. **76**(2): p. 287-99.

63. Rajewsky, K., *Clonal selection and learning in the antibody system.* Nature, 1996. **381**(6585): p. 751-8.

64. Nossal, G.J.V., et al., *Antigens in immunity: VIII. Localization of (125)I-labelled antigens in the secondary response.* Immunology, 1965. **9**(4): p. 349-357.

65. Ada, G.L. and P.G. Lang, *Antigen in tissues: II. State of antigen in lymph node of rats given isotopically-labelled flagellin, haemocyanin or serum albumin.* Immunology, 1966. **10**(5): p. 431-443.

66. Lang, P.G. and G.L. Ada, *Antigen in tissues. IV. The effect of antibody on the retention and localization of antigen in rat lymph nodes.* Immunology, 1967. **13**(5): p. 523-34.

67. Shepherd, A.J., J.E. Downing, and J.A. Miyan, *Without nerves, immunology remains incomplete -in vivo veritas.* Immunology, 2005. **116**(2): p. 145-63.

68. Felten, D.L., et al., *Noradrenergic and peptidergic innervation of lymphoid tissue.* J Immunol, 1985. **135**(2 Suppl): p. 755s-765s.

69. Novotny, G.E. and K.O. Kliche, *Innervation of lymph nodes: a combined silver impregnation and electron-microscopic study.* Acta Anat (Basel), 1986. **127**(4): p. 243-8.

70. Villaro, A.C., M.P. Sesma, and J.J. Vazquez, *Innervation of mouse lymph nodes: nerve endings on muscular vessels and reticular cells.* Am J Anat, 1987. **179**(2): p. 175-85.

71. Fink, T. and E. Weihe, *Multiple neuropeptides in nerves supplying mammalian lymph nodes: messenger candidates for sensory and autonomic neuroimmunomodulation?* Neurosci Lett, 1988. **90**(1-2): p. 39-44.

72. Bellinger, D., et al. *Noradrenergic innervation and acetylcholinesterase activity of lymph nodes in young adult and aging mice*. in *Soc Neurosci Abstr*. 1985.

73. Felten, S.Y. and D.L. Felten, *Innervation of lymphoid tissue.* Psychoneuroimmunology, 1991. **27**.

74. Feldman, R.D., G.W. Hunninghake, and W.L. McArdle, *Beta-adrenergic-receptor-mediated suppression of interleukin 2 receptors in human lymphocytes.* J Immunol, 1987. **139**(10): p. 3355-9.

75. Elenkov, I.J., et al., *Modulation of Lipopolysaccharide-Induced Tumor-Necrosis-Factor-Alpha Production by Selective Alpha-Adrenergic and Beta-Adrenergic Drugs in Mice.* Journal of Neuroimmunology, 1995. **61**(2): p. 123-131.

76. Benschop, R.J., et al., *Adrenergic control of natural killer cell circulation and adhesion.* Brain Behav Immun, 1997. **11**(4): p. 321-32.

77. Sanders, V.M., et al., *Differential expression of the beta2-adrenergic receptor by Th1 and Th2 clones: implications for cytokine production and B cell help.* J Immunol, 1997. **158**(9): p. 4200-10.

78. Hosoi, J., et al., *Regulation of Langerhans cell function by nerves containing calcitonin gene-related peptide.* Nature, 1993. **363**(6425): p. 159-63.

79. Ding, W., et al., *Calcitonin gene-related peptide biases Langerhans cells toward Th2-type immunity.* J Immunol, 2008. **181**(9): p. 6020-6.

80. Sun, J., et al., *Neuronal GPCR controls innate immunity by regulating noncanonical unfolded protein response genes.* Science, 2011. **332**(6030): p. 729-32.

81. Zugasti, O. and J.J. Ewbank, *Neuroimmune regulation of antimicrobial peptide expression by a noncanonical TGF-beta signaling pathway in Caenorhabditis elegans epidermis.* Nat Immunol, 2009. **10**(3): p. 249-56.

82. Nimmerjahn, F. and J.V. Ravetch, *Fc-Receptors as Regulators of Immunity*, in *Advances in Immunology*. 2007, Academic Press. p. 179-204.

83. Qu, L., et al., *Neuronal Fc-gamma receptor I mediated excitatory effects of IgG immune complex on rat dorsal root ganglion neurons.* Brain, behavior, and immunity, 2011. **25**(7): p. 1399-1407.

84. McGeown, J.G., N.G. McHale, and K.D. Thornbury, *The effect of electrical stimulation of the sympathetic chain on peripheral lymph flow in the anaesthetized sheep.* J Physiol, 1987. **393**(1): p. 123-33.

85. McHale, N.G. and T.H. Adair, *Reflex modulation of lymphatic pumping in sheep.* Circ Res, 1989. **64**(6): p. 1165-71.

86. McHale, N.G. and I.C. Roddie, *The effect of intravenous adrenaline and noradrenaline infusion of peripheral lymph flow in the sheep.* J Physiol, 1983. **341**(1): p. 517-26.

87. von Andrian, U.H. and T.R. Mempel, *Homing and cellular traffic in lymph nodes.* Nat Rev Immunol, 2003. **3**(11): p. 867-78.

88. Junt, T., et al., *Subcapsular sinus macrophages in lymph nodes clear lymph-borne viruses and present them to antiviral B cells.* Nature, 2007. **450**(7166): p. 110-4.

89. Phan, T.G., et al., *Subcapsular encounter and complement-dependent transport of immune complexes by lymph node B cells.* Nat Immunol, 2007. **8**(9): p. 992-1000.

90. Carrasco, Y.R. and F.D. Batista, *B cells acquire particulate antigen in a macrophage-rich area at the boundary between the follicle and the subcapsular sinus of the lymph node.* Immunity, 2007. **27**(1): p. 160-71.

91. Agarwal, N., S. Offermanns, and R. Kuner, *Conditional gene deletion in primary nociceptive neurons of trigeminal ganglia and dorsal root ganglia.* Genesis, 2004. **38**(3): p. 122-9.

92. Barthold, S.W., K.A. Bayne, and M.A. Davis, *Guide for the care and use of laboratory animals*. 2011, Washington: National Academy Press.

93. Abrahamsen, B., et al., *The cell and molecular basis of mechanical, cold, and inflammatory pain.* Science, 2008. **321**(5889): p. 702-5.

94. Abadie, V., et al., *Neutrophils rapidly migrate via lymphatics after Mycobacterium bovis BCG intradermal vaccination and shuttle live bacilli to the draining lymph nodes.* Blood, 2005. **106**(5): p. 1843-50.

95. Maletto, B.A., et al., *Presence of neutrophil-bearing antigen in lymphoid organs of immune mice.* Blood, 2006. **108**(9): p. 3094-102.

96. Pesce, J.T., et al., *Neutrophils clear bacteria associated with parasitic nematodes augmenting the development of an effective Th2-type response.* J Immunol, 2008. **180**(1): p. 464-74.

97. Cochran, A.J., D.R. Wen, and D.L. Morton, *Management of the regional lymph nodes in patients with cutaneous malignant melanoma.* World J Surg, 1992. **16**(2): p. 214-21.

98. Fidler, I.J., *The pathogenesis of cancer metastasis: the 'seed and soil' hypothesis revisited.* Nat Rev Cancer, 2003. **3**(6): p. 453-8.

99. Shayan, R., M.G. Achen, and S.A. Stacker, *Lymphatic vessels in cancer metastasis: bridging the gaps.* Carcinogenesis, 2006. **27**(9): p. 1729-38.

100. Morton, D.L., et al., *Technical details of intraoperative lymphatic mapping for early stage melanoma.* Arch Surg, 1992. **127**(4): p. 392-9.

101. Bilchik, A.J., et al., *Universal application of intraoperative lymphatic mapping and sentinel lymphadenectomy in solid neoplasms.* Cancer J Sci Am, 1998. **4**(6): p. 351-8.

102. Nieweg, O.E., P.J. Tanis, and B.B. Kroon, *The definition of a sentinel node.* Ann Surg Oncol, 2001. **8**(6): p. 538-41.

103. Ferris, R.L., et al., *Molecular staging of cervical lymph nodes in squamous cell carcinoma of the head and neck.* Cancer Res, 2005. **65**(6): p. 2147-56.

104. Park, C., et al., *Internal mammary sentinel lymph node mapping for invasive breast cancer: implications for staging and treatment.* Breast J, 2005. **11**(1): p. 29-33.

105. Orchard, T.J., et al., *Type 1 diabetes and coronary artery disease.* Diabetes Care, 2006. **29**(11): p. 2528-38.

106. Secrest, A.M., et al., *All-cause mortality trends in a large population-based cohort with long-standing childhood-onset type 1 diabetes: the Allegheny County type 1 diabetes registry.* Diabetes Care, 2010. **33**(12): p. 2573-9.

107. Soedamah-Muthu, S.S., et al., *All-cause mortality rates in patients with type 1 diabetes mellitus compared with a non-diabetic population from the UK general practice research database, 1992-1999.* Diabetologia, 2006. **49**(4): p. 660-6.

108. Laing, S.P., et al., *Mortality from heart disease in a cohort of 23,000 patients with insulin-treated diabetes.* Diabetologia, 2003. **46**(6): p. 760-5.

109. Laing, S.P., et al., *The British Diabetic Association Cohort Study, I: all-cause mortality in patients with insulin-treated diabetes mellitus.* Diabet Med, 1999. **16**(6): p. 459-65.

110. Skrivarhaug, T., et al., *Long-term mortality in a nationwide cohort of childhood-onset type 1 diabetic patients in Norway.* Diabetologia, 2006. **49**(2): p. 298-305.

111. Secrest, A.M., et al., *Cause-specific mortality trends in a large population-based cohort with long-standing childhood-onset type 1 diabetes.* Diabetes, 2010. **59**(12): p. 3216-22.

112. Livingstone, S.J., et al., *Risk of cardiovascular disease and total mortality in adults with type 1 diabetes: Scottish registry linkage study.* PLoS Med, 2012. **9**(10): p. e1001321.

113. Lind, M., et al., *Glycemic control and excess mortality in type 1 diabetes.* N Engl J Med, 2014. **371**(21): p. 1972-82.

114. Centers for Disease Control and Prevention, *National diabetes statistics report: estimates of diabetes and its burden in the United States, 2014*, in *Atlanta, GA: US Department of Health and Human Services*. 2014.

115. Dall, T.M., et al., *Distinguishing the economic costs associated with type 1 and type 2 diabetes.* Popul Health Manag, 2009. **12**(2): p. 103-10.

116. Atkinson, M.A. and G.S. Eisenbarth, *Type 1 diabetes: new perspectives on disease pathogenesis and treatment.* Lancet, 2001. **358**(9277): p. 221-9.

117. Nelson, P., et al., *Modeling dynamic changes in type 1 diabetes progression: quantifying beta-cell variation after the appearance of islet-specific autoimmune responses.* Math Biosci Eng, 2009. **6**(4): p. 753-78.

118. Morran, M.P., G.S. Omenn, and M. Pietropaolo, *Immunology and genetics of type 1 diabetes.* Mt Sinai J Med, 2008. **75**(4): p. 314-27.

119. Kay, T.W., I.L. Campbell, and L.C. Harrison, *Characterization of pancreatic T lymphocytes associated with beta cell destruction in the non-obese diabetic (NOD) mouse.* J Autoimmun, 1991. **4**(2): p. 263-76.

120. Hawkins, T.A., R.R. Gala, and J.C. Dunbar, *The lymphocyte and macrophage profile in the pancreas and spleen of NOD mice: percentage of interleukin-2 and prolactin receptors on immunocompetent cell subsets.* J Reprod Immunol, 1996. **32**(1): p. 55-71.

121. Anderson, M.S. and J.A. Bluestone, *The NOD mouse: a model of immune dysregulation.* Annu Rev Immunol, 2005. **23**: p. 447-85.

122. van Belle, T.L., K.T. Coppieters, and M.G. von Herrath, *Type 1 diabetes: etiology, immunology, and therapeutic strategies.* Physiol Rev, 2011. **91**(1): p. 79-118.

123. Pugliese, A., et al., *Self-antigen–presenting cells expressing diabetes-associated autoantigens exist in both thymus and peripheral lymphoid organs.* The Journal of clinical investigation, 2001. **107**(5): p. 555-564.

124. Miao, D., L. Yu, and G.S. Eisenbarth, *Role of autoantibodies in type 1 diabetes.* Front Biosci, 2007. **12**: p. 1889-98.

125. Knip, M., et al., *Environmental triggers and determinants of type 1 diabetes.* Diabetes, 2005. **54 Suppl 2**(suppl 2): p. S125-36.

126. Taplin, C.E. and J.M. Barker, *Autoantibodies in type 1 diabetes.* Autoimmunity, 2008. **41**(1): p. 11-8.

127. Wenzlau, J.M., et al., *The cation efflux transporter ZnT8 (Slc30A8) is a major autoantigen in human type 1 diabetes.* Proc Natl Acad Sci U S A, 2007. **104**(43): p. 17040-5.

128. Atkinson, M.A., G.S. Eisenbarth, and A.W. Michels, *Type 1 diabetes.* The Lancet, 2014. **383**(9911): p. 69-82.

129. Pescovitz, M.D., et al., *Rituximab, B-lymphocyte depletion, and preservation of beta-cell function.* N Engl J Med, 2009. **361**(22): p. 2143-52.

130. Wherrett, D.K., et al., *Antigen-based therapy with glutamic acid decarboxylase (GAD) vaccine in patients with recent-onset type 1 diabetes: a randomised double-blind trial.* Lancet, 2011. **378**(9788): p. 319-27.

131. Ludvigsson, J., et al., *GAD65 antigen therapy in recently diagnosed type 1 diabetes mellitus.* N Engl J Med, 2012. **366**(5): p. 433-42.

132. Bach, J.F., *Anti-CD3 antibodies for type 1 diabetes: beyond expectations.* Lancet, 2011. **378**(9790): p. 459-60.

133. Orban, T., et al., *Co-stimulation modulation with abatacept in patients with recent-onset type 1 diabetes: a randomised, double-blind, placebo-controlled trial.* Lancet, 2011. **378**(9789): p. 412-9.

134. Sherry, N., et al., *Teplizumab for treatment of type 1 diabetes (Protege study): 1-year results from a randomised, placebo-controlled trial.* Lancet, 2011. **378**(9790): p. 487-97.

135. Pavlov, V.A., et al., *The cholinergic anti-inflammatory pathway: a missing link in neuroimmunomodulation.* Mol Med, 2003. **9**(5-8): p. 125-34.

136. Pavlov, V.A. and K.J. Tracey, *The cholinergic anti-inflammatory pathway.* Brain Behav Immun, 2005. **19**(6): p. 493-9.

137. Pavlov, V.A., et al., *Central muscarinic cholinergic regulation of the systemic inflammatory response during endotoxemia.* Proc Natl Acad Sci U S A, 2006. **103**(13): p. 5219-23.

138. Pavlov, V.A., et al., *Brain acetylcholinesterase activity controls systemic cytokine levels through the cholinergic anti-inflammatory pathway.* Brain, behavior, and immunity, 2009. **23**(1): p. 41-45.

139. Parrish, W.R., et al., *Modulation of TNF release by choline requires α7 subunit nicotinic acetylcholine receptor-mediated signaling.* Molecular medicine, 2008. **14**(9-10): p. 567.

140. Tracey, K.J., *Reflex control of immunity.* Nat Rev Immunol, 2009. **9**(6): p. 418-28.

141. Rosas-Ballina, M., et al., *Splenic nerve is required for cholinergic antiinflammatory pathway control of TNF in endotoxemia.* Proceedings of the National Academy of Sciences, 2008. **105**(31): p. 11008-11013.

142. Bencherif, M., et al., *Alpha7 nicotinic receptors as novel therapeutic targets for inflammation-based diseases.* Cell Mol Life Sci, 2011. **68**(6): p. 931-49.

143. Olofsson, P.S., et al., *alpha7 nicotinic acetylcholine receptor (alpha7nAChR) expression in bone marrow-derived non-T cells is required for the inflammatory reflex.* Mol Med, 2012. **18**(1): p. 539-43.

144. Mabley, J.G., et al., *Nicotine reduces the incidence of type I diabetes in mice.* J Pharmacol Exp Ther, 2002. **300**(3): p. 876-81.

145. Olofsson, P.S., et al., *Rethinking inflammation: neural circuits in the regulation of immunity.* Immunol Rev, 2012. **248**(1): p. 188-204.

146. Zitnik, R.J., *Treatment of chronic inflammatory diseases with implantable medical devices.* Cleve Clin J Med, 2011. **78 Suppl 1**: p. S30-4.

147. Reichman, W.E., *Current pharmacologic options for patients with Alzheimer's disease.* Ann Gen Hosp Psychiatry, 2003. **2**(1): p. 1.

148. Ellis, J.M., *Cholinesterase inhibitors in the treatment of dementia.* J Am Osteopath Assoc, 2005. **105**(3): p. 145-58.

149. Waldburger, J.M., et al., *Spinal p38 MAP kinase regulates peripheral cholinergic outflow.* Arthritis Rheum, 2008. **58**(9): p. 2919-21.

150. Satapathy, S.K., et al., *Galantamine alleviates inflammation and other obesity-associated complications in high-fat diet-fed mice.* Molecular medicine, 2011. **17**(7-8): p. 599-606.

151. Abiru, N., et al., *Transient insulin autoantibody expression independent of development of diabetes: comparison of NOD and NOR strains.* J Autoimmun, 2001. **17**(1): p. 1-6.

152. Quintana, F.J. and I.R. Cohen, *Autoantibody patterns in diabetes-prone NOD mice and in standard C57BL/6 mice.* J Autoimmun, 2001. **17**(3): p. 191-7.

153. Tisch, R., et al., *Immune response to glutamic acid decarboxylase correlates with insulitis in non-obese diabetic mice.* Nature, 1993. **366**(6450): p. 72-5.

154. Ji, H., et al., *Central cholinergic activation of a vagus nerve-to-spleen circuit alleviates experimental colitis.* Mucosal Immunol, 2014. **7**(2): p. 335-47.

155. Jaakkola, I., S. Jalkanen, and A. Hanninen, *Diabetogenic T cells are primed both in pancreatic and gut-associated lymph nodes in NOD mice.* Eur J Immunol, 2003. **33**(12): p. 3255-64.

156. Holst, J.J., et al., *Autonomic nervous control of the endocrine secretion from the isolated, perfused pig pancreas.* J Auton Nerv Syst, 1986. **17**(1): p. 71-84.

157. Miller, R.E., *Pancreatic neuroendocrinology: peripheral neural mechanisms in the regulation of the Islets of Langerhans.* Endocr Rev, 1981. **2**(4): p. 471-94.

158. Woods, S.C. and D. Porte, Jr., *Neural control of the endocrine pancreas.* Physiol Rev, 1974. **54**(3): p. 596-619.

159. van Westerloo, D.J., et al., *The vagus nerve and nicotinic receptors modulate experimental pancreatitis severity in mice.* Gastroenterology, 2006. **130**(6): p. 1822-30.

160. Yi, C.X., et al., *The role of the autonomic nervous liver innervation in the control of energy metabolism.* Biochim Biophys Acta, 2010. **1802**(4): p. 416-31.

161. Owyang, C. and A. Heldsinger, *Vagal control of satiety and hormonal regulation of appetite.* J Neurogastroenterol Motil, 2011. **17**(4): p. 338-48.

162. Wang, P.Y., et al., *Upper intestinal lipids trigger a gut-brain-liver axis to regulate glucose production.* Nature, 2008. **452**(7190): p. 1012-6.

163. Pavlov, V.A. and K.J. Tracey, *The vagus nerve and the inflammatory reflex--linking immunity and metabolism.* Nat Rev Endocrinol, 2012. **8**(12): p. 743-54.

164. Nicolson, R., B. Craven-Thuss, and J. Smith, *A prospective, open-label trial of galantamine in autistic disorder.* J Child Adolesc Psychopharmacol, 2006. **16**(5): p. 621-9.

165. Chakravarthy, B.K., S. Gupta, and K.D. Gode, *Functional beta cell regeneration in the islets of pancreas in alloxan induced diabetic rats by (-)-epicatechin.* Life Sci, 1982. **31**(24): p. 2693-7.

166. Montana, E., S. Bonner-Weir, and G.C. Weir, *Beta cell mass and growth after syngeneic islet cell transplantation in normal and streptozocin diabetic C57BL/6 mice.* J Clin Invest, 1993. **91**(3): p. 780-7.

167. Yoon, K.-H., et al., *Differentiation and expansion of beta cell mass in porcine neonatal pancreatic cell clusters transplanted into nude mice.* Cell transplantation, 1998. **8**(6): p. 673-689.

168. Xu, G., et al., *Exendin-4 stimulates both beta-cell replication and neogenesis, resulting in increased beta-cell mass and improved glucose tolerance in diabetic rats.* Diabetes, 1999. **48**(12): p. 2270-2276.

169. Shapiro, A.M., et al., *Islet transplantation in seven patients with type 1 diabetes mellitus using a glucocorticoid-free immunosuppressive regimen.* N Engl J Med, 2000. **343**(4): p. 230-8.

170. Ramiya, V.K., et al., *Reversal of insulin-dependent diabetes using islets generated in vitro from pancreatic stem cells.* Nature Medicine, 2000. **6**(3): p. 278-282.

171. Ryan, E.A., et al., *Five-year follow-up after clinical islet transplantation.* Diabetes, 2005. **54**(7): p. 2060-9.

172. Gibly, R.F., et al., *Advancing islet transplantation: from engraftment to the immune response.* Diabetologia, 2011. **54**(10): p. 2494-505.

173. Oparil, S., M.A. Zaman, and D.A. Calhoun, *Pathogenesis of hypertension.* Ann Intern Med, 2003. **139**(9): p. 761-76.

174. *Seventy-Fourth Annual Meeting of the British Medical Association.* Bmj, 1906. **2**(2399): p. 1760-1816.

175. Furchgott, R.F. and J.V. Zawadzki, *The obligatory role of endothelial cells in the relaxation of arterial smooth muscle by acetylcholine.* Nature, 1980. **288**(5789): p. 373-6.

176. Andersson, U. and K.J. Tracey, *Reflex principles of immunological homeostasis.* Annu Rev Immunol, 2012. **30**: p. 313-35.

177. Krump-Konvalinkova, V., et al., *Generation of human pulmonary microvascular endothelial cell lines.* Lab Invest, 2001. **81**(12): p. 1717-27.

178. Ye, X., et al., *Divergent roles of endothelial NF-kappaB in multiple organ injury and bacterial clearance in mouse models of sepsis.* J Exp Med, 2008. **205**(6): p. 1303-15.

179. Kawashima, K., et al., *Reconciling neuronally and nonneuronally derived acetylcholine in the regulation of immune function.* Ann N Y Acad Sci, 2012. **1261**(1): p. 7-17.

180. Dimmeler, S., et al., *Activation of nitric oxide synthase in endothelial cells by Akt-dependent phosphorylation.* Nature, 1999. **399**(6736): p. 601-5.

181. Bearden, S.E., et al., *Arteriolar network architecture and vasomotor function with ageing in mouse gluteus maximus muscle.* J Physiol, 2004. **561**(Pt 2): p. 535-45.

182. Fujimoto, K., et al., *Decreased acetylcholine content and choline acetyltransferase mRNA expression in circulating mononuclear leukocytes and lymphoid organs of the spontaneously hypertensive rat.* Life Sci, 2001. **69**(14): p. 1629-38.

183. Lataro, R.M., et al., *Acetylcholinesterase Inhibition Attenuates the Development of Hypertension and Inflammation in Spontaneously Hypertensive Rats.* Am J Hypertens, 2015. **28**(10): p. 1201-8.

184. June, C., et al., *T-cell therapy at the threshold.* Nat Biotechnol, 2012. **30**(7): p. 611-4.

185. Birmingham, K., et al., *Bioelectronic medicines: a research roadmap.* Nat Rev Drug Discov, 2014. **13**(6): p. 399-400.

186. Famm, K., et al., *Drug discovery: a jump-start for electroceuticals.* Nature, 2013. **496**(7444): p. 159-61.

187. Hansson, G.K., *Inflammation, atherosclerosis, and coronary artery disease.* N Engl J Med, 2005. **352**(16): p. 1685-95.

188. Faraco, G. and C. Iadecola, *Hypertension: a harbinger of stroke and dementia.* Hypertension, 2013. **62**(5): p. 810-7.

189. Harrison, D.G., et al., *Inflammation, immunity, and hypertension.* Hypertension, 2011. **57**(2): p. 132-40.

190. Matrougui, K., et al., *Natural regulatory T cells control coronary arteriolar endothelial dysfunction in hypertensive mice.* Am J Pathol, 2011. **178**(1): p. 434-41.

191. Barhoumi, T., et al., *T regulatory lymphocytes prevent angiotensin II-induced hypertension and vascular injury.* Hypertension, 2011. **57**(3): p. 469-76.

192. McMaster, W.G., et al., *Inflammation, immunity, and hypertensive end-organ damage.* Circ Res, 2015. **116**(6): p. 1022-33.

193. Mizuno, K., et al., *β2-Adrenergic receptor stimulation inhibits LPS-induced IL-18 and IL-12 production in monocytes.* Immunology letters, 2005. **101**(2): p. 168-172.

194. Verhoeckx, K.C., et al., *Inhibitory effects of the β2-adrenergic receptor agonist zilpaterol on the LPS-induced production of TNF-α in vitro and in vivo.* Journal of veterinary pharmacology and therapeutics, 2005. **28**(6): p. 531-537.

195. Kohm, A.P. and V.M. Sanders, *Norepinephrine and beta 2-adrenergic receptor stimulation regulate CD4+ T and B lymphocyte function in vitro and in vivo.* Pharmacol Rev, 2001. **53**(4): p. 487-525.

196. Boyden, E.S., et al., *Millisecond-timescale, genetically targeted optical control of neural activity.* Nat Neurosci, 2005. **8**(9): p. 1263-8.

197. Zhang, F., et al., *Channelrhodopsin-2 and optical control of excitable cells.* Nat Methods, 2006. **3**(10): p. 785-92.

198. Airan, R.D., et al., *Temporally precise in vivo control of intracellular signalling.* Nature, 2009. **458**(7241): p. 1025-9.

199. Novak, T.J. and E.V. Rothenberg, *cAMP inhibits induction of interleukin 2 but not of interleukin 4 in T cells.* Proceedings of the National Academy of Sciences, 1990. **87**(23): p. 9353-9357.